EFFECTS OF PLAN ASPECT RATIO ON SEISMIC RESPONSES OF RC BUILDINGS BY TIME HISTORY ANALYSIS

TOFIQ BIN SAJED

INSTITUTE OF EARTHQUAKE ENGINEERING RESEARCH

CHITTAGONG UNIVERSITY OF ENGINEERING AND TECHNOLOGY

CHATTOGRAM-4349, BANGLADESH

June 2021

EFFECTS OF PLAN ASPECT RATIO ON SEISMIC RESPONSES OF RC BUILDINGS BY TIME HISTORY ANALYSIS

A project

Submitted to

The Institute of Earthquake Engineering Research in partial fulfillment of the requirements for the degree of Postgraduate Diploma in Earthquake Engineering [PG.DIP. (EQE)]

BY

TOFIQ BIN SAJED

INSTITUTE OF EARTHQUAKE ENGINEERING RESEARCH

CHITTAGONG UNIVERSITY OF ENGINEERING AND TECHNOLOGY

CHATTOGRAM-4349, BANGLADESH

June 2021

The project entitled **"Effects of Plan Aspect Ratio on Seismic Responses of RC Buildings by Time History Analysis"** submitted by Tofiq Bin Sajed, Student No: 17PGDEQE004F, and Session: 2017-2018 has been accepted as satisfactory in partial fulfillment of the degree of Postgraduate Diploma in Earthquake Engineering [PG. Dip. (EQE)] on June 29, 2021.

BOARD OF EXAMINERS

Mohammad Raihan Mukhlis
Research Assistant Professor — Chairman (Supervisor)
Institute of Earthquake Engineering Research (IEER)
Chittagong University of Engineering & Technology

Prof. Dr. Md. Rabiul Alam
Director — Member (Ex-Officio)
Institute of Earthquake Engineering Research (IEER)
Chittagong University of Engineering & Technology

Prof. Dr. G. M. Sadiqul Islam
Department of Civil Engineering — Member
Chittagong University of Engineering & Technology

ACKNOWLEDGEMENT

I would like to express my deepest gratitude to my supervisor Mohammad Raihan Mukhlis, Research Assistant Professor, Institute of Earthquake Engineering Research, CUET for his proper guidance, valuable suggestions and sincere supervision throughout the research work.

I would like to thank Prof. Dr. Md. Rabiul Alam, Director, IEER for his valuable suggestions. I would also like to thank Shafayat Bin Ali, Research Assistant Professor, IEER and Sohel Rana, Research Lecturer, IEER, CUET for providing creative ideas and continuous motivation to do research on earthquake related issues and lead me to finish my thesis step by step.

I am grateful to my parents and other family members for their continuous support and encouragement during the research period.

Above all, I am grateful to the almighty Allah, the only source of knowledge that this research work has been completed successfully.

DECLARATION

It is hereby declared that, except where specific references are made to other investigations, the work embodied in this project is the result of investigation carried out by the author under the supervision of Mohammad Raihan Mukhlis, Research Assistant Professor, Institute of Earthquake Engineering Research, CUET, Chattogram - 4349.

Neither this project nor the any part of it has been submitted or is being concurrently submitted in candidature for any degree or diploma at any other institution.

Tofiq Bin Sajed

Student ID Number – 17PGDEQE004F

ABSTRACT

Seismic analysis is one of the major developments in the field of civil engineering. Among many seismic analysis methods, nonlinear time history method is undoubtedly the most realistic method as it directly applies the earthquake load on the structure. Selection of ground motion history is important in time history analysis as it should be compatible with the existing building code of the country. Meanwhile, seismic responses of the structure are greatly influenced by its shape, size and geometry. In this study, nonlinear time history analysis has been used to evaluate the seismic responses of three buildings in both X and Y directions with three different plan aspect ratio (length to width ratio) having same area and height. The selected ground motion history is used in the analysis after matching with the design response spectrum of Bangladesh National Building Code (BNBC). Finally, the effects of plan aspect ratio on seismic responses of the buildings are evaluated in terms of displacements and story drifts. Although, all three building models consist of same plan area, story displacements increase in both X and Y directions with the increase of plan aspect ratios. However, maximum story displacements and story drifts are largely increased in Y direction compared to that in X direction as building models become less stiff in Y direction with the increase of aspect ratios.

TABLE OF CONTENTS

LIST OF FIGURES

LIST OF TABLES

LIST OF ABBREVIATIONS

AR	Aspect Ratio
BNBC	Bangladesh National Building Code
CCA	Chattogram City Area
CDMP	Comprehensive Disaster Management Program
CS	Compressive Stress
CSC	Compressive Strength of Concrete
CDMP	Comprehensive Disaster Management Program
DBE	Design Basis Earthquake
DI	Direct Integration
DOF	Degree of Freedom
DC	Design Code
IEER	Institute of Earthquake Engineering Research
MCE	Maximum Considered Earthquake
MSD	Maximum Story Displacement
NSP	Nonlinear Static Procedure
NDP	Nonlinear Dynamic Procedure
PGA	Peak Ground Acceleration
POA	Pushover Analysis
RSA	Response Spectrum Analysis
RC	Reinforced Concrete
RCC	Reinforced Cement Concrete
RD	Rigid Diaphragm
RCRS	Reinforced Concrete Rectangular Section
SA	Spectral Acceleration
SDR	Story Drift Ratio
THA	Time History Analysis
VDC	Virtual Data Center

Chapter 1
INTRODUCTION

1.1 General

Earthquake loads have been a significant consideration for designing structures. Current building codes recommend different methods of linear/ nonlinear and static/ dynamic analysis based on irregularities in mass and geometry of the building structures (BNBC, 2020 and Eurocode 8, 2004). If the earthquake forces are not taken properly then it might cause serious damage to the building as well as to the life of the people. Hence, the earthquake forces need to be considered properly in different approaches of seismic analysis. But, unfortunately, there is lack of consensus on appropriate selection of ground motion for code based design and seismic performance evaluation of buildings using nonlinear time history analysis (Haselton et.al, 2012). A time history analysis is commonly used to assess a structure's seismic response during dynamic loads from any representative earthquake (Wilkinson and Hiley, 2006). As actual time-dependent behavior of the structural response is considered in time history analysis, it gives a better check for the protection of the structure (BNBC, 2020). Time history analysis is a step-by-step analysis of the dynamic reaction of a structure relative to the ground motion record of any representative earthquake.

In recent years, reinforced concrete (RC) buildings have been badly affected or demolished during earthquakes. An RC building behavior during earthquakes depends mainly on its basic shapes, dimensions, and geometries (Alashker et.al, 2015). Any irregularity in shape size and geometry generally makes a building vulnerable during earthquake excitation. According to damage assessments, following previous earthquakes, buildings with irregular plan configurations may have more severe damage than regular buildings due to increased torsion reactions and stress concentration (Raheem et.al, 2018). One such form of plan irregularity is large plan aspect ratio. Plan aspect ratio is the ratio of the length to the width of the building. Buildings with large plan aspect ratio might reduce the lateral load carrying capacity by producing a weak rigid diaphragm action. The mass of the building is significant at floor levels, and the inertia force is concentrated there during earthquake cracking.

The inertia force is then dispersed according to the stiffness of various lateral load resistance systems (columns and/or structural walls). This is effectively accomplished when the floor slabs are not too distorted in their own horizontal plane. However, inertia forces are allocated based on the tributary area, when floor slabs bend in their own plane, members with lower capacity are overloaded, causing unforeseen damage to buildings (Hujare and Tande, 2017).

The behavior of a building during an earthquake depends on rigidity, sufficient lateral strength, flexibility, and configuration. The conduct of multi-story buildings during earthquake shaking is determined by the distribution of mass, stiffness, and strength in both the horizontal and vertical planes of the structures. Weakness in a building can be caused by isolation in stiffness, mass, or strength along with the diaphragm. In addition, it is necessary to understand the structural performance of buildings with large deformations under seismic loading.

1.2 Objectives with Specific Aims

Based on the above background, the study aims at evaluating the effects of plan aspect ratio on seismic response of multistoried RC buildings using nonlinear time history analysis. In this regard, three multistoried RC buildings of three different aspect ratios are considered keeping same plan area and story height. Nonlinear dynamic analysis of the buildings are performed using three earthquake ground motions time history matched with the design response spectrum of BNBC 2020.

Motivated by the above discussion, the current work is aimed to conduct the following works:

- To determine the maximum story displacement and story drift ratio of RC buildings using time history analysis.
- To compare the effect of plan aspect ratio on story displacement and story drift ratio of RC buildings.

1.3 Organization of the Report

This research report is organized into five chapters. In the present chapter short preface and objectives are presented.

In chapter 2, a comprehensive literature review of earthquake, seismicity of Chittagong and Bangladesh, ground motion, configuration of the buildings, structural analysis, response spectrum and related research are presented.

In chapter 3, Methodology of the whole project work is presented which includes time history analysis (THA) of the buildings as well as design response spectrum and ground motion matching.

In chapter 4, Displacement response at top floor of each building models are formed from time history analysis, Story drift ratio are then determined for each floor by dividing the relative displacements of the floors by the story height as well as maximum story displacement and story drift ratio results are presented.

Lastly chapter 5, conclusions obtained from this project work are presented concisely and it can be concluded that seismic response of buildings increases with the increase of plan aspect ratio if the building is analyzed by time history method.

Chapter 2
LITERATURE REVIEW

2.1 General

In recent years, more people are killed in earthquakes than in any other weather-related disaster. Bangladesh is one of the world's largest deltas, located at the confluence of South Asia and the Bay of Bengal. The earthquake is one of the most devastating natural calamities, wreaking untold havoc on property and human life. Several major earthquakes with epicenters within Bangladesh and its surrounding regions have occurred in the past, according to the historical catalog of Bangladesh and its surrounding regions. Bangladesh has been subjected to seismic calamities from ancient times due to its tectonic location.

2.2 Seismicity

According to the geological location five major faults are active in Bangladesh (Hossain, 1998). Bangladesh is in a dangerous situation due to the presence of these major faults. Earthquake occurs in the world every moment, all of these are not felt which are very minor ($ms \leq 3.0$) and are not vulnerable for us but strong earthquakes ($ms \geq 6.0$) cause terrible situation. An earthquake occurs when energy is released suddenly in the Earth's crust, causing seismic waves. Earthquake or seismic activity in a region refers to the frequency, type, and size of earthquakes observed in a given period of time. The Richter Magnitude (ML) and Moment Magnitude (MW) scales are used to measure earthquakes. The depth at which earthquakes occur is often used to classify them. There are two kinds of earthquakes: shallow and deep. Shallow earthquakes cause more harm. Also, shallow earthquakes have a well-understood mechanism; the process of producing deep earthquakes is not fully understood. Shallow earthquakes are more general, more damaging, and better understood (Roy, 2014).

2.2.1 Seismicity in Bangladesh Region

The historical seismic data and recent seismic activities in Bangladesh and adjacent regions express that Bangladesh is at seismic risk [Fig. 2.1]. As Bangladesh is the most densely inhabited country in the world, any future earthquake will affect a

greater number of people per unit area than earthquakes in other seismically active areas of the world. Experts predict that a large earthquake will strike this region in the near future, resulting in significant human casualties, infrastructure damage, and other losses. The most damaging earthquakes, as shown in Figure 2.1, originate in two well-defined zones or belts: the 'circum-Pacific belt' and the 'Mediterranean-Himalayan seismic belt'.

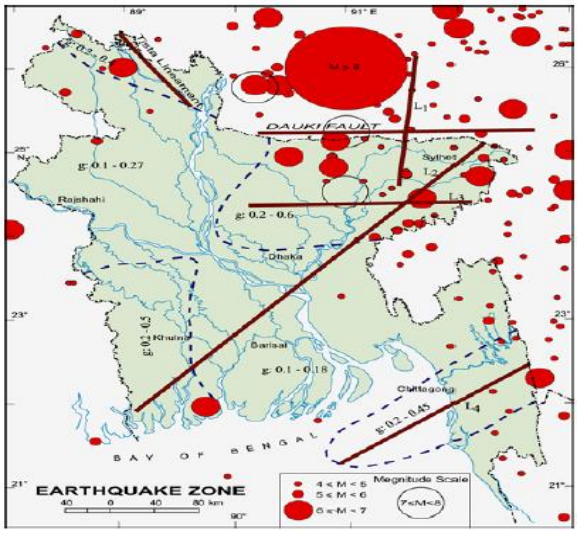

Fig. 2.1: Seismic Activity of Bangladesh (Roy, 2014)

In Bangladesh, there are no comprehensive seismic monitoring systems. In 1954, the Bangladesh Meteorological Department erected a seismic observatory in Chittagong. In 2010, the IEER, CUET established a seismic observatory station. In addition, there are multiple active fault zones in this junction area that are earthquake resources. Mostly around Bangladesh, there are five significant sources of earthquakes were identified by Bolt in 1987 [Table 2.1].

Table 2.1: Seismic sources in Bangladesh (Bolt, 1987)

Faults	Probable magnitude in Bangladesh (in Richter scale)
Assam fault zone	8.0
Tripura fault zone	7.0
Sub Dauki fault zone	7.3
Bogra fault zone	7.0
Shillong plateau	7.0

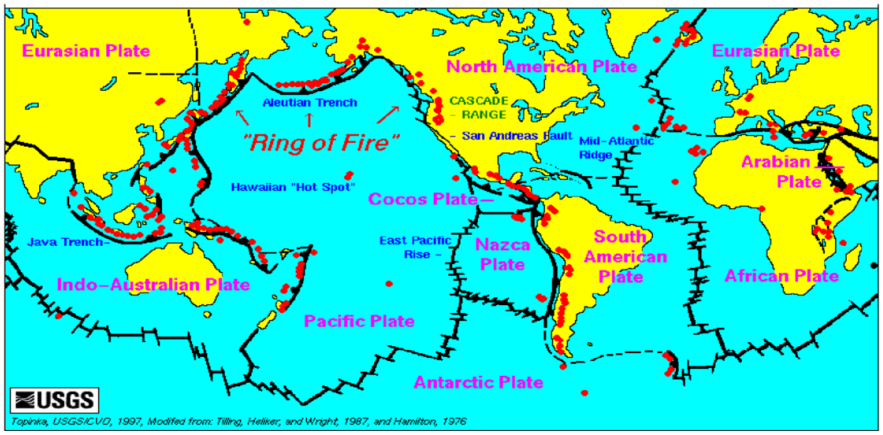

Fig. 2.2: Active Plate Tectonics, "Hot Spots" and the "Ring of Fire" (Wikimedia Commons)

Fig. 2.2 demonstrates that volcanoes occur where magma rises over the Earth's crust in addition to reaching the surface. To achieve this, the magma has to find a weakness within the crustal rocks concerning either the territory or under the seaside. The majority of the volcanoes occur in or close to, your edges of tectonic plates. A recent go-through conducted in the Comprehensive Disaster Management Program (CDMP) phase 1 project. There are five major fault zones in Bangladesh, as shown in Fig. 2.3, i.e., Madhupur fault, Dauki Fault, Plate Boundary Fault -1, Plate Boundary Fault -2, and Plate Boundary Fault -3. Additionally, five scenarios, an exceptional earthquake scenario in which a magnitude-6 earthquake is happening beneath Chittagong Town was recommended, (CDMP, 2009). In such seismic losses analysis, three earthquake circumstances were selected per City Corporation. The first scenario is the circumstances that create the highest level of ground motion in the city among the OIC's list of five examples. The second scenario shows that the remaining four OIC examples are less than they could be in the first situation, and they are not entirely different from each other. The third scenario is a unique situation in which a magnitude six earthquake occurs precisely beneath the town.

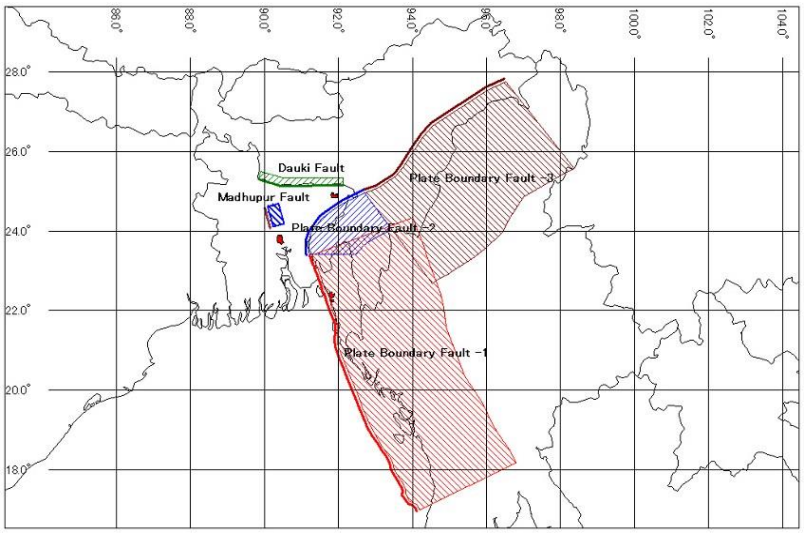

Fig. 2.3: Proposed Earthquake Fault Zones by CDMP in 2009 (CDMP, 2009)

Based on different sources (catalogues, online resources, etc.) the historical earthquakes list was prepared for Bangladesh and its surroundings from 1858 to present. Table 2.2 shows the list of historical earthquakes in and around Bangladesh since 1858. The greatest event was occurred surroundings this region was known as Great Indian Earthquake in 1897 with an estimated magnitude M_s 8.7 (Sabri, 2001). Epicenter of this earthquake was less than 250 km from the capital Dhaka. In the nearby city of Sylhet, which is located in Bangladesh's north eastern region, significant damage was documented, with a death toll of 545. According the trench investigation at Gabrakhari site across the Dauki Fault, the source is inferred to be the Dauki Fault. Another notable earthquake with a magnitude of 7.6 (Sabri, 2001) occurred in 1918 near Sylhet and was known as the Srimangal Earthquake. The earthquake's epicenter was roughly 130 kilometers from Dhaka. Table 2.2 represents some historical earthquakes in and around Bangladesh. Most of these events are strong and major magnitude earthquakes.

Table 2.2: Listing of Major Earthquakes having an effect on Bangladesh (Hussaini et.al, 2015)

Date	Name	Magnitude (Richter)	Epicentral Distance from Dhaka (km)	Epicentral Distance from Sylhet City (km)	Epicentral Distance from Chittagong (km)
10 January, 1869	Cachar Earthquake	7.5	250	70	280
14 July, 1885	Bengal Earthquake	7.0	170	220	350
12 June, 1897	Great Indian Earthquake	8.7	230	80	340
2 July, 1930	Srimongal Earthquake	7.6	150	60	200
2 July, 1930	Dhubri Earthquake	7.1	250	275	415
15 January, 1934	Bihar-Nepal Earthquake	8.3	510	530	580
15 August, 1950	Assam Earthquake	8.5	780	580	540

Fig. 2.4 represents earthquakes that took places around Bangladesh from 1865 to 1995. The Fig. 2.5 represents seismic map in BNBC upgrading project that was undertaken in. The map showing PGA values based on MCE. Design basis earthquake (DBE) with return period of 475 years including local soil effects and corresponding to PGA value of $\frac{2}{3}$ Zg or 0.19g, where as BNBC 2020 map (see in Fig. 2.5) presents a coefficient of 0.28 g (MCE).

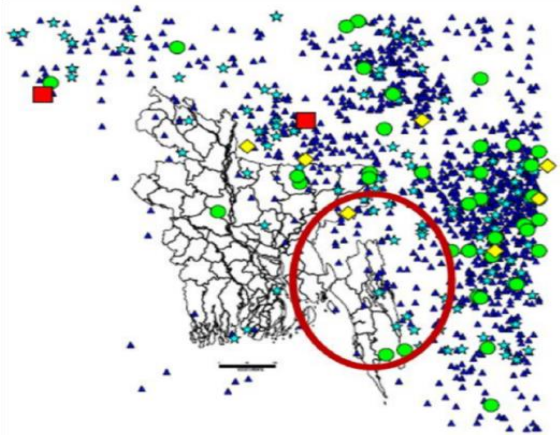

Fig. 2.4: Seismic zoning map for Bangladesh based on a return period of 2475years

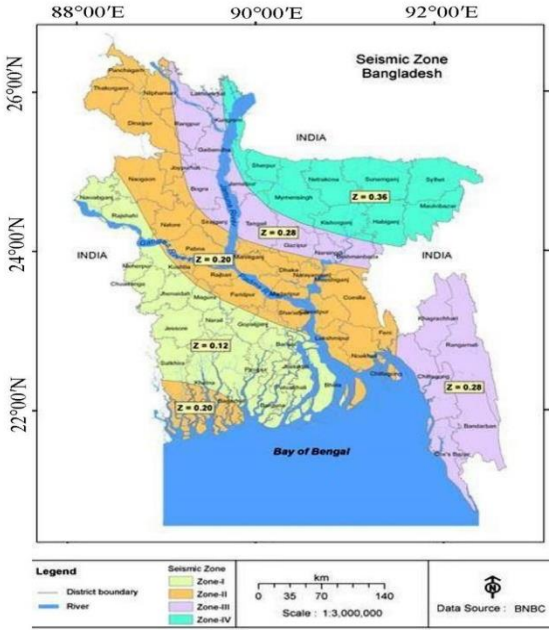

Fig. 2.5: Earthquake Zoning Map of Bangladesh, BNBC 2020

2.2.2 Seismicity in Chattogram Region

Chittagong has a long history of earthquakes. There are hundreds of evidences associated with the earthquakes that jolted Chittagong and its adjoining areas. In 1762, in the southern portion of Chittagong division, one of the greatest earthquakes in history struck Arakan. Although the magnitude was not documented at the time, it caused significant damage. The magnitude 8.6 Assam earthquake of 1950 was felt in the same area, causing severe shaking. If we look at the current situation, we can see that this region has undergone around 200 light and moderate earthquakes since 1996 (Karmakar, 2003). Many of the earthquake sources were near Myanmar's border region. The magnitude of the 1997 Jaintapur earthquake on the India-Bangladesh border was 5.6. It was eventually felt mainly with Chittagong and also within Rangpur, Sylhet together with Meghalaya on 21st November. A magnitude 5.7 earthquake on the India-Bangladesh border jolted these areas violently, and it was felt across the country. But it was Chittagong that wreaked the most havoc. On this occasion, a five-story RCC structure collapsed, killing 23 people. Another earthquake of magnitude 5.2 struck Moheshkhali Island in the Chittagong division on July 22,

1999. This quake was followed by a few aftershocks, causing significant damage and killing at least 6 people and injuring over 500 more. The concrete structures of cyclone shelters developed cracks, while mud dwellings suffered significant damage.

The most remarkable recent earthquake that triggered Chittagong city and the adjoining hill districts occurred on 27 July, 2003. The magnitude of this earthquake was 5.6 (surface-wave magnitude). Its epicenter was at Kalabunia village of Barkal Upazila of Rangamati district (Ansary and Sadek 2006; Karim 2003; Khan, 2003). Two people died and around three hundred people were injured during the earthquake. About 150 buildings including a school were damaged throughout the region, among them the Union Parishad building and the roof of a health complex collapsed. Chittagong city is relatively close to the Rangamati district. Many minor to major cracks developed in several buildings, including Public Library, Chittagong Jail and Polytechnic buildings. Cracks also developed in buildings of Cox's Bazar, Moheshkhali, Kutubdia and Sonadia Island. Many mild aftershocks of different magnitude were felt in Barkal and Rangamati. At the time of last 3 years approximately 7 light-size earthquakes took sites surrounding the 100-kilometre radius of Chittagong, which makes us aware of the future safety factors in this region.

Tables 2.3 for Chattogram City Area show the input parameters for these selected earthquake scenarios. Deterministic Calculation of scenario earthquake ground shaking chosen for the HAZUS hazard analysis. The Table 2.3 represents the earthquake scenario for Chattogram region (Khair et.al, 2014).

Table 2.3: Earthquake Scenario Parameters for Chattogram City Area

Case	Coordinate of Epicenter		Mw	Depth to top of fault (km)	Dip Angle	Fault type	Description
	Latitude	Longitude					
1	21.1	92.1	8.5	17.5	30°	Reverse	Plate Boundary Fault-1
2	23.8	91.1	8.0	3	20°	Reverse	Plate Boundary Fault-2
3	22.4	91.8	6.0	25	90°	Reverse	Mw 6.0 beneath the city

2.3 Ground motion

Earthquakes occur by the rupture of the bedrock beneath the earth's crust. This is linked to the release involving stored strain power from the fault location, which radiates out in all directions in the form of seismic waves that travels around through the body in addition to along the Earth's surface area. These seismic waves, which are primarily of two categories: body waves and surface waves, are caused by a tremble of the ground (Earth's surface) on which those structures are built. The acceleration, velocity, and displacement of the ground motion can all be measured. Seismographs are devices that measure these reduced displacements. The ground shakes violently in the region of big earthquake epicenters. Seismographs become saturated as a result of their design, which causes them to become useless at capturing ground displacement under large displacement shaking. Engineers, on the other hand, are interested in determining the ground vibration levels at which structures are destroyed and are familiar with the stresses involved (as a component of a building's design). As a result, the invention of equipment known as Accelerographs, which monitor the acceleration of an earthquake vibration as a function of time at the spot in which the sensor is situated, was motivated. Even in the closest cases of seismic faults, where the tremors are intense, these instruments successfully capture ground tremors.

2.3.1 Accelerograms

An accelerogram is a recording made with an accelerograph, which shows the fluctuation in ground acceleration over time at a specific location on the ground during an earthquake. The type of isolation in the bedrock, the geology along the path from the source to the surface of the earth, and the local soil all influence the nature of accelerograms. Accelerograms contain specific information about ground shaking, such as peak amplitude, strong shaking duration, and frequency response (Specifically, the frequencies when the earthquake carries significant Vibrating force). Three essential criteria that define the features of accelerated ground motion at a station are the type of eruption, geology along the travel route, and geotechnical layer beneath the building [Fig. 2.6].

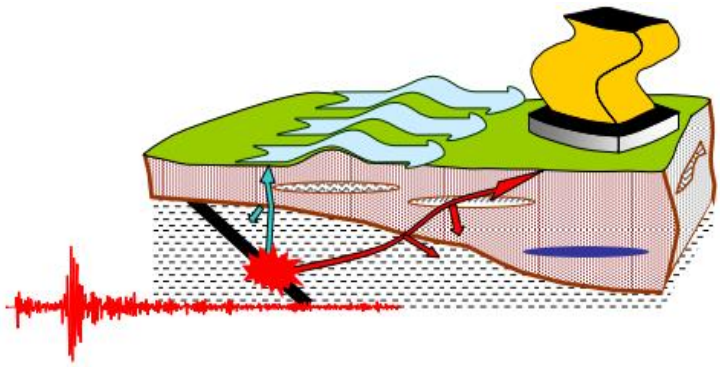

Fig. 2.6: During earthquakes, the ground shakes (Murty et.al, 2013)

The duration of an earthquake cannot make a difference in a building that is resilient during an entire earthquake. On the other hand, the duration of an earthquake makes a significant difference for another building that is damaged during an earthquake. Maximum ground acceleration, strong vibration duration, and frequency response all affect the building's inelastic conditions.

2.3.2 Acceleration Response Spectrum of a Ground Motion

Structures are typically designed using the greatest force created in the structure as a result of earthquake shaking. There are two methods to define force: (i) mass m time's acceleration a, which represents inertia force; (ii) stiffness k times displacement x, which represents elastic force, i.e.

$$F = ma \text{ or } F = kx.$$

Furthermore, the upper limit of such a response is effective in design, so a different natural period T and SDoF are built for the exact damping under the ground motion of the same earthquake. The acceleration response spectrum for 5% damp based on the El Centro 1940 earthquake is a response spectrum that correlates to the acceleration of the building. Time history of El Centro 1940 is shown in Fig. 2.7.

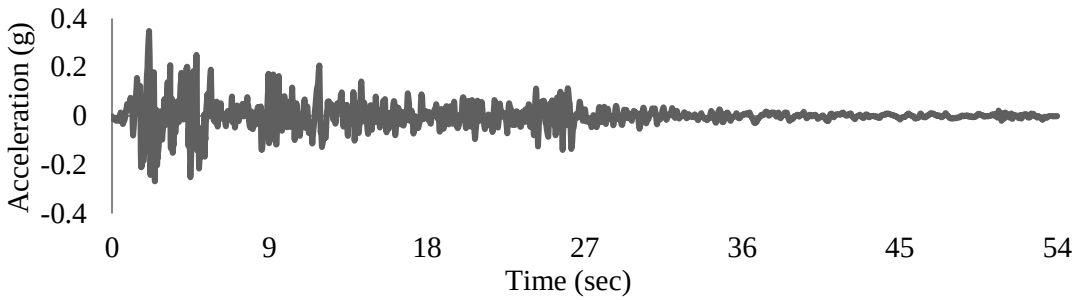

Fig. 2.7: Time history of El Centro 1940

It is easy to calculate the effective mass of a building during an earthquake, known as seismic mass (Gravity G is equal to the seismic weight divided by the acceleration), This is to analyze the overall strength compared to the real building. Acceleration response is the absolute maximum acceleration (or spectral acceleration) response of the spectra of structures with different basic translatable natural periods but with the same dampness and the same considered ground motion

The resultant force is known as the seismic design lateral load of the building or the seismic design base shear of the building, and seismic design regulations provide a design response spectrum for the design process. Maximum spectral acceleration of original El Centro 1940 ground motion is 0.91g. Matching of original acceleration response spectrum of El Centro 1940 as shown in Fig. 2.8

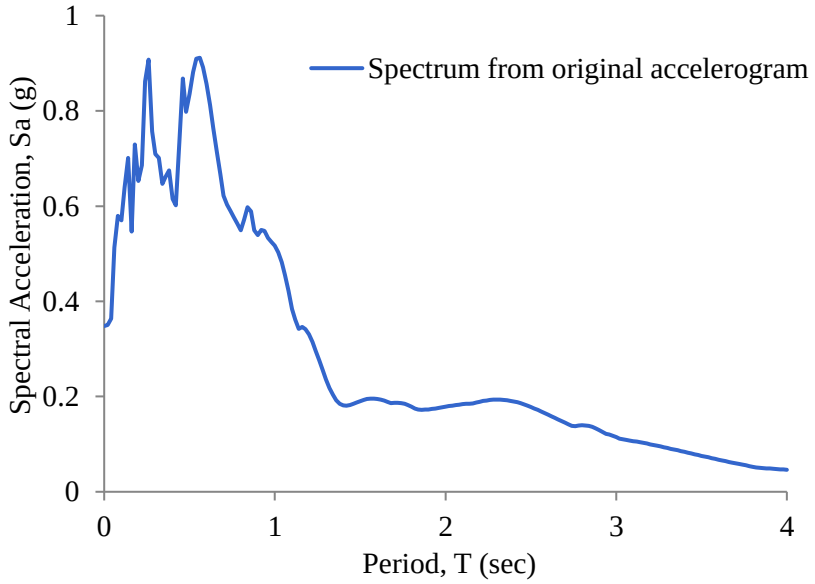

Fig. 2.8: Matching of original acceleration response spectrum of El Centro 1940

2.4 Configuration of the buildings

During an earthquake, a building's configuration can have a substantial impact on its overall performance. The ratio between the length (typically the longer dimension) and the width (typically the shorter dimension) of a rectangular shape is known as the aspect ratio. The aspect ratio has no units and is merely a number because it is defined as the ratio of two lengths. An object with a large aspect ratio appears slender when compared to one with a small aspect ratio. The stresses in a floor serving as a horizontal distribution diaphragm in a transverse direction grow as the length of a building grows. As a result, building length proportions must be carefully considered (Ahmed et.al, 2019). Floors and floor systems serve as horizontal diaphragms in the structure of a building. These gather and transmit inertia forces to lateral resistant systems' vertical components. They also make sure that under gravity and seismic loads, vertical components work together. Simple and complicated buildings are the most common types of structures. Stagnation and central opening buildings, on the other hand, place geometric barriers on inertia forces requiring forces to curve prior to reaching the bottom. The smooth and direct conduction of inertial forces created by people of structural and non-structural elements is enabled by the plan and equal distribution of structural elements at heights (Guleria, 2014).

The architect chooses the configuration of a structure and directly affects the structural system of the bearing components in a building (building shape and dimensions). Non-bearing walls and apertures in horizontal structural components or exterior facade covering elements, as well as the kind, location, and dimensions of major structural members (columns, walls, floors, and staircases), all influence how a structure behaves during earthquakes. Buildings seismic performance is highly dependent on their configuration. Overall geometry, structural systems, and load paths are all essential factors that influence building seismic configuration. This section covers a variety of topics relating to seismic configuration. Plan Aspect Ratio 1, it is not good to keep the structure with such huge estimates, having buildings with big plan aspect ratios is not good. Inertia force is absorbed in the building during earthquake shaking, mainly on the ground floor where the mass is massive. The action of rigid diaphragms occurs when floor slabs help to transfer inertia forces to different lateral load resistance systems in proportion to their strength. When floor

slabs deform in their plane, the inertia force, on the other hand, is distributed according to the tributary area. As a result, members with lower capacity are overloaded, resulting in unnecessary structural damage (Drazic and Vatin, 2016).

2.5 Structural Analysis

Analyze a structural system to detect distortions and forces caused by applied loads or ground tensions at the required design stage of earthquake-resistant construction. The following are requirements for a structural analysis process:

a) Modeling of a structure.

b) A representation of ground motion caused by the effect of an earthquake or ground motion.

c) The management equations are constructed and solved using an analytic method.

Depending on the design process analysis goals, various methods can be applied, from simple plastics assessment to a dynamic analysis of complex non-linear, full-structured models.

The concept of a linear or nonlinear connection among forces and displacements is critical in structural analysis. For decades, structural design has relied on static and dynamic load linear analysis. Nonlinear behavior must be represented in the evolving performance-based recommendations. Nonlinear behavior might come from two different places. The first is a nonlinear force-deformation relationship caused by material characteristics such as flexible yield, stiffness, energy loss, or fragility fractures. The inclusion of substantial displacement in the case of consistency and balanced relationships causes the second type of nonlinear behavior. Axial loads and ground motion delegation at the building's location are usually included in an earthquake analysis. A dynamic analysis is used in many design methods, including presenting the site's expected ground motion response spectrum (Chopra, 1995). The structural analysis methods utilized in earthquake-resistant design are tabulated in Table 2.4 (Bozorgnia and Bertero, 2004). Almost every structural analysis of earthquake-resistant design is carried out using software that uses one or more of the approaches provided in this section. The forces and malformations produced from such an investigation are generally displayed in modern software utilizing graphical components. The Engineer must perform a shred of verifiable evidence before

employing any new structural assessment equipment to ensure accurate findings (Bozorgnia and Bertero, 2004).

When a structure is pressed against the seismic pressure that identifies a hazard on a building site, the primary goal is to evaluate the force and distortion globally and locally:

Table 2.4: Structural analysis procedures (Bozorgnia and Bertero, 2004)

Analysis procedure	Analysis method
Linear static procedure (LSP)	Equivalent linear static analysis
Linear dynamic procedure (LDP)	Response spectrum analysis (RSA)
Nonlinear static procedure (NSP)	Pushover analysis (POA)
Nonlinear dynamic procedure (NDP)	Time history analysis (THA)

2.5.1 Nonlinear Time-History Analysis

The most appropriate and comprehensive analysis method for assessing the structure's non-linear earthquake response is the seismic analysis of nonlinear-time history. Another statement is that today's state-of-the-art methodology for forecasting building reaction to earthquake ground motion is nonlinear dynamic earthquake analysis (Sam, 2008).

Direct reconciliation of movement conditions is needed for time history investigation, which can be accomplished utilizing either the mathematically dissipative-combination calculation (Hilber et.al, 1977) Or the Newmark scheme, better known as the later special case (Newmark, 1959). Because of the nonlinearity of the investigation conspire; a gradual iterative arrangement strategy should be utilized: this implies that heaps are applied in predefined increases and equilibrated utilizing an iterative plan where the interior powers relating to every dislodging augmentation are registered until one or the other combination or the greatest number of emphases is reached.

The selecting of time step size is an important part of nonlinear time history analysis. The accuracy, stability, and rate of convergence of the solution algorithm are all affected by the size of the time step. Because nonlinear time history analysis makes fewer assumptions than nonlinear static analysis, it has fewer constraints. The intricacies of the analytic model and how it catches the primary behavioral impacts, on the other hand, define the correctness of the results. Maximum structural element deflections are frequently adjusted to levels where degradation is managed, and nonlinear dynamic analysis methods are dependable by selection criteria. Because of the inherent diversity in the reaction of buildings to seismic vibrations, should be taken numerous simplification assumptions utilized in research, the results of any linear or nonlinear study for seismic behavior with caution. In theory, nonlinear dynamic analyses should provide more realistic answers than previous approaches, but their accuracy is dependent on modeling concepts and variables. In time history analysis, the time to load history is separated into several small receive instant. In contrast, in the static analysis, the axial load is divided into various little pressure installments. During a limited period or force increment, the building's response is supposed to be completely elastic. The incremental stiffness is changed for the following time or load increment as nonlinear behavior occurs. As a result, the reaction of a sequence of stability analyses with variable stiffness computes the reaction of the dynamic function (Anderson, 2000).

Rigidity, dampening, and load can all be affected by displacement, velocity, and time in nonlinear analysis. This requires an iterative arrangement of the motion conditions. The time-history analysis is used to determine a structure's dynamic behavior to random loading. The equations to be solved are dynamic system formulas:

$$Ku(t) + C\dot{u}(t) + M\ddot{u}(t) = r(t) \qquad (1)$$

Where,

K is the stiffness matrix;

C is the damping matrix;

M is the diagonal mass matrix;

u(t) is displacements of structures;

$\dot{u}(t)$ is velocities of structures;

$\ddot{u}$(t) is accelerations of structures;

r(t) is the applied load.

These are two alternative solutions, each by means of advantages and disadvantages. In perfect situations, two options should produce identical results for a given problem (Teferra, 2018). Dynamic equation can be solved by following methods,

a) Nonlinear modal time-history analysis

The method is highly efficient, especially for structural systems with a small number of preset nonlinear elements that are essentially linear elastic. However, cannot be considered the limitations of nonlinear components until appropriate modes are available. The simplest way to do this is to use a significant proportion of Ritz variables. The FNA solutions nonlinearity is restricted to the Link/Support parts. The complete stiffness matrix, K, and the mass matrix, M, are used in modal analysis. It is strongly advised that the Ritz variables method be used for the modal analysis.

b) Nonlinear direct-integration time-history analysis

Although modal superposition is typically more efficient and accurate, direct integration does have the accompanying benefits:

- It is possible to consider full damping that couples the modes.
- Direct integration may be more efficient in solving influence and wave propagation issues that may ignite a high proportion of modes.
- In a nonlinear direct integration analysis, every sort of nonlinearity can be considered.

Always conduct direct-integration analyses by reducing time-step values until the gradation shape is little enough not to affect the results. The following factors are taken into account when performing nonlinear direct-integration time-history analysis: Material non-linearity and geometric non-linearity are two types of non-linearity.

2.5.2 Material Non-Linearity

In seismic engineering, the behavior of structures to deformation in their inhospitable regions is significant when significant earthquakes occur. This subject is the focus of

this discussion. The deformation of a member in a non-linear inelastic analysis does not have to be proportional to the internal force. For increasing amounts of internal force, there occurs plastic deformation and energy absorption in a member. Material nonlinearity is the term for this type of nonlinear behavior.

A nonlinear direct-joining time-application investigation will consider all material nonlinearity defined in the model. It is firmly urged that you utilize similar mathematical nonlinearity boundaries for the current case as you utilized for the past model if you are proceeding from a past nonlinear analysis. During an earthquake, structures experience oscillatory motion and deformation reversal. Regarding concrete elements, component ensembles, and lowered structural models, and little comprehensive buildings, cyclic tests simulating this condition have been done. The experimental results demonstrate that a structure's cyclic force-deformation behavior is influenced by both the structural material and the structural system. During cycling aberrations, the force deformation charts show velocity profiles due to energy dissipation. The structural system and materials determine the geometry of these loops (Chopra, 1995).

When properly supported by approximations and models, nonlinear time-history analyses are a very effective tool. The analysis is inherently difficult and time-consuming (Pecker, 2007). When simulating rigid parts of structures, many engineers utilize big values for element properties. For static and dynamic analytic problems, this can result in significant mistakes in the results. The practice of employing unreasonably big numbers in nonlinear analysis can cause slow convergence and extended computer execution times (Wilson, 2002).

2.5.3 Geometric Non-Linearity

Vertical forces acting on the buildings distorted configuration cause geometric nonlinear effects, causing internal factors in elements and junctions to grow. The two forms of geometric nonlinear effects are P-D effects, which are related to aberrations across the elements and usually controlled to the joint chord, and P-D effects, which are evaluated among element endpoints and frequently linked in story drifts structures. P-D effects are significantly more of a problem in buildings susceptible to

earthquakes than P-D effects, provided particular elements comply with the slenderness restrictions of subject matter in severe earthquake areas. In most nonlinear earthquake studies, P-D effects are not required to be modeled. P-D effects, then again, should be demonstrated since they can result in longitudinal resistance decrease over time. The internal force and moment demands are magnified by large lateral deflections (D), resulting in a reduction in effective lateral stiffness. As internal factors increase, the amount of power designed to protect vertical forces decreases, resulting in a drop in effective lateral power (pecker, 2007).

- P-delta effects
- Large displacement effects

2.5.4 Stress Strain Curve

Nonlinearity increases with increase in stress post peak response is not really material response rather it is structural response under the same stress. Stronger concrete exhibits lower strain Post peak response is more brittle for stronger concrete. Confined concrete have higher strain than unconfined concrete. Post peak response is more brittle for stronger concrete. The expression describes the connection among compression load (σ_c) and shortens strain (εc) for simple un-axial forcing.

$$\frac{\sigma c}{fcm} = \frac{k\eta - \eta 2}{1+(k-2)\eta} \qquad (2)$$

Where,

$\eta = \varepsilon c/\varepsilon c_1$

εc_1 is the strain at peak stress

$K = 1.05E_{cm}\,\varepsilon c_1/f_{cm}$ $\qquad E_{cm} = 22x\,(f_{cm}/10)^{0.3}$

$\varepsilon c_1\,(\%\,o) = 0.7 f_{cm}{}^{0.31} \leq 2.8$ $\quad f_{cm} = f_{ck} + 8Mpa$

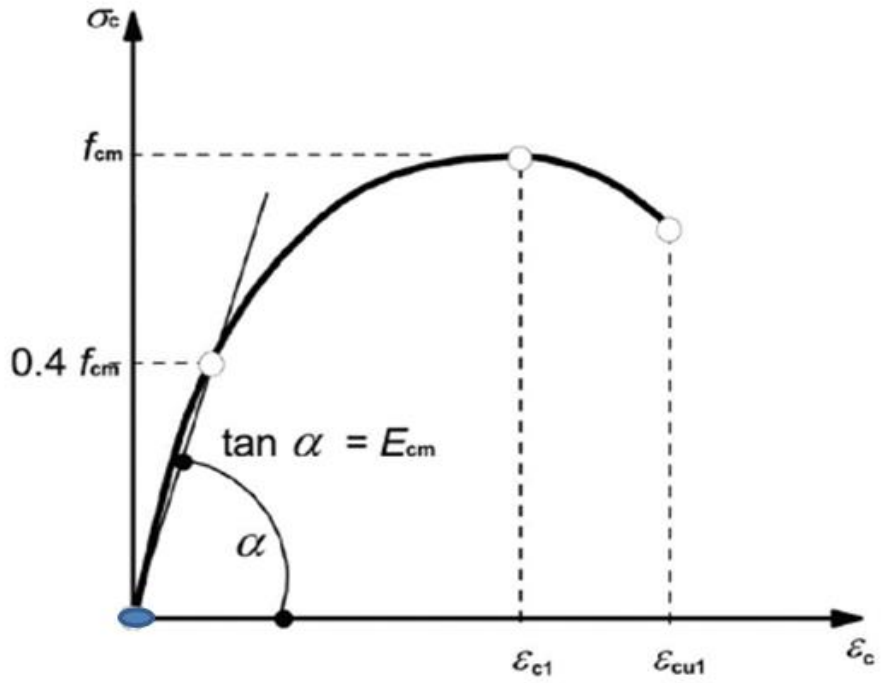

Fig. 2.9: Stress-strain relation of structural analysis (Teferra, 2018)

2.6 Response Spectrum

In comparison to the Fourier spectrum of horizontal components, a response spectrum is a conceptual spectrum. It's a collection of one-degree-of-freedom (dof) subsystems' required time period reactions at different natural harmonics. Critical data like phase shift is missing from the presented response spectrum. Furthermore, the given response spectrum can be used to create thousands of artificial time histories.

- For the horizontal elements of a seismic event, the elastic reaction spectrum Cs is determined by the following (BNBC, 2020).

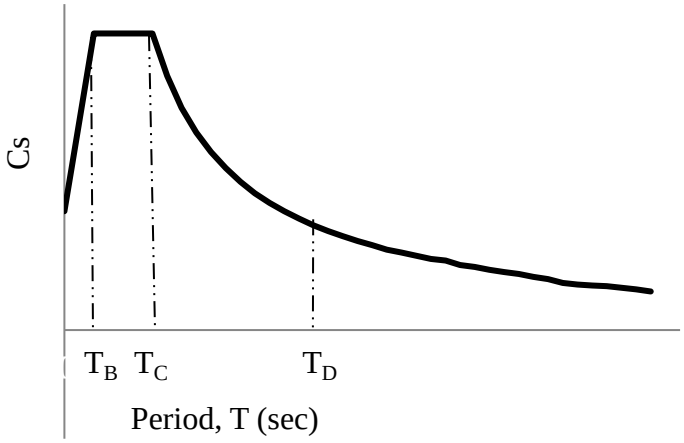

Fig. 2.10: Typical shape of the elastic reaction spectrum coefficient Cs (BNBC, 2020)

- The ground variety affects the values of the periods T_B, T_C and T_D as well as the soil factor S that describes the form of the elastic reaction spectrum (BNBC, 2020).
- It is advised that the type 1 spectrum be used if the earthquakes that add the most to the seismic hazard assessed for the area for the purpose of probability hazard analysis have a surface-wave magnitude. Otherwise use type 2 (BNBC, 2020).

$$0 \leq T \leq T_B : C_s = S[1 + \frac{T}{T_B}(2.5\,\eta - 1)] \quad (3)$$

$$T_B \leq T \leq T_c : C_s = 2.5 S\eta \quad (4)$$

$$T_c \leq T \leq T_D : C_S = 2.5\, S\eta\, [\frac{T_c}{T}] \quad (5)$$

$$T_D \leq T \leq 4sec : C_s = 2.5\, S\eta\, [\frac{Tc\ T_D}{T_2}] \quad (6)$$

Where,

Cs is the elastic reaction spectrum;

T_B is the time of the fixed spectral acceleration chapter's upper limit;

T_C is the highest limit of the time of the spectrum's fixed displacement reaction range;

T_D is the value defining the start of the fixed displacement reaction range of the spectrum;

S is the soil factor;

η =1 for 5% thick damping.

2.7 Related Research

Alashker et.al (2015) studied the seismic performance of three buildings with three distinct layouts with the same area and height was evaluated using nonlinear pushover analysis. This method determines the building's base shear capacity and the performance level of each component under various levels of seismic activity. In terms of displacement, base shear, and plastic hinge pattern, the effects of various plans on seismic response of structures were demonstrated.

Ahmed et.al (2019) discussed using the parameters for the design as per the BNBC-1993 for the seismic zone-2, six building models with G+ 10 storey's intermediate moments resisting frame buildings but different horizontal aspect ratios such as 1, 2, 4, 6, 8, and 10 have also been regarded and their effects on the conduct of the RCC buildings are expressed. Its results of the seismic responses of structures are summarized using software in the form of graphs and tables. The outputs of the analysis were investigated in order to determine the best horizontal aspect ratio for a building subjected to seismic loadings.

Ahirwal et.al (2019) studied CSI SAP200 software to model an existing structure with irregular diaphragms and compare seismic performance to a building without membrane discontinuities. A static and dynamic linear analysis was performed. The modal time period, base shear, storey drift, and joint displacement of two buildings were compared.

Drazic and Vatin (2016) studied building configuration is determined at the early stages of design when it is possible to assess a structure's regularity and see the impact of a proposed design solution on the structural condition (structure analysis, dimensioning, and modeling). It entails the design of regular buildings (configuration) where the most cost-effective design, construction, and highest predictability of the necessary seismic performances are required.

Hujare and Tande (2017) discussed nonlinear pushover analysis to assess the seismic performance of four distinct building layouts with the same area and height. The impacts of plan aspect ratio on building seismic response are presented in terms of displacement and base shear. Also, acquired is the best construction configuration for the highest base shear at the performance point.

Modi et.al (2016) evaluated reinforced concrete structure pushover analysis. In this experiment, a G+4 RC construction was pushed in the X and Y directions for various aspect ratios. ETABS was used for the analysis. According to the performance point, get from the analysis, everyone gets to know whether or not the construct will perform well and also not during seismic activity. For varied aspect ratios, the graph of the pushover curve was presented in terms of base shear – roof displacement. In addition, for various aspect ratios, the number of hinges generated and the maximum story drift are studied in both the X and Y directions.

Raheem et.al (2018) studied structural seismic response demand for the L-shaped building class by assessing the plan configuration irregularity of re-entrant corners and the impacts of lateral–torsion coupling on observed seismic behavior demands. Story drift, inter-story drift, story shear force, overturning moment, bending moment at the base and across building height, and torsional irregularity ratio are among the responses measured. As reference models, a three-dimensional finite element models for nine-story symmetrical buildings was built. In addition, six L-shaped building models are created using the reference building model's design as a starting point. The findings show that physical models with significant irregularity are more unstable than conventional buildings due to stress concentration and horizontal torsional couplings performance.

Vimala and Kumar (2015) evaluated the impact of aspect ratio on total damage structures due to seismic loads discussed in this work. A numerical investigation is carried out in this research for three benchmark structures with aspect ratios of 3, 1, and 0.3 to determine failure patterns in nonlinear states. To understand the capacity of the structure, a nonlinear static pushover analysis is done, and expended energy based on thorough investigation is employed to calculate the damage. The damage, displacement, and plastic hinge pattern of the results are compared.

2.8 Synopsis

Firstly in this chapter, Seismicity in Bangladesh region and seismicity in Chattogram region are discussed. Building earthquake response is influenced by ground shaking characteristics as well as building attributes. The acceleration and displacement of the ground motion can be measured. Configuration is critical to excellent seismic performance of structures. Overall geometry, structural systems, and load paths are all essential factors that influence building seismic configuration. Several issues related to seismic configuration are mentioned in this section. The methodologies for structural analysis utilized in earthquake-resistant design are discussed, as well as nonlinear time history analysis.

Chapter 3

METHODOLOGY

3.1 General

In this study, effects of plan aspect ratio on seismic response of RC buildings have been evaluated using nonlinear time history analysis as per BNBC Guideline. The methodology has been described as follows.

3.2 Geometric Details of Building Models

Three different six storied buildings are selected for this study having same plan area but different plan aspect ratios. The selected plan aspect ratios are 1, 1.5 and 2. All buildings are modelled using nonlinear seismic analysis software SeismoStruct and Etabs. On the basis of difference in aspect ratios, three plan areas are chosen for three different six storied buildings as shown in Fig. 3.1. The plan areas in Figs. 3.1(a), 3.1(b), 3.1(c) are representing building models with plan aspect ratios of 1, 1.5 and 2 respectively. For Model 1 (AR=1), the structure is 20 m in X-direction and 20 m in Y-direction. For Model 2 (AR=1.5), the structure is 25 m in X-direction and 16 m in Y-direction. For Model 3 (AR=2), the structure is 28 m in X-direction and 14 m in Y-direction. Model 1 consists of uniform span of 4 m in both x and y direction while model 3 consists of uniform span of 3.5 m in both x and y direction [Fig. 3.1]. On the other hand, model 2 consists of uniform span of 5 m in x direction but 4 m in y direction [Fig. 3.1]. Support conditions are considered to be fixed neglecting soil-structure interaction. Story heights are taken as 3m. Material properties considered for models are shown in Table 3.1.

Table 3.1: Material properties

Compressive Strength of Concrete (For Column)	24 MPa
Compressive Strength of Concrete (For Beam and Slab)	21 MPa
Steel Grade (Yield Strength)	420 MPa

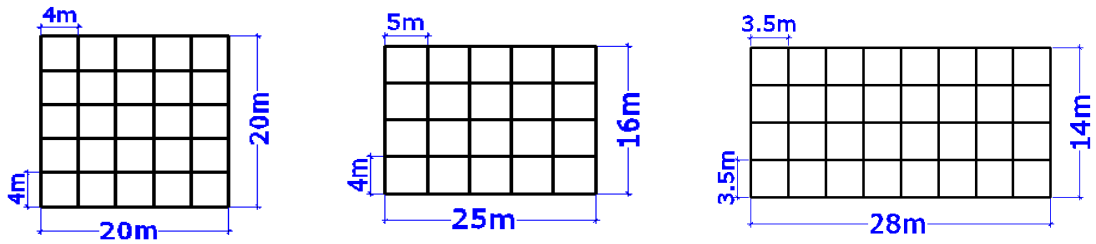

(a) (b) (c)

Fig. 3.1: Plan of building models: (a) Model 1: AR = 1 (b) Model 2: AR = 1.5 (c) Model 3: AR = 2

3.3 Equivalent Linear Static Analysis for Size Determination

In this study, the analysis of three different six storey Building of different plan aspect ratios is carried out by equivalent linear static method to estimate the size of structural components. The Analysis is carried out through ETABS software as it is more user friendly and versatile program. So, ETABS software has been used to check the size of beams and columns. The details of the seismic and other various parameters are mentioned in the Tables below.

3.3.1 Details of Loading Conditions

Details of loading condition have been determined in accordance with BNBC (2020). The loading conditions considered in the study are listed in Table 3.2.

Table 3.2: Details of loading conditions

Load type	Intensity of load
Live load: Ordinary roof	1 KN/m^2
Live load: Floors	2 KN/m^2
Floor finish	0.862 KN/m^2
Beam wall load	7 KN/m

3.3.2 Seismic Parameters

The different seismic parameters are taken following the BNBC (2020) guidelines. The detailed descriptions about seismic parameter are given in the Table 3.3.

Table 3.3: Seismic parameters

Seismic zone	III
Zone factor	0.28
Importance factor	1
Occupancy category (For Residential)	II
Response reduction factor	8
Site Class	SC
Seismic Design Category	D

3.3.3 Size Determination of Structural Components

The sizes of beams and columns are finally checked for the considered loading conditions using equivalent linear static analysis. Selected dimensions of structural components are shown in Table 3.4.

Table 3.4: Selected dimensions of structural components

Story height	3 m
Size of columns	400 mm × 400 mm
Size of beams	400 mm × 300 mm
Slab thickness	125 mm
Design code	ACI 318-99

3.4 Time History Analysis (THA) of the Buildings

In general, Time history analysis gives a nonlinear assessment of structural reaction during impact loading which may fluctuate as indicated by the specified time function. Non-linear dynamic time history analysis is usually considered the most accurate approach of assessing demand. But the correctness of the analysis mostly depends on the selecting of the ground motion accelerations which might affect a building during its service life. In this regard, selected ground motion should be matched with the design response spectrum of specific seismic zone and soil class over which the building will be constructed.

3.4.1 Analytical Model

The buildings are analytically modeled as 3-dimensional beam column rigid frame system as shown in Fig. 3.2 and Fig. 3.3. The entire modeling is performed in nonlinear seismic analysis software SeismoStruct and ETABS.

3.4.1.1 Modeling in SeismoStruct

Beams and columns are modeled with original geometric dimension as inelastic force-based frame elements while in-plane rigidity of the slab is simulated using rigid diaphragm action. All beams and columns are discretized with 150 section fibres with 5 integration sections. Nodes are necessary to express the geometry with the structure and element connectivity module to be able to add the structural elements (columns and beams). Constraining conditions of the structure are defined by means of nodal constraints type Rigid Diaphragms. Restrain all are selected at the base of the structural nodes. The tributary loads over slab are calculated and distributed over adjacent beams as uniformly distributed element loads. The ground motion accelerations are applied at the base of all columns in single direction in a model. The selection of ground motion accelerations are discussed in the next section. The bases of the columns are assumed to be fixed neglecting the foundation movement effect.

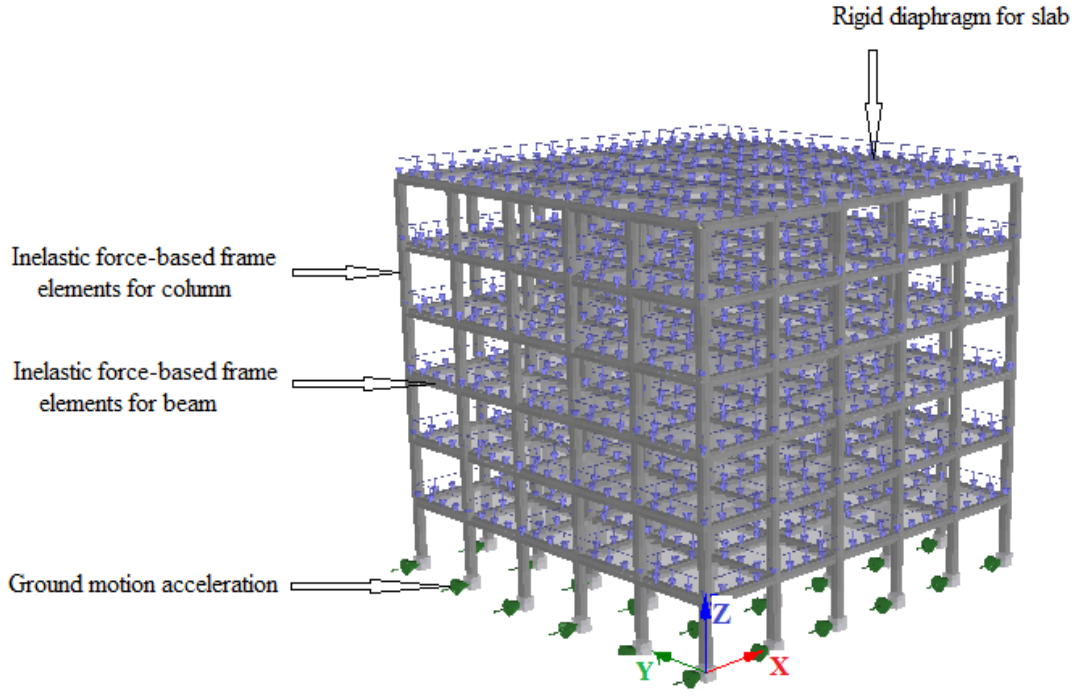

(a)

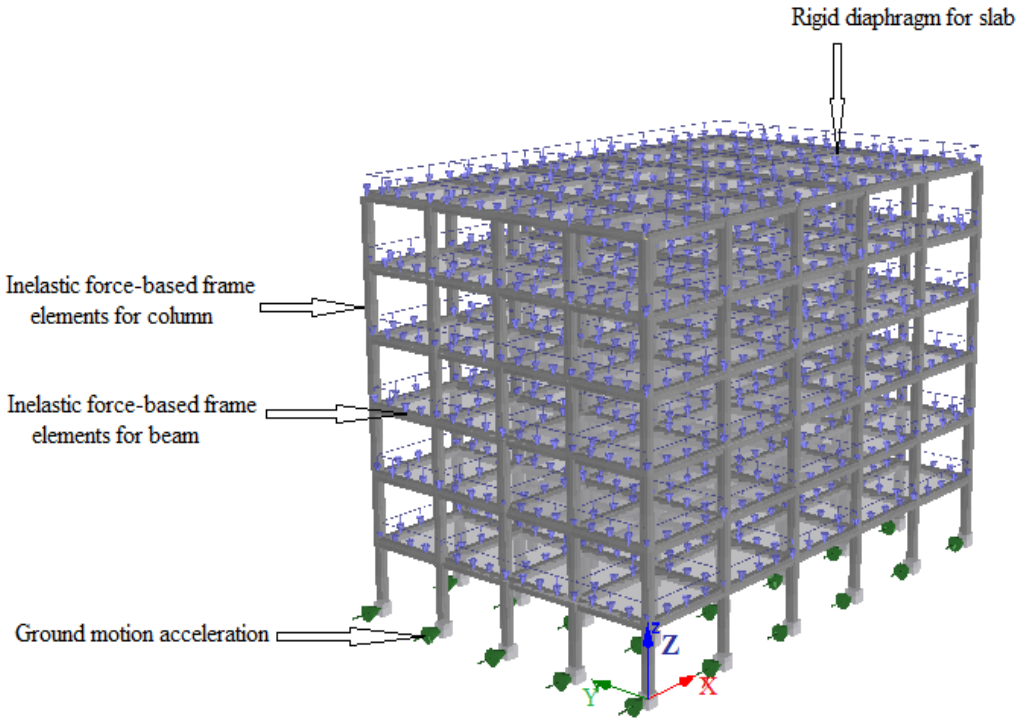

(b)

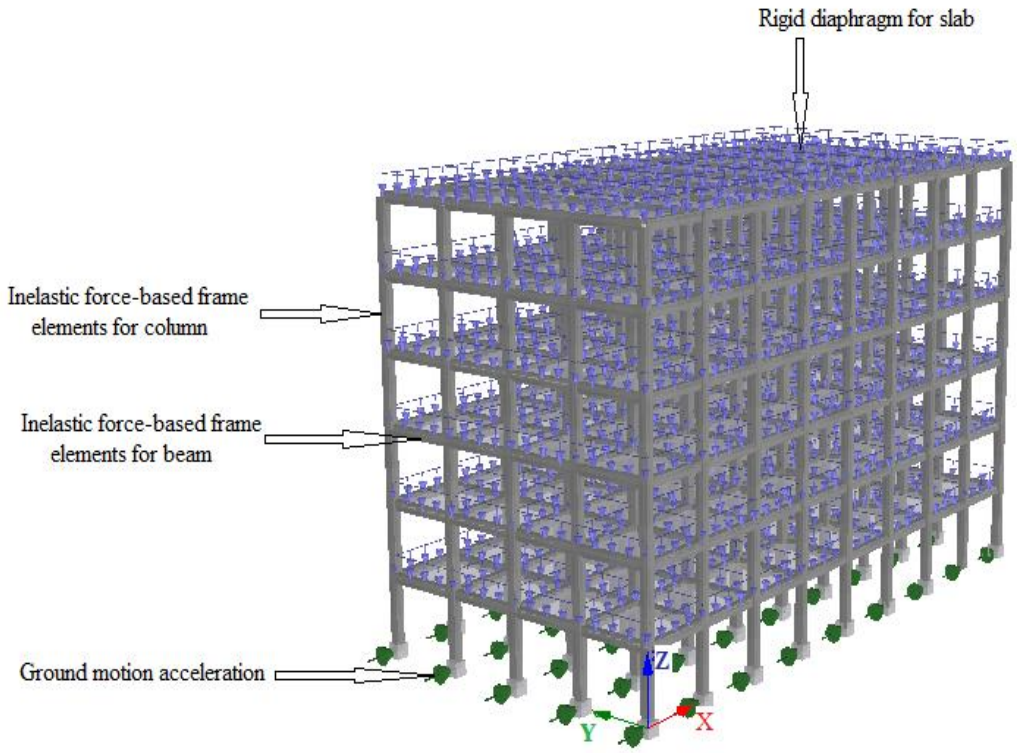

(c)

Fig. 3.2: Modeling in SeismoStruct: (a) Model 1 (b) Model 2 (c) Model 3

3.4.1.2 Modeling in ETABS

The finite element analysis-FEM based software ETABS is used to create 3D model and run all analyses. The software is able to predict the geometric nonlinear behavior of space frames under dynamic loadings, taking into account both geometric nonlinearity and material inelasticity. For structural analysis moment of inertia is taken as - 70% of gross moment of inertia of column and 35% of gross moment of inertia of beam. The bases of the columns are assumed to be fixed neglecting the foundation movement effect.

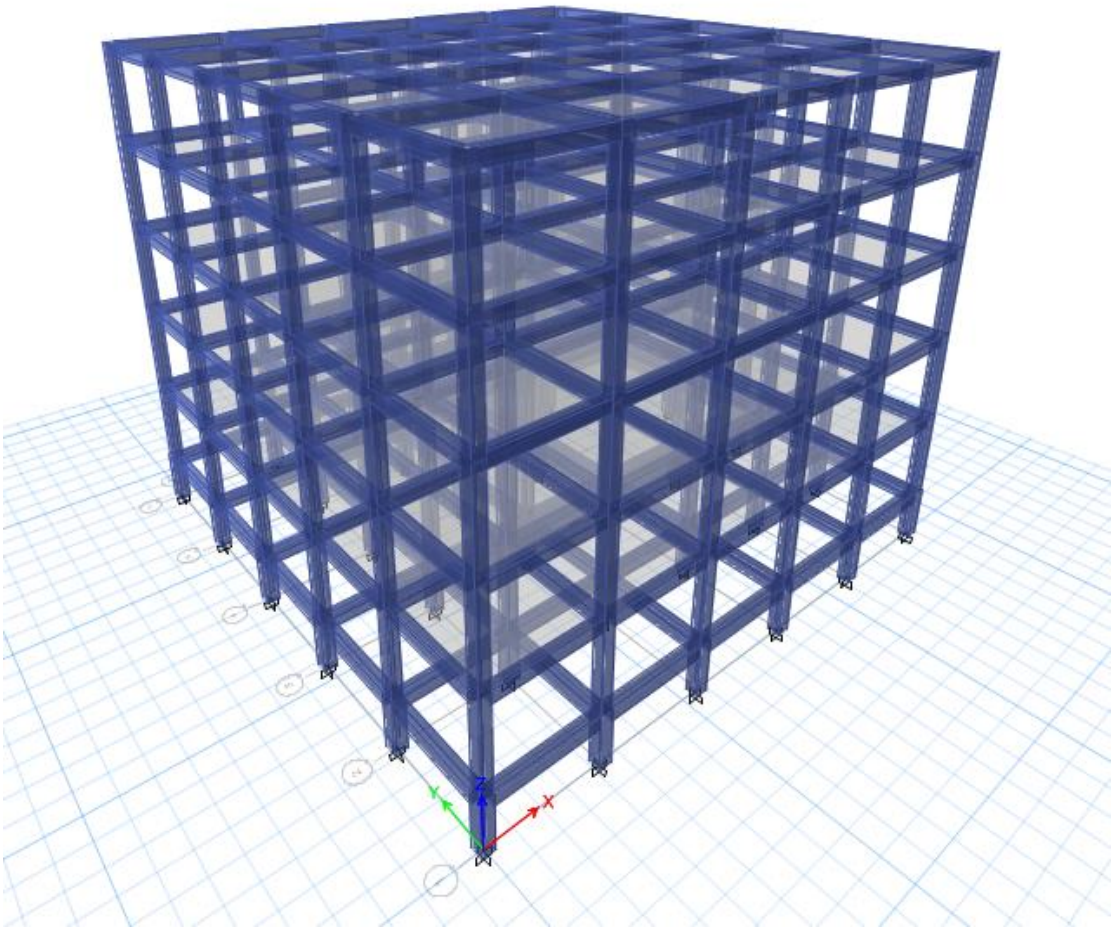

(a)

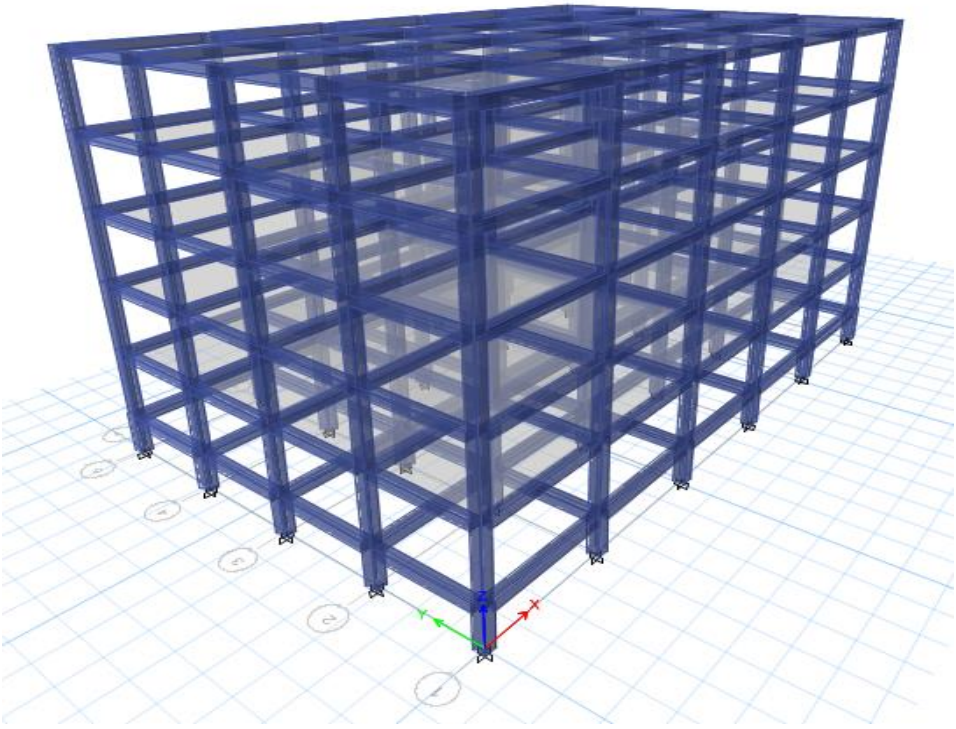

(b)

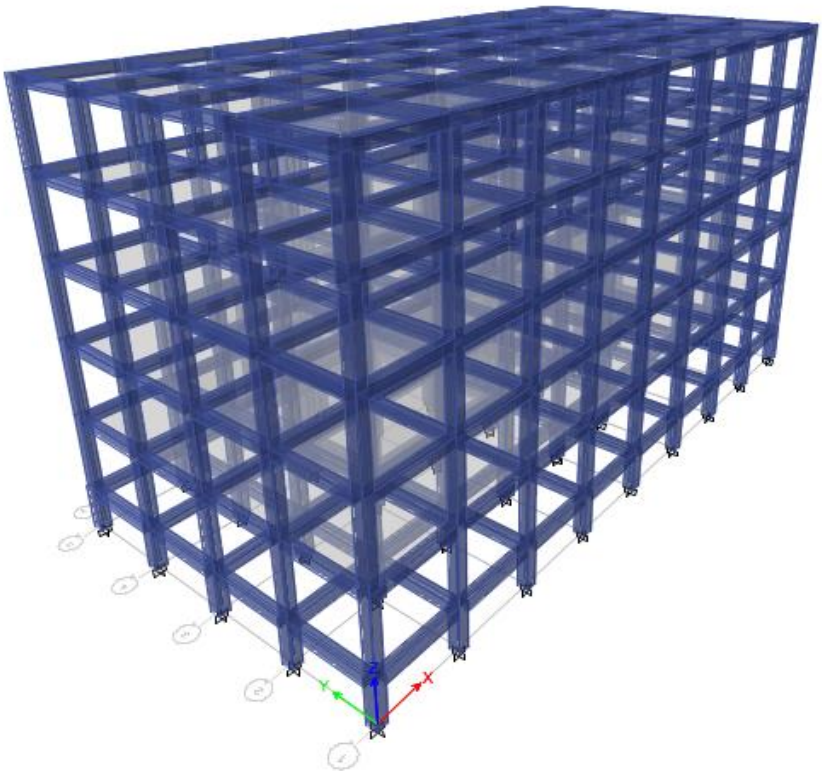

(c)

Fig. 3.3: Modeling in ETABS: (a) Model 1 (b) Model 2 (c) Model 3

3.4.2 Selected Ground Motions for THA

The seismic resistance design guidelines recommend choosing at least three or seven ground motion records that are suitable with the design spectrum for time-history analysis. Not less than three ground motion sets (consisting of two horizontal elements and one vertical element, if required) need to be considered.

3.4.2.1 El Centro 1940

Ground motion accelerations of El Centro 1940 earthquake with peak ground accelerations (PGA) of 0.35g (g = 9.81 m/s^2), recorded at the Imperial Valley site at a distance of 12.2 kilometers from the hypocenter, are selected for the time history analysis. El Centro earthquake records are acquired from COSMOS Virtual Data Center (VDC) database [Fig. 3.4].

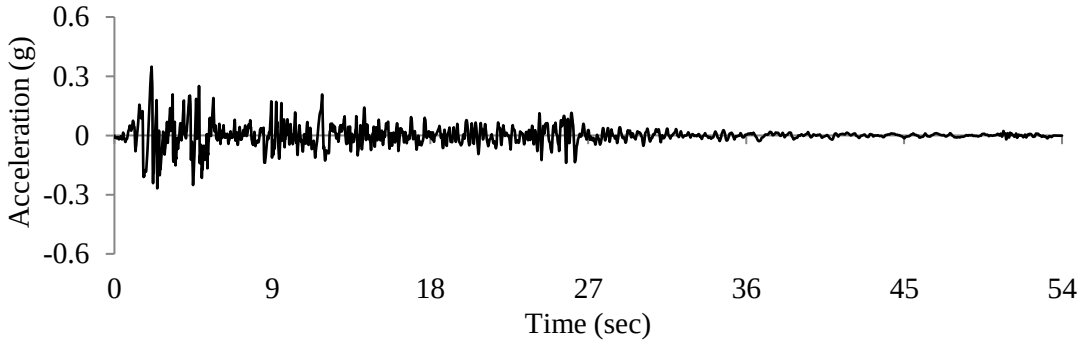

Fig. 3.4: Seismic ground motion accelerations of El Centro 1940

3.4.2.2 Kobe 1995

Ground motion accelerations of Kobe 1995 earthquake with peak ground accelerations (PGA) of -0.51g (g = 9.81 m/s^2), recorded at Nishi-Akashi site at a distance of 19.9 kilometers from the hypocenter, are selected for the time history analysis. Kobe earthquake records are acquired from COSMOS Virtual Data Center (VDC) database [Fig. 3.5].

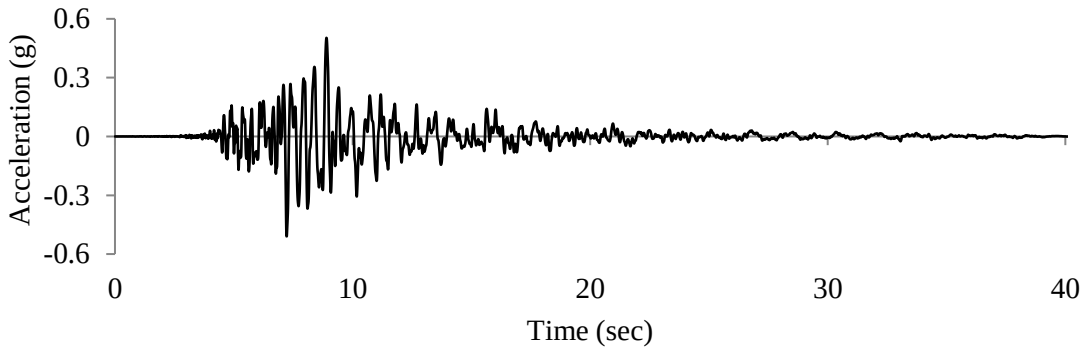

Fig. 3.5: Seismic ground motion accelerations of Kobe 1995

3.4.2.3 Tabas 1978

Ground motion accelerations of Tabas 1978 earthquake with peak ground accelerations (PGA) of 0.37g (g = 9.81 m/s^2), recorded at Dayhook site at a distance of 18 kilometers from the hypocenter, are selected for the time history analysis. Tabas earthquake records are acquired from COSMOS Virtual Data Center (VDC) database [Fig. 3.6].

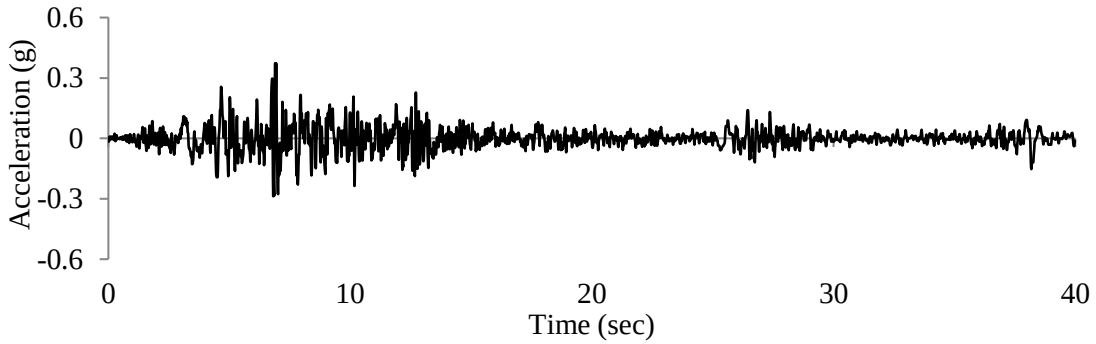

Fig. 3.6: Seismic ground motion accelerations of Tabas 1978

3.4.3 Design Response Spectrum

The study buildings are assumed to be constructed in a moderate seismic zone with zone coefficient, Z= 0.28 representing a probable PGA of 0.28g for a seismic event with a return period of 2475 years representing maximum considered earthquake (MCE). It is also assumed that shear wave velocity of soils beneath the building site will be in the range of 180-360 m/s representing deep deposits of dense or medium dense sand, gravel or stiff clay classified as soil type SC with soil factor, S=1.15 according to BNBC. For inelastic (nonlinear) analysis, real design acceleration spectrum is used, where, response modification factor, R=1 and structural importance factor, I=1. The actual design acceleration response spectrum is the genuine depiction

of the expected ground motion i.e. design basis earthquake (DBE) with return period of 475 years including local soil effects and corresponding to PGA value of $\frac{2}{3}$Zg or 0.19g for this case. Real design acceleration response spectrum for PGA of 0.28g (MCE) or design acceleration response spectrum for PGA of 0.19g (DBE) for site class SC is shown in Fig. 3.7. Maximum spectral acceleration of design response spectrum is 0.55g within 0.2 to 0.6 sec.

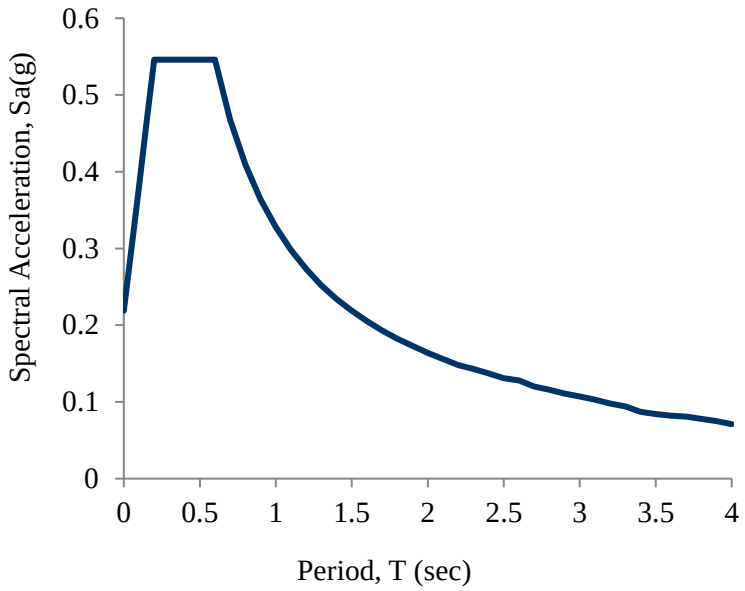

Fig. 3.7: Design acceleration response spectrum for PGA of 0.19g for site class SC

3.4.4 Ground Motion Matching

The magnitude, fault distance, and source mechanisms of the chosen time histories should be similar to the design ground motion at the site. Selected time histories must be matched with design response spectra of the site using Seismomatch software.

3.4.4.1 Matching with El Centro 1940

Selected ground motion El Centro acceleration time histories are matched with design response spectrum for PGA of 0.19g (DBE) for the site class SC using SeismoMatch software. SeismoMatch is an earthquake software program that uses the wavelets algorithm to adjust the ground motion accelerograms of an earthquake to match a specific target response spectrum. Matching of response spectrum of original El Centro 1940 ground motion acceleration with design acceleration response spectrum of selected site are shown in Fig. 3.8. Maximum spectral acceleration of original El

Centro 1940 ground motion is 0.91g which is reduced to 0.56g after matching with design response spectrum for PGA of 0.19g regarding maximum and mean misfit.

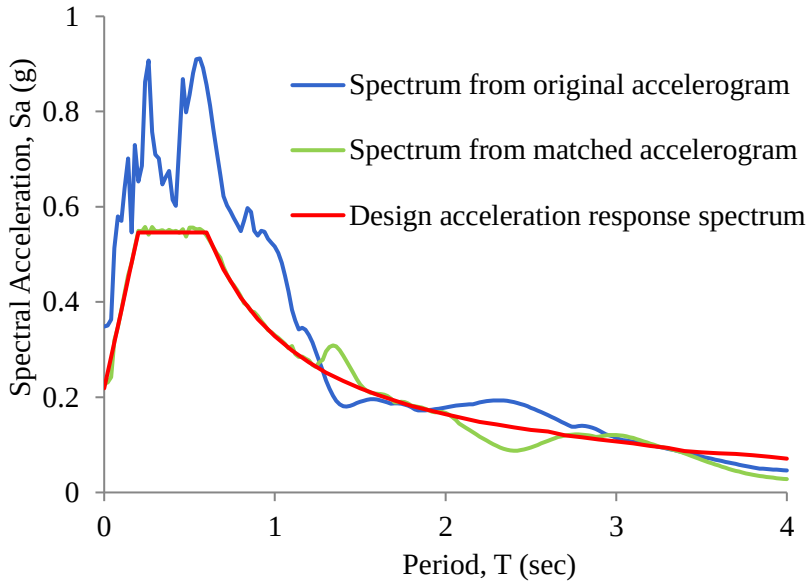

Fig. 3.8: Matching of original acceleration response spectrum with design acceleration response spectrum

Matched ground motion time history of El Centro 1940 is also generated from SeismoMatch software after matching response spectra of original El Centro 1940 with design response spectrum for PGA of 0.19g (DBE). The comparison of original acceleration and matched acceleration time histories of El Centro 1940 is shown in Fig. 3.9. The PGA of original El Centro 1940 ground motion history is reduced to 0.23g from 0.35g regarding maximum and mean misfit of matching.

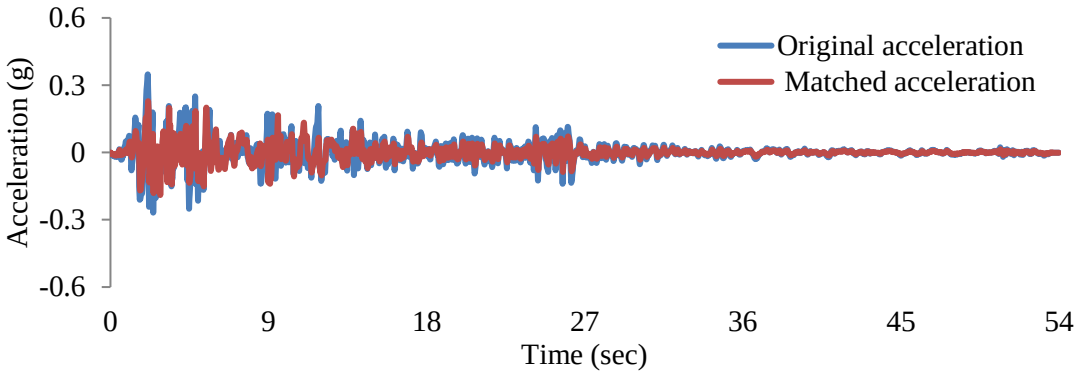

Fig. 3.9: Comparison of original acceleration and matched acceleration time histories of El Centro 1940

3.4.4.2 Matching with Kobe 1995

Selected ground motion kobe 1995 acceleration time histories are matched with design response spectrum for PGA of 0.19g (DBE) for the site class SC using SeismoMatch software. . SeismoMatch is an earthquake software program that uses the wavelets algorithm to adjust the ground motion accelerograms of an earthquake to match a specific target response spectrum. Matching of response spectrum of original Kobe 1995 ground motion acceleration with design acceleration response spectrum of selected site are shown in Fig. 3.10. Maximum spectral acceleration of original Kobe 1995 ground motion is 2.26g which is reduced to 0.56g after matching with design response spectrum for PGA of 0.19g regarding maximum and mean misfit.

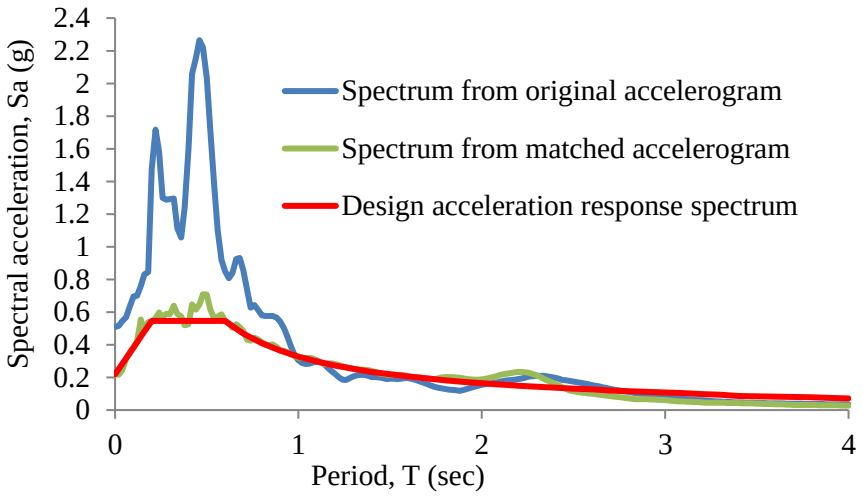

Fig. 3.10: Matching of original acceleration response spectrum with design acceleration response spectrum

Matched ground motion time history of Kobe 1995 is also generated from SeismoMatch software after matching response spectra of original Kobe 1995 with design response spectrum for PGA of 0.19g (DBE). The comparison of original acceleration and matched acceleration time histories of Kobe 1995 is shown in Fig. 3.11. The PGA of original Kobe 1995 ground motion history is reduced to 0.22g from 0.51g regarding maximum and mean misfit of matching.

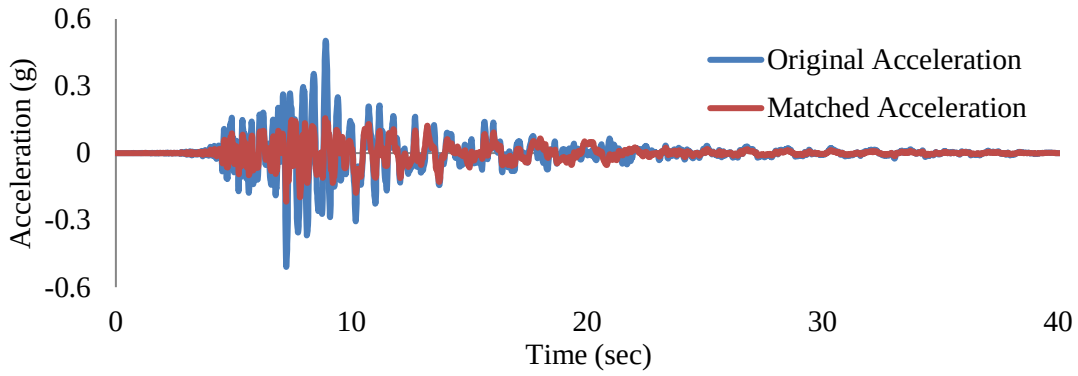

Fig. 3.11: Comparison of original acceleration and matched acceleration time histories of Kobe 1995

3.4.4.3 Matching with Tabas 1978

Selected ground motion Tabas 1978 acceleration time histories are matched with design response spectrum for PGA of 0.19g (DBE) for the site class SC using SeismoMatch software. . SeismoMatch is an earthquake software program that uses the wavelets algorithm to adjust the ground motion accelerograms of an earthquake to match a specific target response spectrum. Matching of response spectrum of original Tabas 1978 ground motion acceleration with design acceleration response spectrum of selected site are shown in Fig. 3.12. Maximum spectral acceleration of original Tabas 1978 ground motion is 1.4g which is reduced to 0.56g after matching with design response spectrum for PGA of 0.19g regarding maximum and mean misfit.

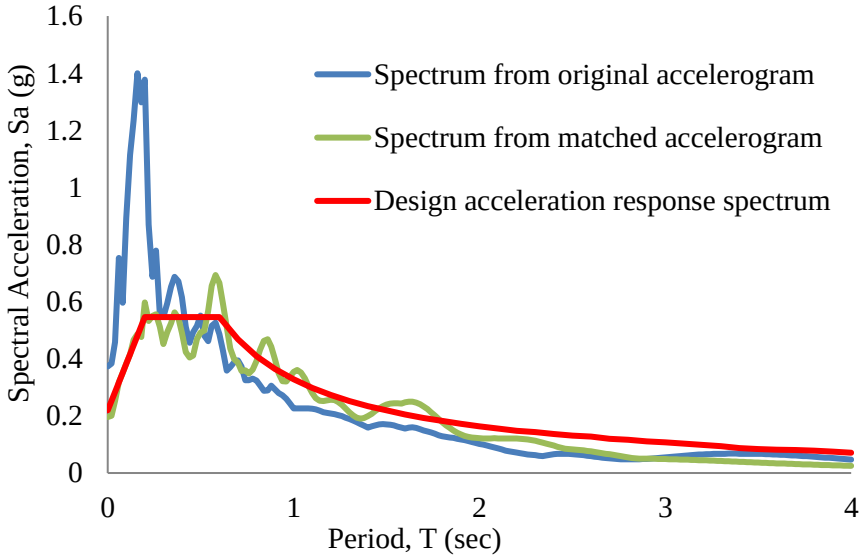

Fig. 3.12: Matching of original acceleration response spectrum with design acceleration response spectrum

Matched ground motion time history of Tabas 1978 is also generated from SeismoMatch software after matching response spectra of original Tabas 1978 with design response spectrum for PGA of 0.19g (DBE). The comparison of original acceleration and matched acceleration time histories of Tabas 1978 is shown in Fig. 3.13. The PGA of original Tabas 1978 ground motion history is reduced to 0.20g from 0.37g regarding maximum and mean misfit of matching.

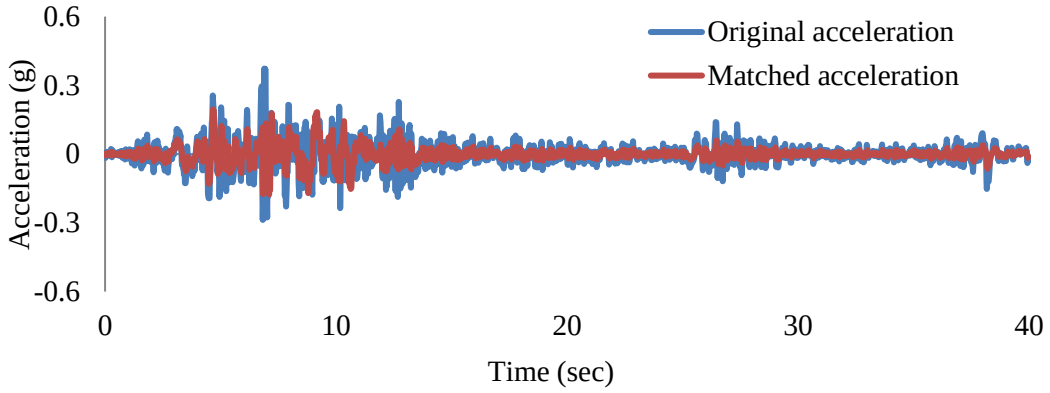

Fig. 3.13: Comparison of original acceleration and matched acceleration time histories of Tabas 1978

3.4.5 Time History Analysis

The matched acceleration time histories are applied in all three building models of SeismoStruct in X and Y direction separately. The applications of time history acceleration at the base of all columns in X direction are shown in Fig. 3.2. The application of ground motion accelerations in the both directions simultaneously are neglected in the nonlinear time history analysis. Dynamic time-history loads (accelerations or forces) fluctuate as per different load diagrams in the existing time domain. The magnitude of the load applied to the structure is determined by the dynamic time-history load of their constant nominal value and the variable load factor calculated from their load curve (accelerogram) at any given time. The dynamic time history X direction and Y direction loads are shown in Fig. 3.14.

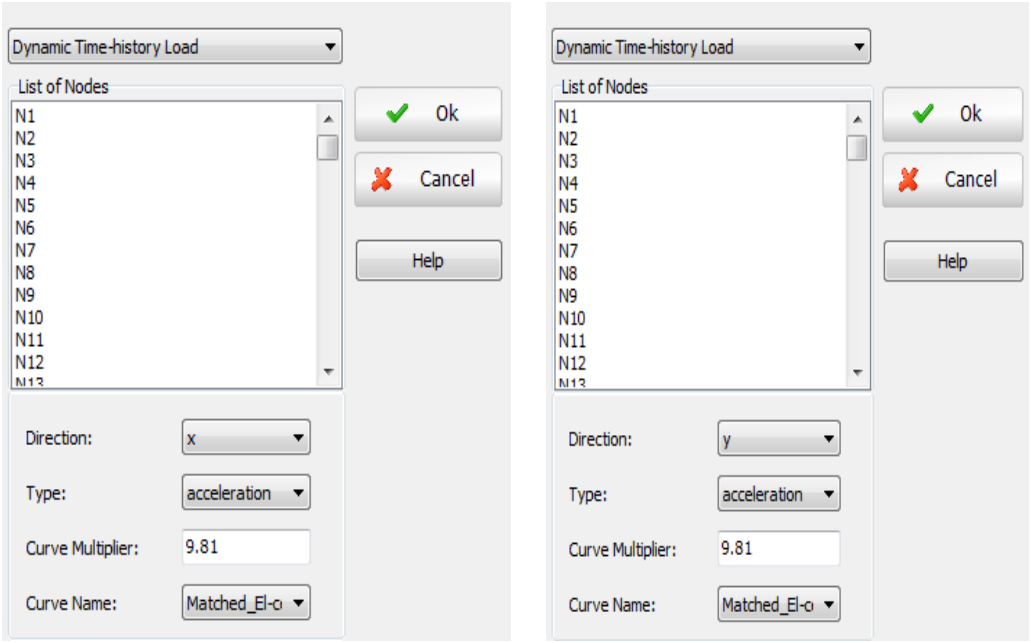

Fig. 3.14: Dynamic time history loads: (a) X direction (b) Y direction

Verification for Convergence criteria at each individual degree-of-freedom of the structure that the current iteration displacement/rotation is less than or equal to a user's specific tolerance gives the user direct control over the degree of accuracy or, conversely, approximate, problem-solving. Furthermore, and for the vast majority of analyses, a local precision check is adequate to ensure the overall accuracy of the result. Therefore, the criterion for this convergence test is the default alternative to SeismoStruct, with a displacement tolerance of 0.0001 m and a rotation tolerance of 0.0001 rad as shown in Fig. 3.15, In the vast majority of circumstances, this results in exact and durable solutions. The convergence criteria are given in Table 3.5.

Table 3.5: Convergence criteria

Displacement tolerance	0.0001 m
Rotation tolerance	0.0001 rad
Largest acceptable increase of norms	100
Element loop convergence tolerance	1.0000000E-005
Element loop maximum iterations	300

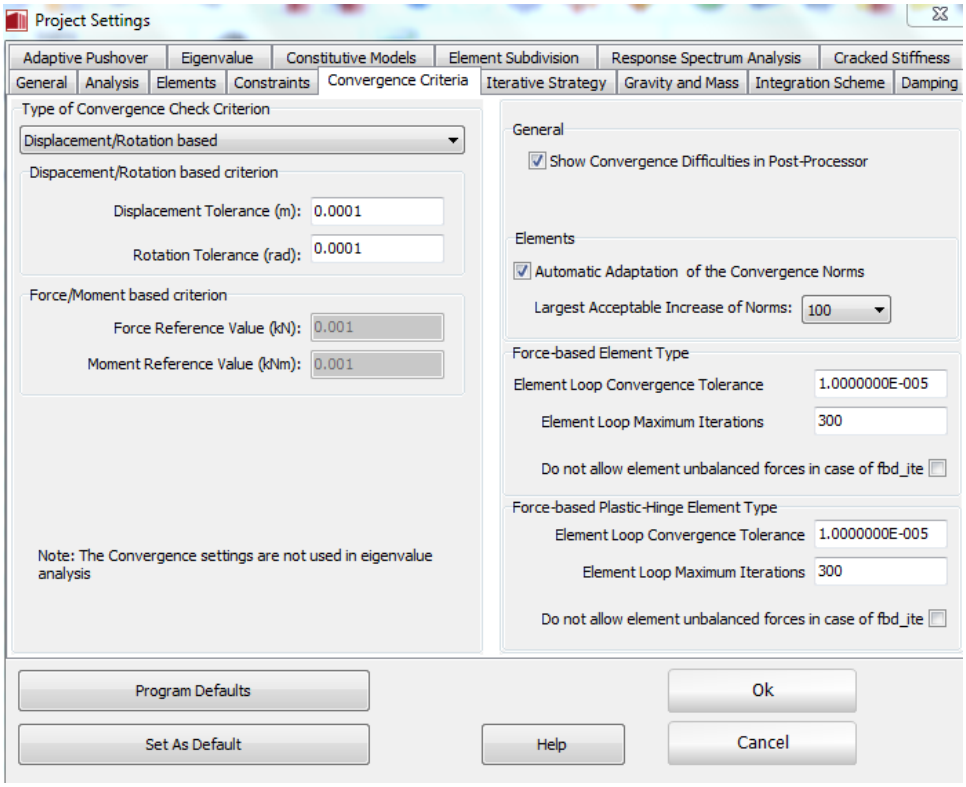

Fig. 3.15: Convergence criteria - Displacement/Rotation based

Finally, the response of the building models are observed for application of three different ground motion time histories.

3.5 Synopsis

Three six storied buildings with three different plan aspect ratios are modeled in SeismoStruct and ETABS. The selected three ground motion histories (El Centro 1940, Kobe 1995 and Tabas 1978) are used in the analysis after matching with the design response spectrum as per BNBC for PGA of 0.19g (DBE) for the site class SC using SeismoMatch software. The matched acceleration time histories are applied at the base of all columns in X and Y direction separately. Finally, the responses of the building models are observed to investigate the effect of plan aspect ratio.

Chapter 4
RESULTS & DISCUSSIONS

4.1 General

The seismic responses of building models are evaluated in terms of maximum story displacement and story drift in both X and Y directions separately. Maximum story displacements occur in the top floor of the buildings. Inter story drifts or story drifts are then determined for each floor by dividing the relative displacements of the floors by the story height.

4.2 Response of Buildings

Displacement response at top floor of each building models are formed from time history analysis. This response are found from SeismoStruct.

4.2.1 El Centro 1940

The displacement response of the three-building models in the X-direction under El Centro 1940 is shown in Fig. 4.1 to 4.3.

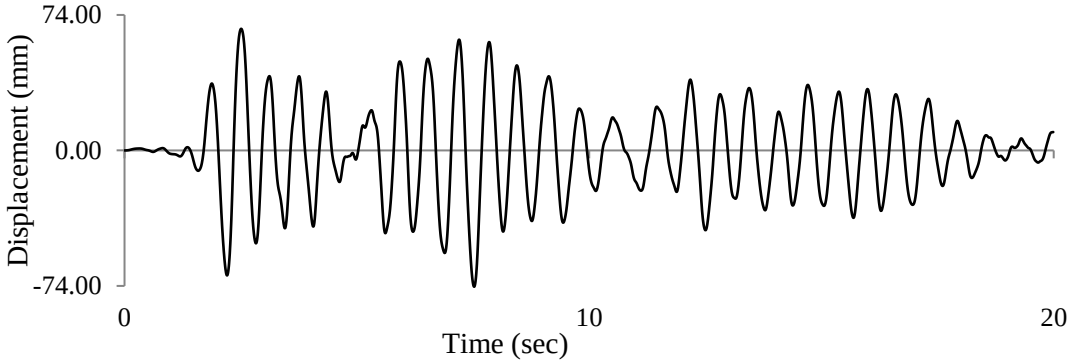

Fig. 4.1: El Centro 1940 in X direction for model 1

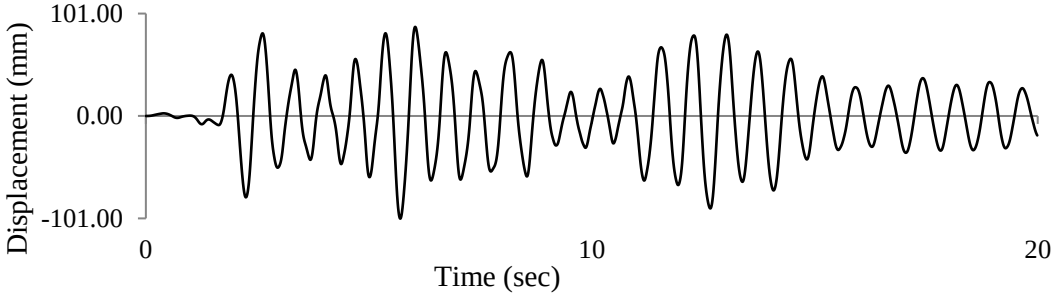

Fig. 4.2: El Centro 1940 in X direction for model 2

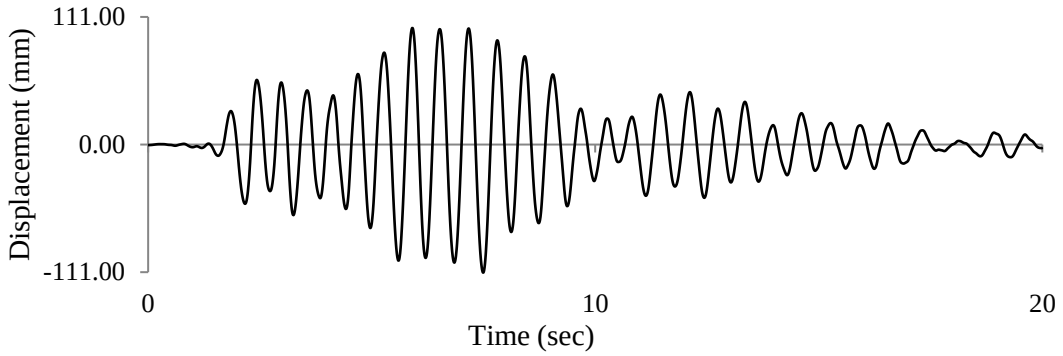

Fig. 4.3: El Centro 1940 in X direction for model 3

4.2.2 El Centro 1940

The displacement response of the three-building models in the Y-direction under El Centro 1940 is shown in Fig. 4.4 to 4.6.

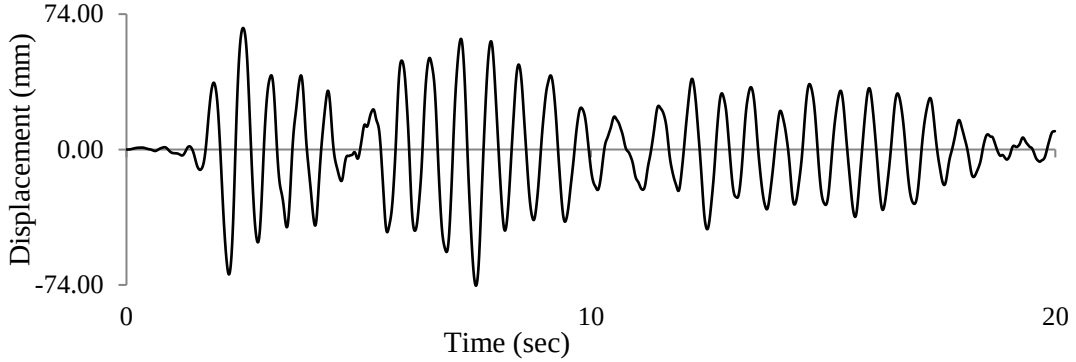

Fig. 4.4: El Centro 1940 in Y direction for model 1

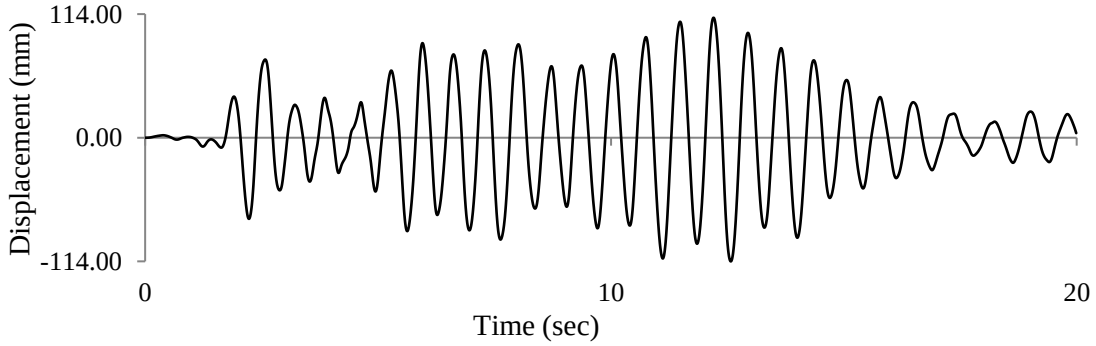

Fig. 4.5: El Centro 1940 in Y direction for model 2

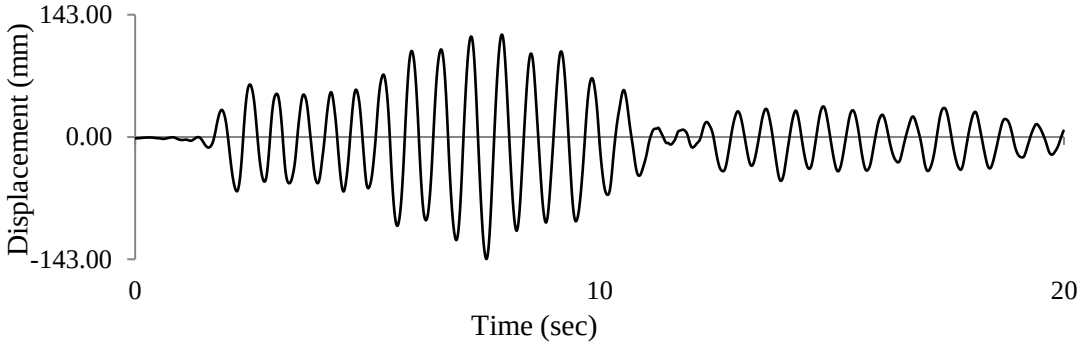

Fig. 4.6: El Centro 1940 in Y direction for model 3

4.2.3 Kobe 1995

The displacement response of the three-building models in the X-direction under Kobe 1995 is shown in Fig. 4.7 to 4.9.

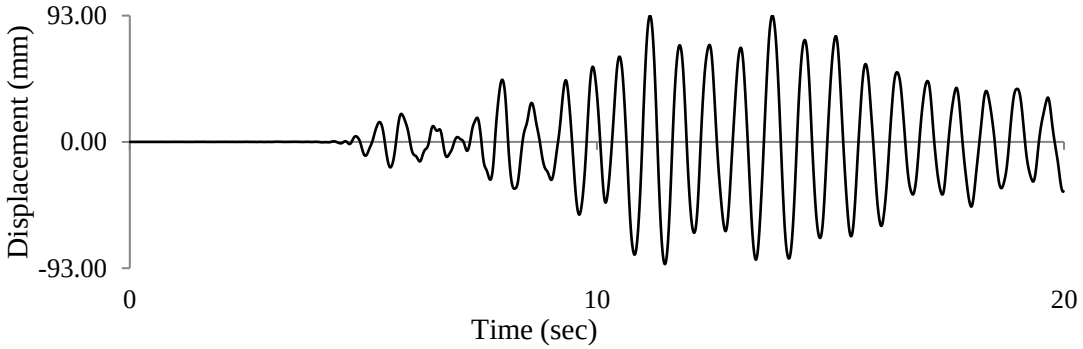

Fig. 4.7: Kobe 1995 in X direction for model 1

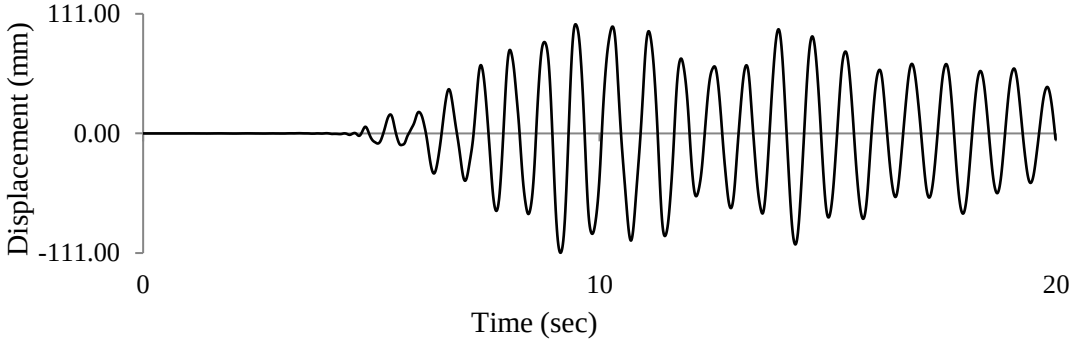

Fig. 4.8: Kobe 1995 in X direction for model 2

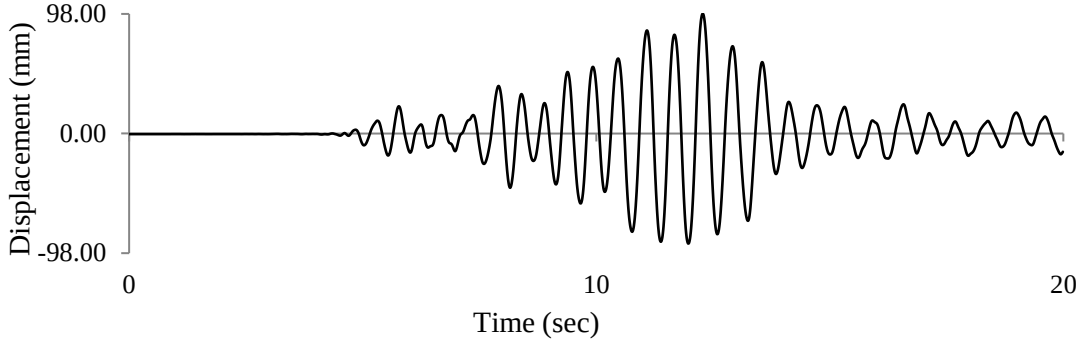

Fig. 4.9: Kobe 1995 in X direction for model 3

4.2.4 Kobe 1995

The displacement response of the three-building models in the Y-direction under Kobe 1995 is shown in Fig. 4.10 to 4.12.

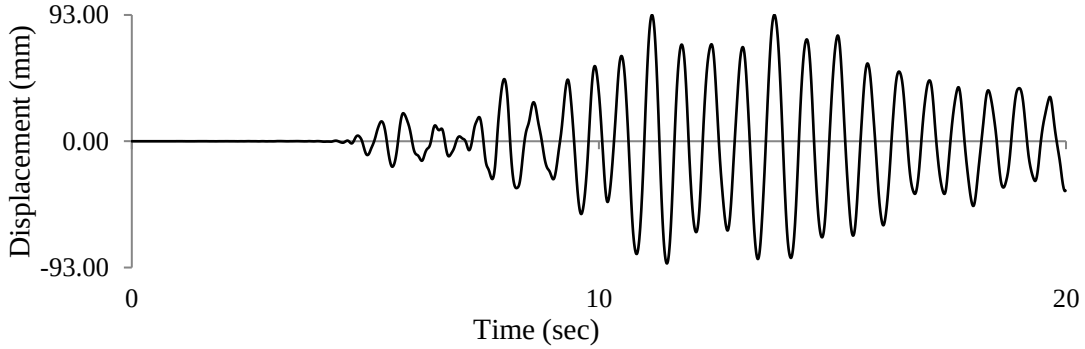

Fig. 4.10: Kobe 1995 in Y direction for model 1

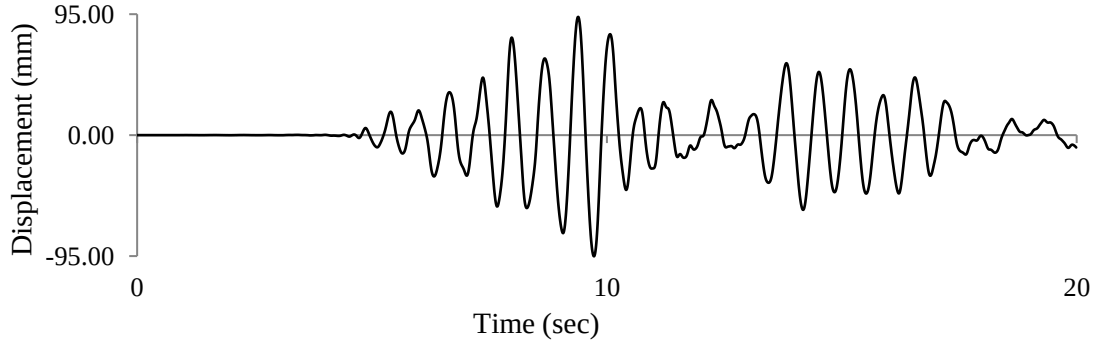

Fig. 4.11: Kobe 1995 in Y direction for model 2

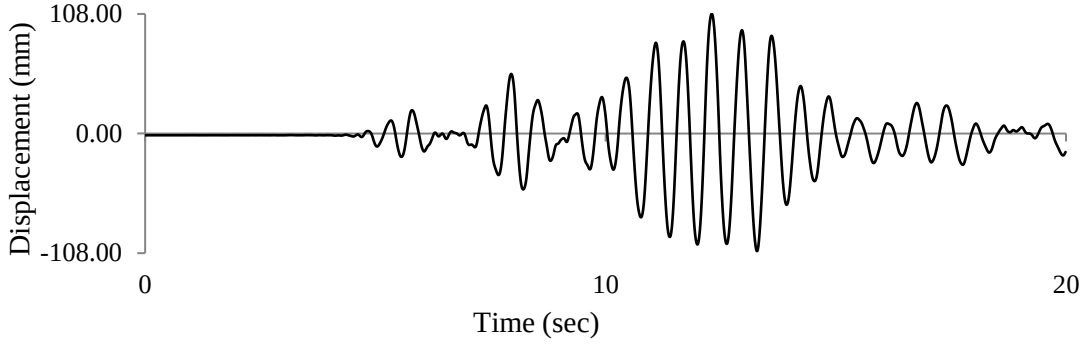

Fig. 4.12: Kobe 1995 in Y direction for model 3

4.2.5 Tabas 1978

The displacement response of the three-building models in the X-direction under Tabas 1978 is shown in Fig. 4.13 to 4.15.

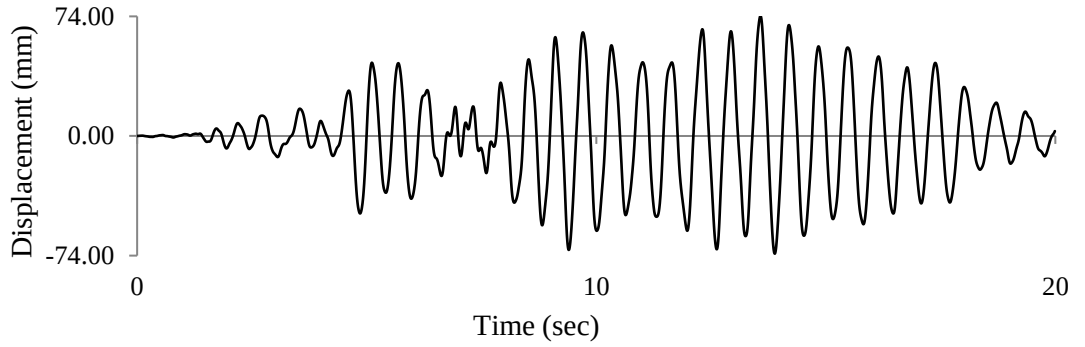

Fig. 4.13: Tabas 1978 in X direction for model 1

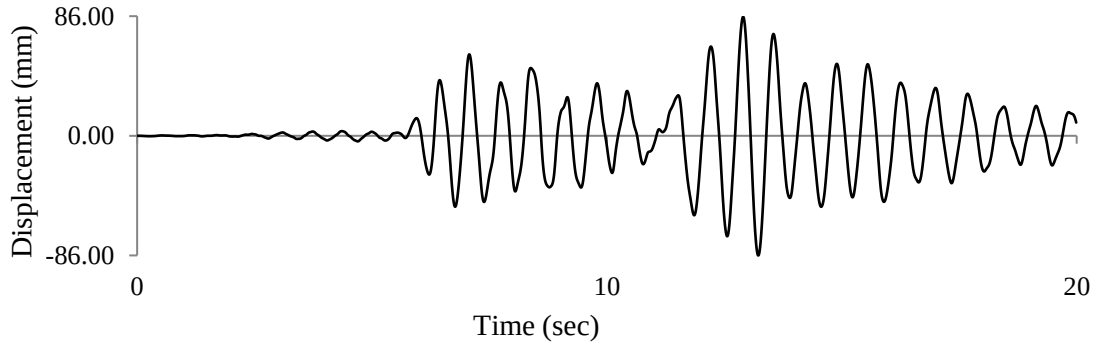

Fig. 4.14: Tabas 1978 in X direction for model 2

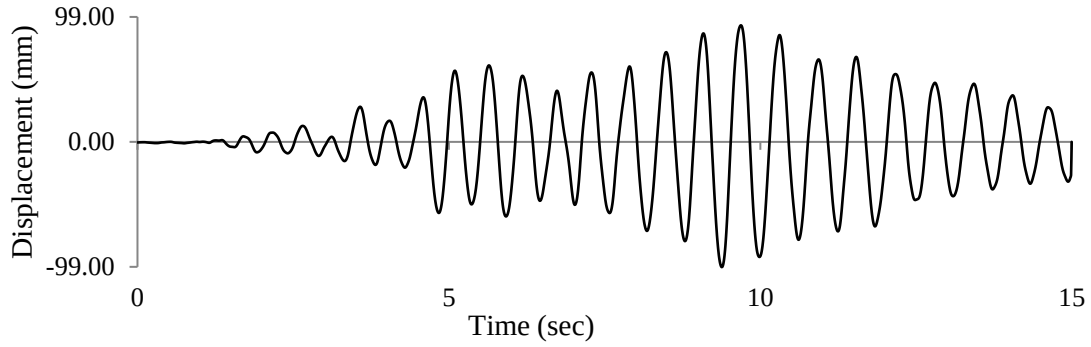

Fig. 4.15: Tabas 1978 in X direction for model 3

4.2.6 Tabas 1978

The displacement response of the three-building models in the Y-direction under Tabas 1978 is shown in Fig. 4.16 to 4.18.

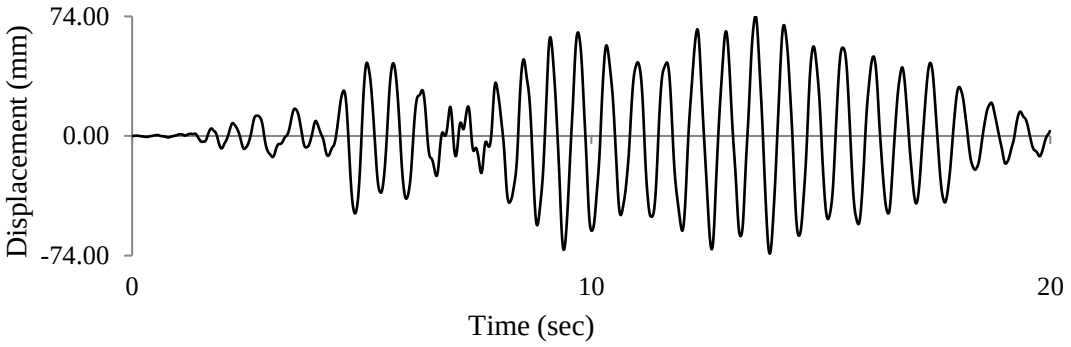

Fig. 4.16: Tabas 1978 in Y direction for model 1

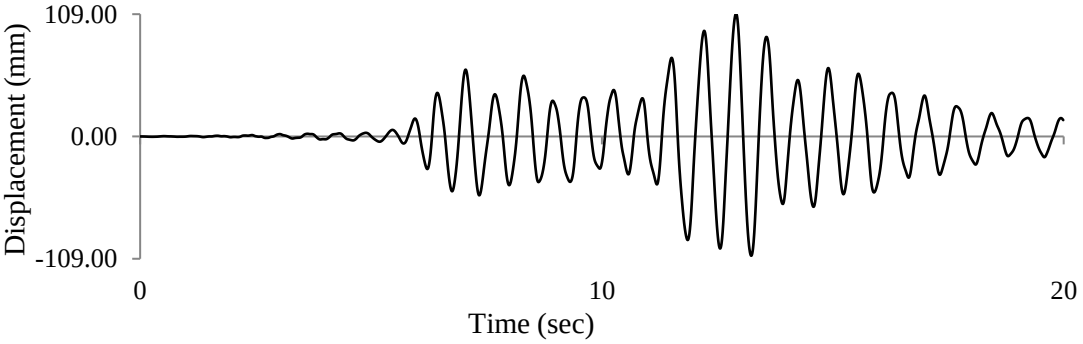

Fig. 4.17: Tabas 1978 in Y direction for model 2

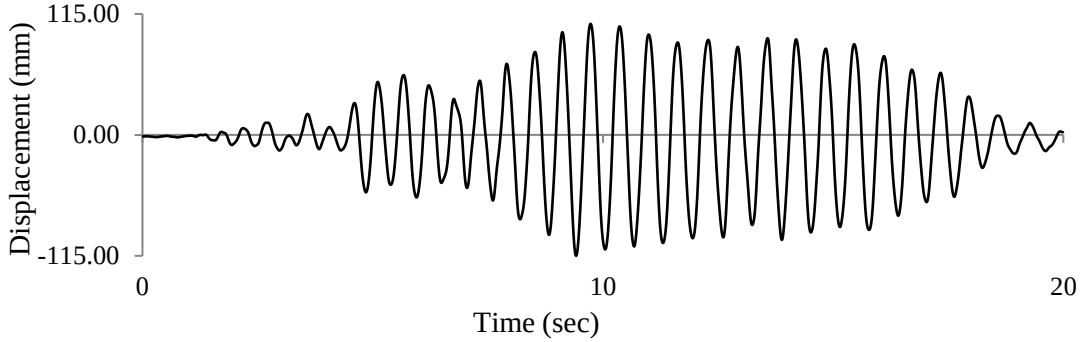

Fig. 4.18: Tabas 1978 in Y direction for model 3

4.3 Comparison in Seismostruct Software

4.3.1 Maximum Story Displacement

4.3.1.1 El Centro 1940

The maximum story displacement values in X and Y directions for all three building models with different aspect ratios (AR) are shown in Fig. 4.1. For Model 1 (AR = 1), maximum story displacement is found to be 74 mm in both X and Y directions. For Model 2 (AR = 1.5), maximum story displacement is found to be 101 mm in X direction and 114 mm in Y direction. For Model 3 (AR = 2), maximum story displacement is found to be 111 mm in X direction and 143 mm in Y direction. Although, all three building models consist of same plan area, maximum story displacements increase in both X and Y directions with the increase of plan aspect ratios. There are 35% and 50% increase of maximum story displacements in X direction due to increase of aspect ratio 1.5 and 2 times respectively from basic square shape of plan. On the other hand, there are 55% and 95% increase of maximum story displacements in Y direction due to increase of aspect ratio 1.5 and 2 times respectively from basic square shape of plan.

Table 4.1: Maximum story displacement in X and Y directions for El Centro 1940

Aspect Ratio	Maximum story displacement (mm)	
	X direction	Y direction
1	74	74
1.5	101	114
2	111	143

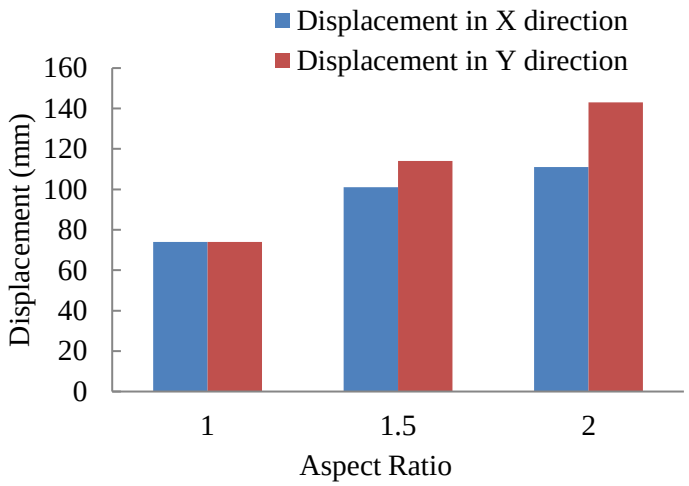

Fig. 4.19: Maximum story displacements along X and Y directions for El Centro 1940

4.3.1.2 Kobe 1995

The maximum story displacement values in X and Y directions for all three building models with different aspect ratios (AR) are shown in Fig. 4.2. For Model 1 (AR = 1), maximum story displacement is found to be 93 mm in both X and Y directions. For Model 2 (AR = 1.5), maximum story displacement is found to be 111 mm in X direction and 95 mm in Y direction. For Model 3 (AR = 2), maximum story displacement is found to be 98 mm in X direction and 108 mm in Y direction. Although, all three building models consist of same plan area but it is observed that the maximum story displacement is reduced for aspect ratio 2, while the displacement is maximum for aspect ratio 1.5 in X direction and maximum story displacement increase in Y direction with the increase of plan aspect ratios. There are 20% and 6% increase of maximum story displacements in X direction due to increase of aspect ratio 1.5 and 2 times respectively from basic square shape of plan. On the other hand, there are 3% and 16% increase of maximum story displacements in Y direction due to increase of aspect ratio 1.5 and 2 times respectively from basic square shape of plan.

Table 4.2: Maximum story displacement in X and Y directions for Kobe 1995

Aspect Ratio	Maximum story displacement (mm)	
	X direction	Y direction
1	93	93
1.5	111	95
2	98	108

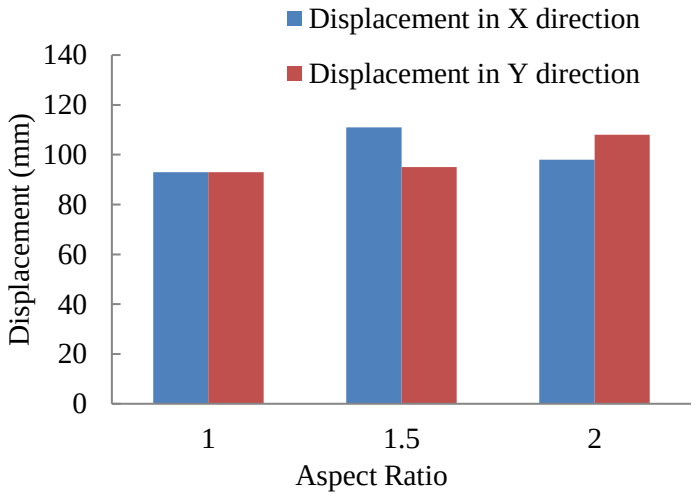

Fig. 4.20: Maximum story displacements along X and Y directions for Kobe 1995

4.3.1.3 Tabas 1978

The maximum story displacement values in X and Y directions for all three building models with different aspect ratios (AR) are shown in Fig. 4.3. For Model 1 (AR = 1), maximum story displacement is found to be 74 mm in both X and Y directions. For Model 2 (AR = 1.5), maximum story displacement is found to be 86 mm in X direction and 109 mm in Y direction. For Model 3 (AR = 2), maximum story displacement is found to be 99 mm in X direction and 115 mm in Y direction. Although, all three building models consist of same plan area, maximum story displacements increase in both X and Y directions with the increase of plan aspect ratios. There are 17% and 34% increase of maximum story displacements in X direction due to increase of aspect ratio 1.5 and 2 times respectively from basic square shape of plan. On the other hand, there are 48% and 56% increase of maximum story displacements in Y direction due to increase of aspect ratio 1.5 and 2 times respectively from basic square shape of plan.

Table 4.3: Maximum story displacement in X and Y directions for Tabas 1978

Aspect Ratio	Maximum story displacement (mm)	
	X direction	Y direction
1	74	74
1.5	86	109
2	99	115

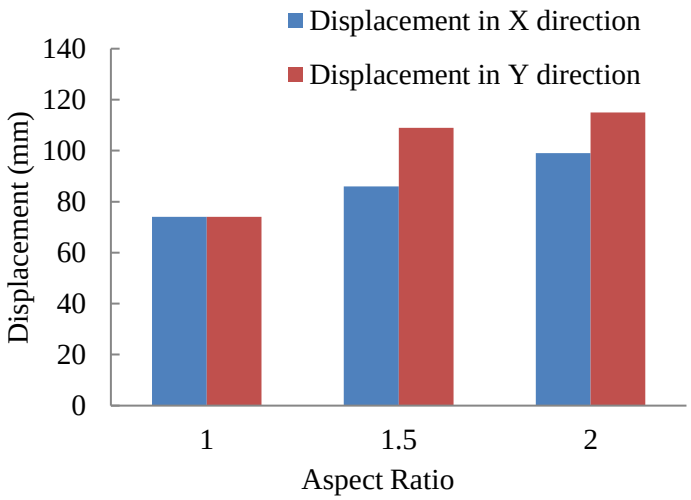

Fig. 4.21: Maximum story displacements along X and Y directions for Tabas 1978

4.3.2 Story Drift Ratio

4.3.2.1 El Centro 1940

The story drift ratio has been compared for all three building models with different aspect ratios (AR) in both X and Y directions are shown in Fig. 4.22 and Fig. 4.23 respectively. Similar to the maximum story displacement, story drift ratio are also increased in both X and Y directions with the increase of aspect ratios. However, story drift ratio are found maximum at 2nd story for ground motion time histories applied in both X and Y directions. Maximum story drift ratio values are found to be 0.006, 0.008 and 0.009 for building models with aspect ratios 1, 1.5 and 2 respectively in X direction. On the other hand, maximum story drift ratio values are found to be 0.006, 0.01 and 0.012 for building models with aspect ratios 1, 1.5 and 2 respectively in Y direction. It is observed that, there are 35% and 50% increase of maximum story drift ratio in X direction due to increase of aspect ratio 1.5 and 2 times respectively from basic square shape of plan. Similarly, there are 65% and 100% increase of maximum story drift ratio in Y direction due to increase of aspect ratio 1.5 and 2

times respectively from basic square shape of plan. As building models become less stiff in Y direction with the increase of aspect ratios in X direction, maximum story displacements and story drift ratio are largely increased in Y direction compared to that in X direction.

Table 4.4: Story drift ratio in X direction for different aspect ratios for El Centro 1940

Story No.	Story drift ratio		
	AR=1	AR=1.5	AR=2
6	0.0013	0.0027	0.002
5	0.0033	0.0047	0.0043
4	0.0043	0.0063	0.0063
3	0.0053	0.0073	0.0087
2	0.006	0.008	0.009
1	0.0043	0.005	0.0067
0	0	0	0

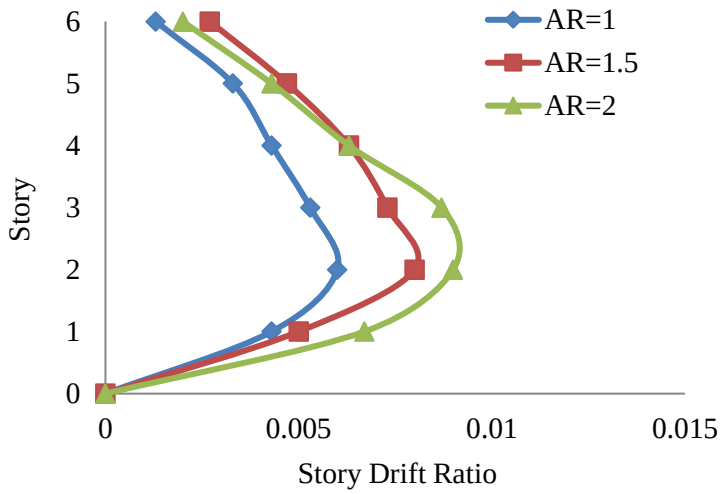

Fig. 4.22: Story drift ratio in X direction for different aspect ratios for El Centro 1940

Table 4.5: Story drift ratio in Y direction for different aspect ratios for El Centro 1940

Story No.	Story drift ratio		
	AR=1	AR=1.5	AR=2
6	0.0013	0.002	0.003
5	0.0033	0.0043	0.0057
4	0.0043	0.0067	0.0083
3	0.0053	0.0087	0.011
2	0.006	0.01	0.012
1	0.0043	0.0067	0.0083
0	0	0	0

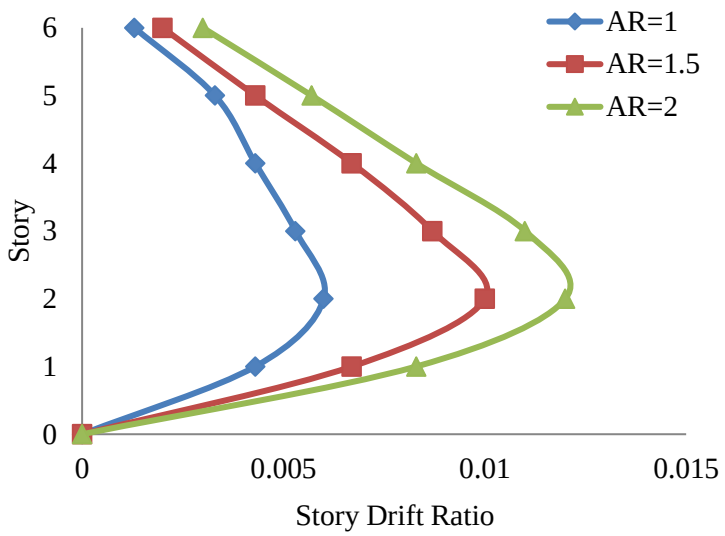

Fig. 4.23: Story drift ratio in Y direction for different aspect ratios for El Centro 1940

4.3.2.2 Kobe 1995

The story drift ratio has been compared for all three building models with different aspect ratios (AR) in both X and Y directions are shown in Fig. 4.24 and Fig. 4.25 respectively. For Model 1 with aspect ratio of 1 shows the least value among all the three models in both X and Y directions. However, story drift ratio are found maximum at 2nd story for ground motion time histories applied in both X and Y directions. Maximum story drift ratio values are found to be 0.0077, 0.0097 and 0.0083 for building models with aspect ratios 1, 1.5 and 2 respectively in X direction. On the other hand, maximum story drift ratio values are found to be 0.0077, 0.0080 and 0.0090 for building models with aspect ratios 1, 1.5 and 2 respectively in Y direction. It is observed that, there are 26% and 8% increase of maximum story drift ratio in X direction due to increase of aspect ratio 1.5 and 2 times respectively from basic square shape of plan. Similarly, there are 4% and 17% increase of maximum story drift ratio in Y direction due to increase of aspect ratio 1.5 and 2 times respectively from basic square shape of plan. For Model 2 (AR = 1.5), maximum story displacements and story drift ratio are increased in X direction compared to that in Y direction and For Model 3 (AR = 2), maximum story displacements and story drift ratio are increased in Y direction compared to that in X direction.

Table 4.6: Story drift ratio in X direction for different aspect ratios for Kobe 1995

Story No.	Story drift ratio		
	AR=1	AR=1.5	AR=2
6	0.0017	0.0017	0.0013
5	0.0037	0.0040	0.0033
4	0.0053	0.0063	0.0057
3	0.0073	0.0090	0.0077
2	0.0077	0.0097	0.0083
1	0.0053	0.0063	0.0063
0	0	0	0

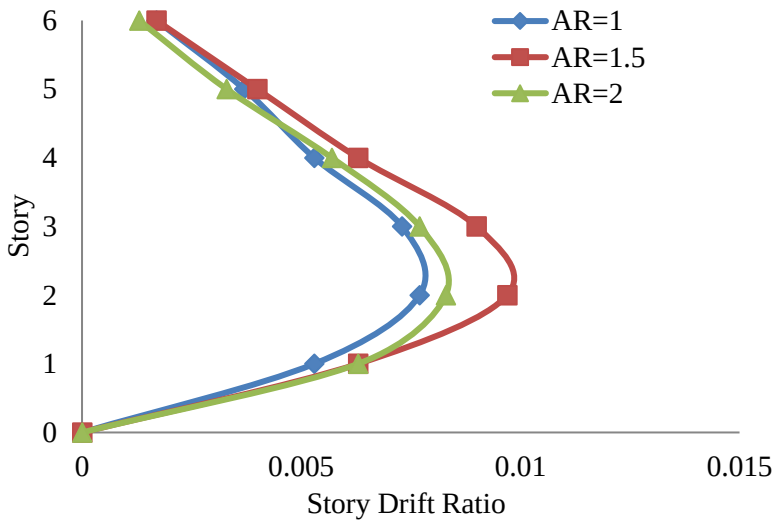

Fig. 4.24: Story drift ratio in X direction for different aspect ratios for Kobe 1995

Table 4.7: Story drift ratio in Y direction for different aspect ratios for Kobe 1995

Story No.	Story drift ratio		
	AR=1	AR=1.5	AR=2
6	0.0017	0.0020	0.0017
5	0.0037	0.0040	0.0040
4	0.0053	0.0057	0.0060
3	0.0073	0.0073	0.0083
2	0.0077	0.0080	0.0090
1	0.0053	0.0050	0.0070
0	0	0	0

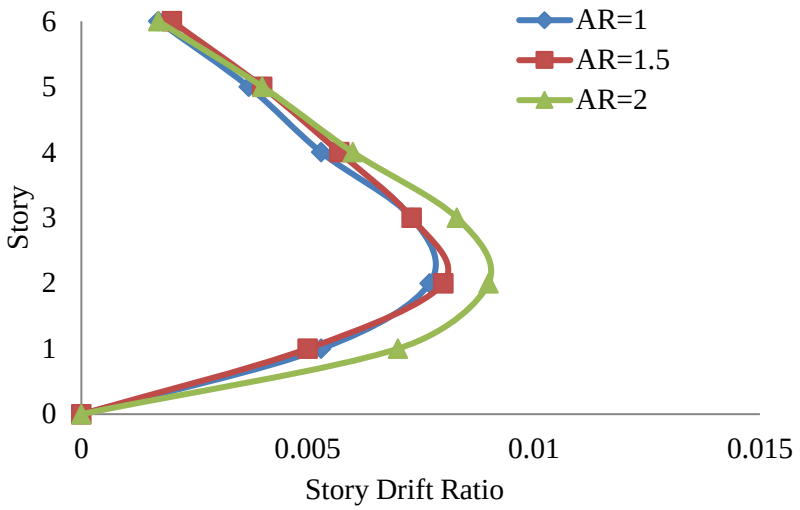

Fig. 4.25: Story drift ratio in Y direction for different aspect ratios for Kobe 1995

4.3.2.3 Tabas 1978

The story drift ratio has been compared for all three building models with different aspect ratios (AR) in both X and Y directions are shown in Fig. 4.26 and Fig. 4.27 respectively. Similar to the maximum story displacement, story drift ratio are also increased in both X and Y directions with the increase of aspect ratios. However, story drift ratio are found maximum at 2nd story for ground motion time histories applied in both X and Y directions. Maximum story drift ratio values are found to be 0.0053, 0.0070 and 0.0083 for building models with aspect ratios 1, 1.5 and 2 respectively in X direction. On the other hand, maximum story drift ratio values are found to be 0.0053, 0.0083 and 0.0093 for building models with aspect ratios 1, 1.5 and 2 respectively in Y direction. It is observed that, there are 32% and 57% increase of maximum story drift ratio in X direction due to increase of aspect ratio 1.5 and 2 times respectively from basic square shape of plan. Similarly, there are 57% and 76% increase of maximum story drift ratio in Y direction due to increase of aspect ratio 1.5 and 2 times respectively from basic square shape of plan. As building models become less stiff in Y direction with the increase of aspect ratios in X direction, maximum story displacements and story drift ratio are largely increased in Y direction compared to that in X direction.

Table 4.8: Story drift ratio in X direction for different aspect ratios for Tabas 1978

Story No.	Story drift ratio		
	AR=1	AR=1.5	AR=2
6	0.0020	0.0020	0.0017
5	0.0040	0.0043	0.0037
4	0.0050	0.0053	0.0060
3	0.0047	0.0060	0.0077
2	0.0053	0.0070	0.0083
1	0.0037	0.0040	0.0057
0	0	0	0

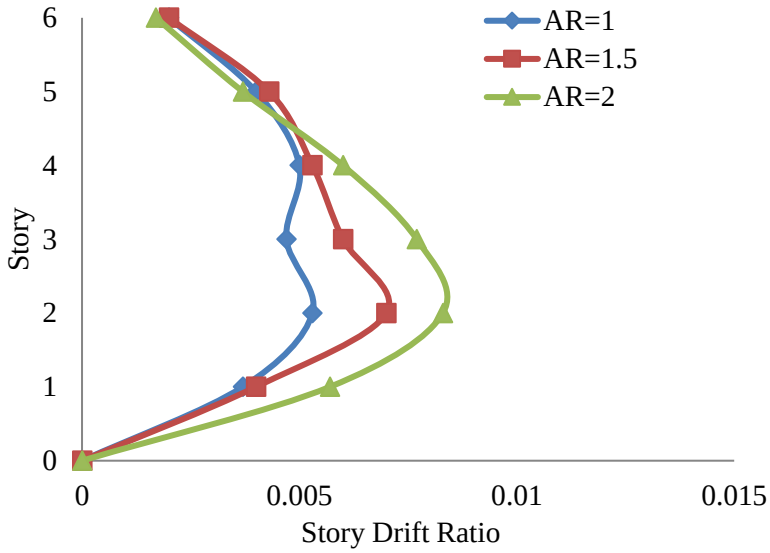

Fig. 4.26: Story drift ratio in X direction for different aspect ratios for Tabas 1978

Table 4.9: Story drift ratio in Y direction for different aspect ratios for Tabas 1978

Story No.	Story drift ratio		
	AR=1	AR=1.5	AR=2
6	0.0020	0.0027	0.0027
5	0.0040	0.0050	0.0053
4	0.0050	0.0067	0.0060
3	0.0047	0.0080	0.0083
2	0.0053	0.0083	0.0093
1	0.0037	0.0057	0.0067
0	0	0	0

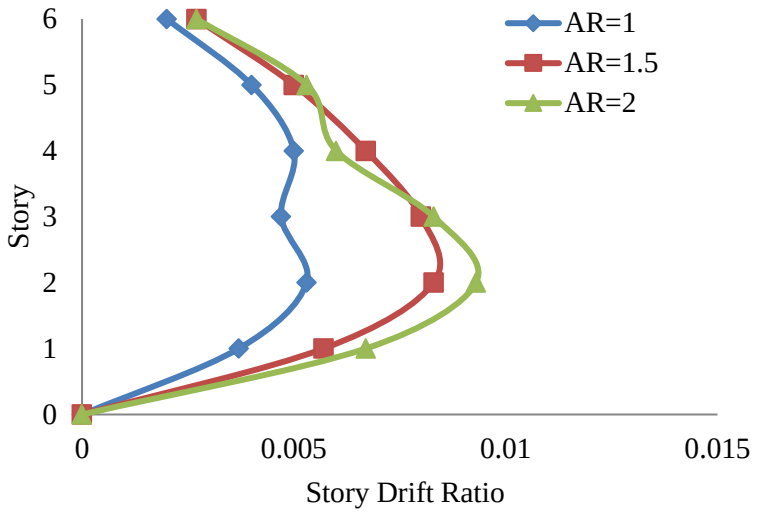

Fig. 4.27: Story drift ratio in Y direction for different aspect ratios for Tabas 1978

4.3.3 Comparison of Story Displacement for Different Ground Motions

4.3.3.1 All Models in X direction

The maximum story displacement values in X direction for building model 1, model 2 and model 3 (AR = 1, AR=1.5 and AR= 2) with three ground motions are shown in Fig. 4.28. For El Centro 1940, maximum story displacement model 1 is found to be 74 mm, model 2 is found to be 101 mm and model 3 is found to be 111 mm in X direction. For Kobe 1995, maximum story displacement model 1 is found to be 93 mm, model 2 is found to be 111 mm and model 3 is found to be 98 mm in X direction. For Tabas 1978, maximum story displacement model 1 is found to be 74 mm, model 2 is found to be 86 mm and model 3 is found to be 99 mm in X direction. Although, all three building models consist of same plan area, story displacement maximum Kobe 1995 and El Centro 1940 in both model 2 and model 3. Seismic responses of buildings are assessed in terms of maximum story displacement in X direction. The maximum displacement value between these three ground motions (El Centro, Kobe and Tabas), that will do work with response.

Table 4.10: Maximum story displacement in X direction for all Models

Model	Maximum story displacement (mm)		
	El Centro 1940	Kobe 1995	Tabas 1978
Model 1	74	93	74
Model 2	101	111	86
Model 3	111	98	99

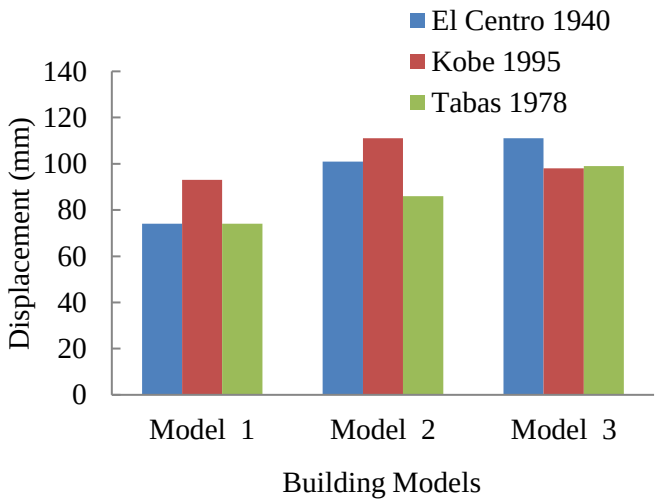

Fig. 4.28: Maximum story displacement in X direction for all Models

4.3.3.2 All Models in Y direction

The maximum story displacement values in Y direction for building model 1, model 2 and model 3 (AR = 1, AR=1.5 and AR= 2) with three ground motions are shown in Fig. 4.29. For El Centro 1940, maximum story displacement model 1 is found to be 74 mm, model 2 is found to be 114 mm and model 3 is found to be 143 mm in Y direction. For Kobe 1995, maximum story displacement model 1 is found to be 93 mm, model 2 is found to be 95 mm and model 3 is found to be 108 mm in Y direction. For Tabas 1978, maximum story displacement model 1 is found to be 74 mm, model 2 is found to be 109 mm and model 3 is found to be 115 mm in Y direction. Although, all three building models consist of same plan area, story displacement maximum El Centro 1940 in model 3. Seismic responses of buildings are assessed in terms of maximum story displacement in Y direction. The maximum displacement value between these three ground motions (El Centro, Kobe and Tabas), that will do work with response.

Table 4.11: Maximum story displacement in Y direction for all Models

Model	Maximum story displacement (mm)		
	El Centro 1940	Kobe 1995	Tabas 1978
Model 1	74	93	74
Model 2	114	95	109
Model 3	143	108	115

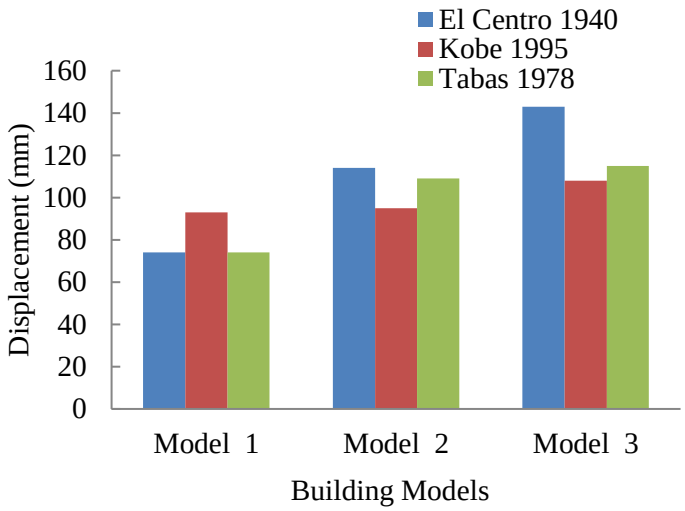

Fig. 4.29: Maximum story displacement in Y direction for all Models

4.3.4 Comparison of Story Drift Ratio

4.3.4.1 Model 1 (X direction)

The story drift ratio have been compared for building model 1 (AR = 1) with three ground motions in X direction are shown in Fig. 4.30. However, story drift ratio is found maximum at 2nd story for ground motion time histories applied in X direction. Maximum story drift ratio values are found to be 0.0060, 0.0077 and 0.0053 for building model 1 with ground motions El Centro, Kobe and Tabas respectively in X direction. Kobe 1995 shows the highest story drift ratio values among all the three ground motions.

Table 4.12: Story drift ratio in X direction for Model 1

Story No.	Story drift ratio		
	El Centro 1940	Kobe 1995	Tabas 1978
6	0.0013	0.0017	0.0020
5	0.0033	0.0037	0.0040
4	0.0043	0.0053	0.0050
3	0.0053	0.0073	0.0047
2	0.0060	0.0077	0.0053
1	0.0043	0.0053	0.0037
0	0	0	0

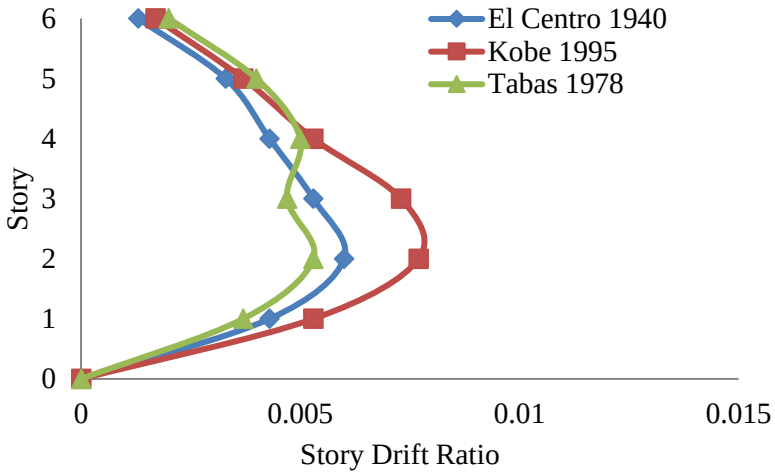

Fig. 4.30: Story drift ratio in X direction for Model 1

The maximum permissible limit for story drift ratio is 0.020 (BNBC, 2020). The maximum story drift ratio among all the cases is 0.0077 ≤ 0.020; hence Building Model 1 in X direction is found safe for all ground motions in term of story drift ratio as shown in the Table 4.13, 4.14 and 4.15.

Table 4.13: El Centro 1940 in X direction

Story No.	Displacement δ_x	$\Delta_x=\delta_x-\delta_{x-1}$	Floor height	Story drift ratio	Story drift ratio limit	Remarks
6	74 mm	4 mm	3 m	0.0013	≤ 0.020	Ok
5	70 mm	10 mm	3 m	0.0033	≤ 0.020	Ok
4	60 mm	13 mm	3 m	0.0043	≤ 0.020	Ok
3	47 mm	16 mm	3 m	0.0053	≤ 0.020	Ok
2	31 mm	18 mm	3 m	0.0060	≤ 0.020	Ok
1	13 mm	13 mm	3 m	0.0043	≤ 0.020	Ok

Table 4.14: Kobe 1995 in X direction

Story No.	Displacement δ_x	$\Delta_x=\delta_x-\delta_{x-1}$	Floor height	Story drift ratio	Story drift ratio limit	Remarks
6	93 mm	5 mm	3 m	0.0017	≤ 0.020	Ok
5	88 mm	11 mm	3 m	0.0037	≤ 0.020	Ok
4	77 mm	16 mm	3 m	0.0053	≤ 0.020	Ok
3	61 mm	22 mm	3 m	0.0073	≤ 0.020	Ok
2	39 mm	23 mm	3 m	0.0077	≤ 0.020	Ok
1	16 mm	16 mm	3 m	0.0053	≤ 0.020	Ok

Table 4.15: Tabas 1978 in X direction

Story No.	Displacement δ_x	$\Delta_x=\delta_x-\delta_{x-1}$	Floor height	Story drift ratio	Story drift ratio limit	Remarks
6	74 mm	6 mm	3 m	0.0020	≤ 0.020	Ok
5	68 mm	12 mm	3 m	0.0040	≤ 0.020	Ok
4	56 mm	15 mm	3 m	0.0050	≤ 0.020	Ok
3	41 mm	14 mm	3 m	0.0047	≤ 0.020	Ok
2	27 mm	16 mm	3 m	0.0053	≤ 0.020	Ok
1	11 mm	11 mm	3 m	0.0037	≤ 0.020	Ok

4.3.4.2 Model 1 (Y direction)

The story drift ratio have been compared for building model 1 (AR = 1) with three ground motions in Y direction are shown in Fig. 4.31. However, story drift ratio is found maximum at 2nd story for ground motion time histories applied in Y direction. Maximum story drift ratio values are found to be 0.0060, 0.0077 and 0.0053 for building model 1 with ground motions El Centro, Kobe and Tabas respectively in Y direction. Kobe 1995 shows the highest story drift ratio values among all the three ground motions.

Table 4.16: Story drift ratio in Y direction for Model 1

Story No.	Story drift ratio		
	El Centro 1940	Kobe 1995	Tabas 1978
6	0.0013	0.0017	0.0020
5	0.0033	0.0037	0.0040
4	0.0043	0.0053	0.0050
3	0.0053	0.0073	0.0047
2	0.0060	0.0077	0.0053
1	0.0043	0.0053	0.0037
0	0	0	0

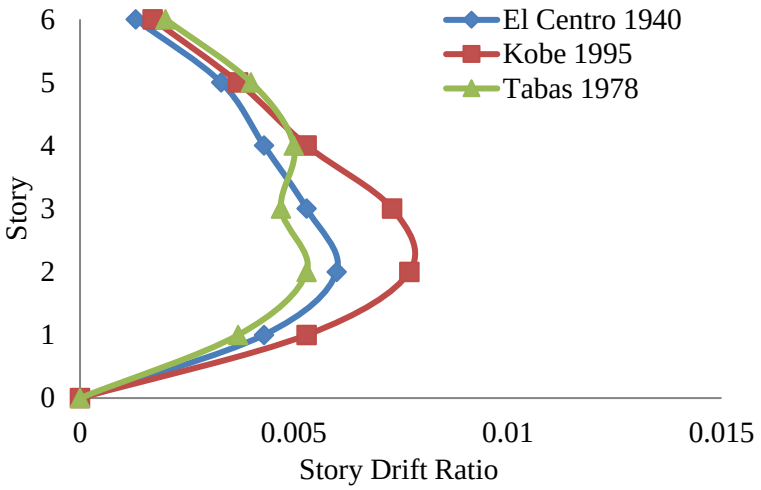

Fig. 4.31: Story drift ratio in Y direction for Model 1

The maximum permissible limit for story drift ratio is 0.020 (BNBC, 2020). The maximum story drift ratio among all the cases is 0.0077 ≤ 0.020; hence Building Model 1 in Y direction is found safe for all ground motions in term of story drift ratio as shown in the Table 4.17, 4.18 and 4.19.

Table 4.17: El Centro 1940 in Y direction

Story No.	Displacement δ_x	$\Delta_x=\delta_x-\delta_{x-1}$	Floor height	Story drift ratio	Story drift ratio limit	Remarks
6	74 mm	4 mm	3 m	0.0013	≤ 0.020	Ok
5	70 mm	10 mm	3 m	0.0033	≤ 0.020	Ok
4	60 mm	13 mm	3 m	0.0043	≤ 0.020	Ok
3	47 mm	16 mm	3 m	0.0053	≤ 0.020	Ok
2	31 mm	18 mm	3 m	0.0060	≤ 0.020	Ok
1	13 mm	13 mm	3 m	0.0043	≤ 0.020	Ok

Table 4.18: Kobe 1995 in Y direction

Story No	Displacement δ_x	$\Delta_x=\delta_x-\delta_{x-1}$	Floor height	Story drift ratio	Story drift ratio limit	Remarks
6	93 mm	5 mm	3 m	0.0017	≤ 0.020	Ok
5	88 mm	11 mm	3 m	0.0037	≤ 0.020	Ok
4	77 mm	16 mm	3 m	0.0053	≤ 0.020	Ok
3	61 mm	22 mm	3 m	0.0073	≤ 0.020	Ok
2	39 mm	23 mm	3 m	0.0077	≤ 0.020	Ok
1	16 mm	16 mm	3 m	0.0053	≤ 0.020	Ok

Table 4.19: Tabas 1978 in Y direction

Story No.	Displacement δ_x	$\Delta_x=\delta_x-\delta_{x-1}$	Floor height	Story drift ratio	Story drift ratio limit	Remarks
6	74 mm	6 mm	3 m	0.0020	≤ 0.020	Ok
5	68 mm	12 mm	3 m	0.0040	≤ 0.020	Ok
4	56 mm	15 mm	3 m	0.0050	≤ 0.020	Ok
3	41 mm	14 mm	3 m	0.0047	≤ 0.020	Ok
2	27 mm	16 mm	3 m	0.0053	≤ 0.020	Ok
1	11 mm	11 mm	3 m	0.0037	≤ 0.020	Ok

4.3.4.3 Model 2 (X direction)

The story drift ratio have been compared for building model 2 (AR = 1.5) with three ground motions in X direction are shown in Fig. 4.32. However, story drift ratio is found maximum at 2nd story for ground motion time histories applied in X direction. Maximum story drift ratio values are found to be 0.0080, 0.0097 and 0.0070 for building model 2 with ground motions El Centro, Kobe and Tabas respectively in X direction. Kobe 1995 shows the highest story drift ratio values among all the three ground motions.

Table 4.20: Story drift ratio in X direction for Model 2

Story No.	Story drift ratio		
	El Centro 1940	Kobe 1995	Tabas 1978
6	0.0027	0.0017	0.0020
5	0.0047	0.0040	0.0043
4	0.0063	0.0063	0.0053
3	0.0073	0.0090	0.0060
2	0.0080	0.0097	0.0070
1	0.0050	0.0063	0.0040
0	0	0	0

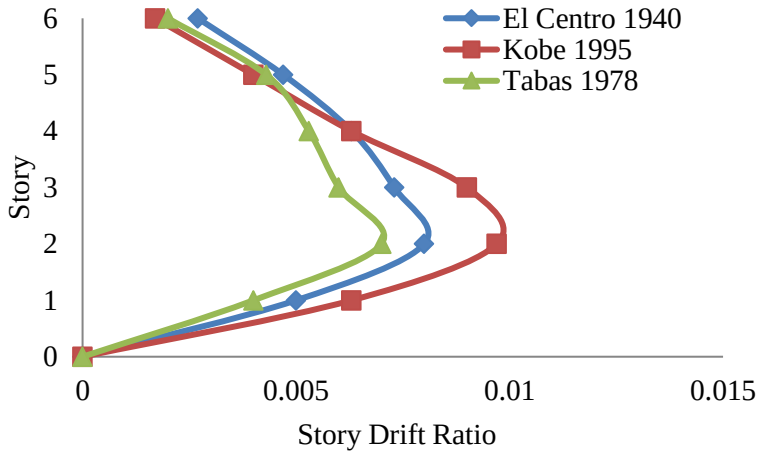

Fig. 4.32: Story drift ratio in X direction for Model 2

The maximum permissible limit for story drift ratio is 0.020 (BNBC, 2020). The maximum story drift ratio among all the cases is 0.0097 ≤ 0.020; hence Building Model 2 in X direction is found safe for all ground motions in term of story drift ratio as shown in the Table 4.21, 4.22 and 4.23.

Table 4.21: El Centro 1940 in X direction

Story No.	Displacement δ_x	$\Delta_x=\delta_x-\delta_{x-1}$	Floor height	Story drift ratio	Story drift ratio limit	Remarks
6	101 mm	8 mm	3 m	0.0027	≤ 0.020	Ok
5	93 mm	14 mm	3 m	0.0047	≤ 0.020	Ok
4	79 mm	19 mm	3 m	0.0063	≤ 0.020	Ok
3	60 mm	22 mm	3 m	0.0073	≤ 0.020	Ok
2	38 mm	23 mm	3 m	0.0080	≤ 0.020	Ok
1	15 mm	15 mm	3 m	0.0050	≤ 0.020	Ok

Table 4.22: Kobe 1995 in X direction

Story No	Displacement δ_x	$\Delta_x=\delta_x-\delta_{x-1}$	Floor height	Story drift ratio	Story drift ratio limit	Remarks
6	111 mm	5 mm	3 m	0.0017	≤ 0.020	Ok
5	106 mm	12 mm	3 m	0.0040	≤ 0.020	Ok
4	94 mm	19 mm	3 m	0.0063	≤ 0.020	Ok
3	75 mm	27 mm	3 m	0.0090	≤ 0.020	Ok
2	48 mm	29 mm	3 m	0.0097	≤ 0.020	Ok
1	19 mm	19 mm	3 m	0.0063	≤ 0.020	Ok

Table 4.23: Tabas 1978 in X direction

Story No.	Displacement δ_x	$\Delta_x=\delta_x-\delta_{x-1}$	Floor height	Story drift ratio	Story drift ratio limit	Remarks
6	86 mm	6 mm	3 m	0.0020	≤ 0.020	Ok
5	80 mm	13 mm	3 m	0.0043	≤ 0.020	Ok
4	67 mm	16 mm	3 m	0.0053	≤ 0.020	Ok
3	51 mm	18 mm	3 m	0.0060	≤ 0.020	Ok
2	33 mm	21 mm	3 m	0.0070	≤ 0.020	Ok
1	12 mm	12 mm	3 m	0.0040	≤ 0.020	Ok

4.3.4.4 Model 2 (Y direction)

The story drift ratio have been compared for building model 2 (AR = 1.5) with three ground motions in Y direction are shown in Fig. 4.33. However, story drift ratio is found maximum at 2nd story for ground motion time histories applied in Y direction. Maximum story drift ratio values are found to be 0.01, 0.0080 and 0.0083 for building model 2 with ground motions El Centro, Kobe and Tabas respectively in Y direction. El Centro 1940 shows the highest story drift ratio values among all the three ground motions.

Table 4.24: Story drift ratio in Y direction for Model 2

Story No.	Story drift ratio		
	El Centro 1940	Kobe 1995	Tabas 1978
6	0.002	0.0020	0.0027
5	0.0043	0.0040	0.0050
4	0.0067	0.0057	0.0067
3	0.0087	0.0073	0.0080
2	0.01	0.0080	0.0070
1	0.0067	0.0050	0.0040
0	0	0	0

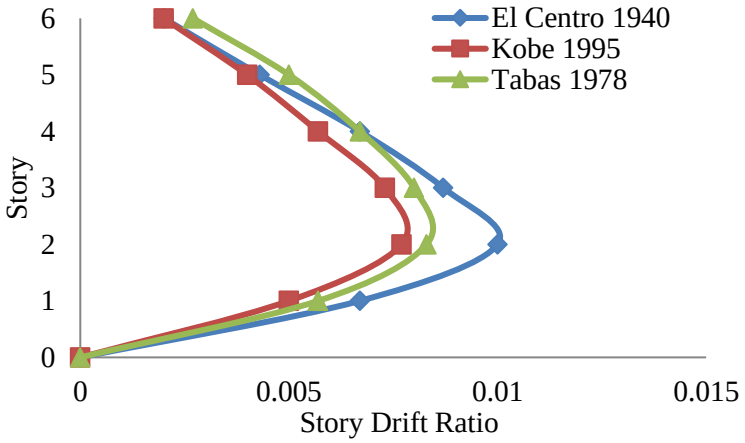

Fig. 4.33: Story drift ratio in Y direction for Model 2

The maximum permissible limit for story drift ratio is 0.020 (BNBC, 2020). The maximum story drift ratio among all the cases is 0.01 ≤ 0.020; hence Building Model 2 in Y direction is found safe for all ground motions in term of story drift ratio as shown in the Table 4.25, 4.26 and 4.27.

Table 4.25: El Centro 1940 in Y direction

Story No.	Displacement δ_x	$\Delta_x=\delta_x-\delta_{x-1}$	Floor height	Story drift ratio	Story drift ratio limit	Remarks
6	114 mm	6 mm	3 m	0.0020	≤ 0.020	Ok
5	108 mm	13 mm	3 m	0.0043	≤ 0.020	Ok
4	95 mm	20 mm	3 m	0.0067	≤ 0.020	Ok
3	75 mm	26 mm	3 m	0.0087	≤ 0.020	Ok
2	49 mm	29 mm	3 m	0.01	≤ 0.020	Ok
1	20 mm	20 mm	3 m	0.0067	≤ 0.020	Ok

Table 4.26: Kobe 1995 in Y direction

Story No.	Displacement δ_x	$\Delta_x=\delta_x-\delta_{x-1}$	Floor height	Story drift ratio	Story drift ratio limit	Remarks
6	95 mm	6 mm	3 m	0.0020	≤ 0.020	Ok
5	89 mm	12 mm	3 m	0.0040	≤ 0.020	Ok
4	77 mm	17 mm	3 m	0.0057	≤ 0.020	Ok
3	60 mm	22 mm	3 m	0.0073	≤ 0.020	Ok
2	38 mm	23 mm	3 m	0.0080	≤ 0.020	Ok
1	15 mm	15 mm	3 m	0.0050	≤ 0.020	Ok

Table 4.27: Tabas 1978 in Y direction

Story No.	Displacement δ_x	$\Delta_x=\delta_x-\delta_{x-1}$	Floor height	Story drift ratio	Story drift ratio limit	Remarks
6	109 mm	8 mm	3 m	0.0027	≤ 0.020	Ok
5	101 mm	15 mm	3 m	0.0050	≤ 0.020	Ok
4	86 mm	20 mm	3 m	0.0067	≤ 0.020	Ok
3	66 mm	24 mm	3 m	0.0080	≤ 0.020	Ok
2	42 mm	25 mm	3 m	0.0083	≤ 0.020	Ok
1	17 mm	17 mm	3 m	0.0057	≤ 0.020	Ok

4.3.4.5 Model 3 (X direction)

The story drift ratio have been compared for building model 3 (AR = 2) with three ground motions in X direction are shown in Fig. 4.34. However, story drift ratio is found maximum at 2nd story for ground motion time histories applied in X direction. Maximum story drift ratio values are found to be 0.0090, 0.0083 and 0.0083 for building model 3 with ground motions El Centro, Kobe and Tabas respectively in X direction. El Centro 1940 shows the highest story drift ratio values among all the three ground motions.

Table 4.28: Story drift ratio in X direction for Model 3

Story No.	Story drift ratio		
	El Centro 1940	Kobe 1995	Tabas 1978
6	0.0020	0.0013	0.0017
5	0.0043	0.0033	0.0037
4	0.0063	0.0057	0.0060
3	0.0087	0.0077	0.0077
2	0.0090	0.0083	0.0083
1	0.0067	0.0063	0.0057
0	0	0	0

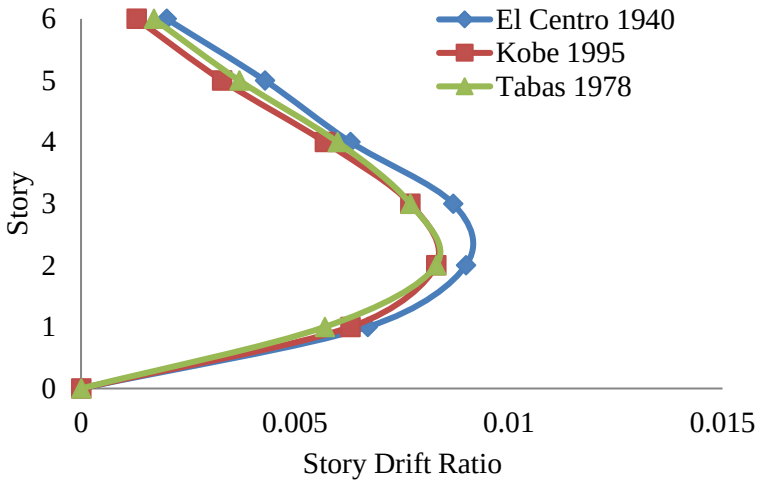

Fig. 4.34: Story drift ratio in X direction for Model 3

The maximum permissible limit for story drift ratio is 0.020 (BNBC, 2020). The maximum story drift ratio among all the cases is 0.0090 ≤ 0.020; hence Building Model 3 in X direction is found safe for all ground motions in term of story drift ratio as shown in the Table 4.29, 4.30 and 4.31.

Table 4.29: El Centro 1940 in X direction

Story No.	Displacement δ_x	$\Delta_x=\delta_x-\delta_{x-1}$	Floor height	Story drift ratio	Story drift ratio limit	Remarks
6	111 mm	6 mm	3 m	0.0020	≤ 0.020	Ok
5	105 mm	13 mm	3 m	0.0043	≤ 0.020	Ok
4	92 mm	19 mm	3 m	0.0063	≤ 0.020	Ok
3	73 mm	26 mm	3 m	0.0087	≤ 0.020	Ok
2	47 mm	27 mm	3 m	0.0090	≤ 0.020	Ok
1	20 mm	20 mm	3 m	0.0067	≤ 0.020	Ok

Table 4.30: Kobe 1995 in X direction

Story No.	Displacement δ_x	$\Delta_x=\delta_x-\delta_{x-1}$	Floor height	Story drift ratio	Story drift ratio limit	Remarks
6	98 mm	4 mm	3 m	0.0013	≤ 0.020	Ok
5	94 mm	10 mm	3 m	0.0033	≤ 0.020	Ok
4	84 mm	17 mm	3 m	0.0057	≤ 0.020	Ok
3	67 mm	23 mm	3 m	0.0077	≤ 0.020	Ok
2	44 mm	25 mm	3 m	0.0083	≤ 0.020	Ok
1	19 mm	19 mm	3 m	0.0063	≤ 0.020	Ok

Table 4.31: Tabas 1978 in X direction

Story No.	Displacement δ_x	$\Delta_x=\delta_x-\delta_{x-1}$	Floor height	Story drift ratio	Story drift ratio limit	Remarks
6	99 mm	5 mm	3 m	0.0017	≤ 0.020	Ok
5	94 mm	11 mm	3 m	0.0037	≤ 0.020	Ok
4	83 mm	18 mm	3 m	0.0060	≤ 0.020	Ok
3	65 mm	23 mm	3 m	0.0077	≤ 0.020	Ok
2	42 mm	25 mm	3 m	0.0083	≤ 0.020	Ok
1	17 mm	17 mm	3 m	0.0057	≤ 0.020	Ok

4.3.4.6 Model 3 (Y direction)

The story drift ratio have been compared for building model 3 (AR = 2) with three ground motions in Y direction are shown in Fig. 4.35. However, story drift ratio is found maximum at 2nd story for ground motion time histories applied in Y direction. Maximum story drift ratio values are found to be 0.012, 0.0090 and 0.0093 for building model 3 with ground motions El Centro, Kobe and Tabas respectively in Y direction. El Centro 1940 shows the highest story drift ratio values among all the three ground motions.

Table 4.32: Story drift ratio in Y direction for Model 3

Story No.	Story drift ratio		
	El Centro 1940	Kobe 1995	Tabas 1978
6	0.0030	0.0017	0.0027
5	0.0057	0.0040	0.0053
4	0.0083	0.0060	0.0060
3	0.011	0.0083	0.0083
2	0.012	0.0090	0.0093
1	0.0083	0.0070	0.0067
0	0	0	0

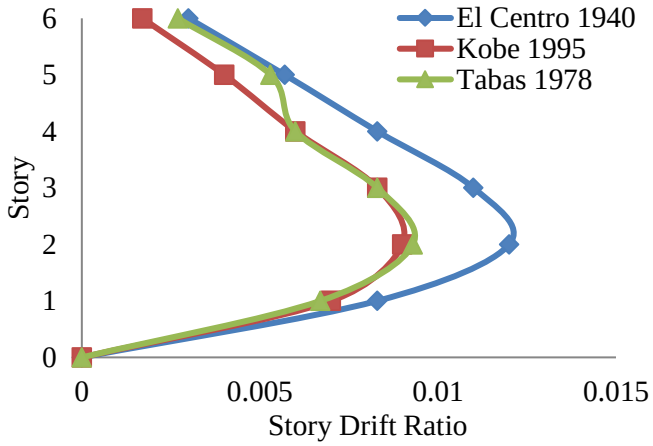

Fig. 4.35: Story drift ratio in Y direction for Model 3

The maximum permissible limit for story drift ratio is 0.020 (BNBC, 2020). The maximum story drift ratio among all the cases is 0.012 ≤ 0.020; hence Building Model 3 in Y direction is found safe for all ground motions in term of story drift ratio as shown in the Table 4.33, 4.34 and 4.35.

Table 4.33: El Centro 1940 in Y direction

Story No.	Displacement δ_x	$\Delta_x=\delta_x-\delta_{x-1}$	Floor height	Story drift ratio	Story drift ratio limit	Remarks
6	143 mm	9 mm	3 m	0.0030	≤ 0.020	Ok
5	134 mm	17 mm	3 m	0.0057	≤ 0.020	Ok
4	117 mm	25 mm	3 m	0.0083	≤ 0.020	Ok
3	92 mm	32 mm	3 m	0.011	≤ 0.020	Ok
2	60 mm	35 mm	3 m	0.012	≤ 0.020	Ok
1	25 mm	25 mm	3 m	0.0083	≤ 0.020	Ok

Table 4.34: Kobe 1995 in Y direction

Story No.	Displacement δ_x	$\Delta_x=\delta_x-\delta_{x-1}$	Floor height	Story drift ratio	Story drift ratio limit	Remarks
6	108 mm	5 mm	3 m	0.0017	≤ 0.020	Ok
5	103 mm	12 mm	3 m	0.0040	≤ 0.020	Ok
4	91 mm	18 mm	3 m	0.0060	≤ 0.020	Ok
3	73 mm	25 mm	3 m	0.0083	≤ 0.020	Ok
2	48 mm	27 mm	3 m	0.0090	≤ 0.020	Ok
1	21 mm	21 mm	3 m	0.0070	≤ 0.020	Ok

Table 4.35: Tabas 1978 in Y direction

Story No.	Displacement δ_x	$\Delta_x=\delta_x-\delta_{x-1}$	Floor height	Story drift ratio	Story drift ratio limit	Remarks
6	115 mm	8 mm	3 m	0.0027	≤ 0.020	Ok
5	107 mm	16 mm	3 m	0.0053	≤ 0.020	Ok
4	91 mm	18 mm	3 m	0.0060	≤ 0.020	Ok
3	73 mm	25 mm	3 m	0.0083	≤ 0.020	Ok
2	48 mm	28 mm	3 m	0.0093	≤ 0.020	Ok
1	20 mm	20 mm	3 m	0.0067	≤ 0.020	Ok

4.4 Comparison in Etabs Software

4.4.1 Maximum Story Displacement

4.4.1.1 El Centro 1940

The maximum story displacement values in X and Y directions for all three building models with different aspect ratios (AR) are shown in Fig. 4.36. For Model 1 (AR = 1), maximum story displacement is found to be 157 mm in both X and Y directions. For Model 2 (AR = 1.5), maximum story displacement is found to be 181 mm in X direction and 193 mm in Y direction. For Model 3 (AR = 2), maximum story displacement is found to be 210 mm in X direction and 233 mm in Y direction. Although, all three building models consist of same plan area, maximum story displacements increase in both X and Y directions with the increase of plan aspect ratios. There are 15% and 35% increase of maximum story displacements in X direction due to increase of aspect ratio 1.5 and 2 times respectively from basic square shape of plan. On the other hand, there are 23% and 50% increase of maximum story displacements in Y direction due to increase of aspect ratio 1.5 and 2 times respectively from basic square shape of plan.

Table 4.36: Maximum story displacement in X and Y directions for El Centro 1940

Aspect Ratio	Maximum story displacement (mm)	
	X direction	Y direction
1	157	157
1.5	181	193
2	210	233

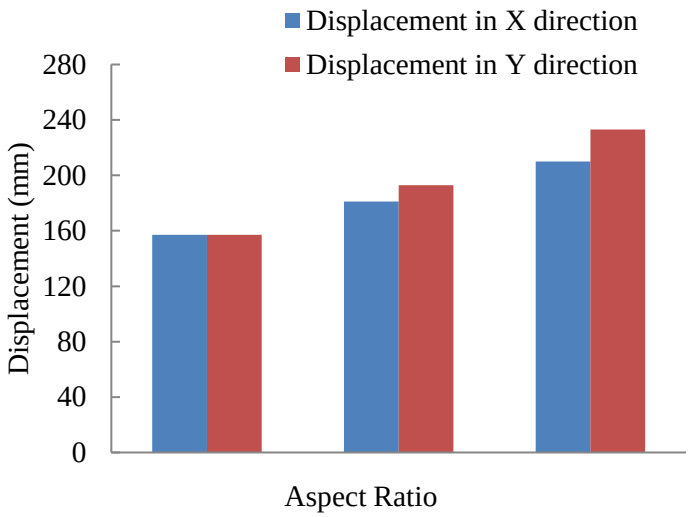

Fig. 4.36: Maximum story displacements along X and Y directions for El Centro 1940

4.4.1.2 Kobe 1995

The maximum story displacement values in X and Y directions for all three building models with different aspect ratios (AR) are shown in Fig. 4.37. For Model 1 (AR = 1), maximum story displacement is found to be 123 mm in both X and Y directions. For Model 2 (AR = 1.5), maximum story displacement is found to be 140 mm in X direction and 151 mm in Y direction. For Model 3 (AR = 2), maximum story displacement is found to be 150 mm in X direction and 159 mm in Y direction. Although, all three building models consist of same plan area, maximum story displacements increase in both X and Y directions with the increase of plan aspect ratios. There are 15% and 30% increase of maximum story displacements in X direction due to increase of aspect ratio 1.5 and 2 times respectively from basic square shape of plan. On the other hand, there are 23% and 35% increase of maximum story displacements in Y direction due to increase of aspect ratio 1.5 and 2 times respectively from basic square shape of plan.

Table 4.37: Maximum story displacement in X and Y directions for Kobe 1995

Aspect Ratio	Maximum story displacement (mm)	
	X direction	Y direction
1	123	123
1.5	140	151
2	158	164

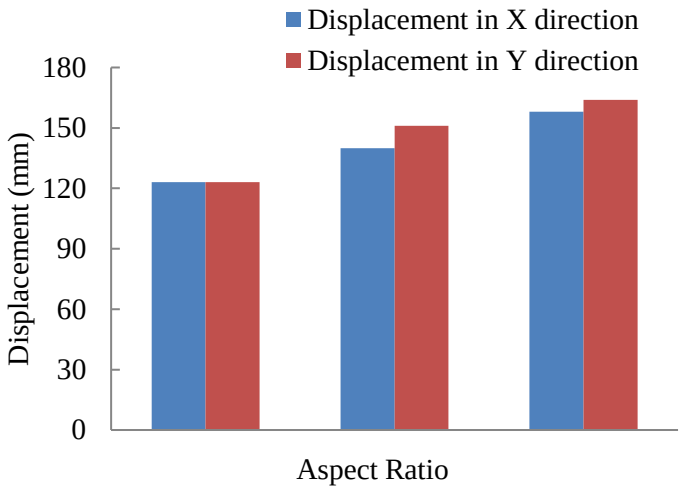

Fig. 4.37: Maximum story displacements along X and Y directions for Kobe 1995

4.4.1.3 Tabas 1978

The maximum story displacement values in X and Y directions for all three building models with different aspect ratios (AR) are shown in Fig. 4.38. For Model 1 (AR = 1), maximum story displacement is found to be 126 mm in both X and Y directions. For Model 2 (AR = 1.5), maximum story displacement is found to be 148 mm in X direction and 157 mm in Y direction. For Model 3 (AR = 2), maximum story displacement is found to be 170 mm in X direction and 180 mm in Y direction. Although, all three building models consist of same plan area, maximum story displacements increase in both X and Y directions with the increase of plan aspect ratios. There are 18% and 35% increase of maximum story displacements in X direction due to increase of aspect ratio 1.5 and 2 times respectively from basic square shape of plan. On the other hand, there are 25% and 43% increase of maximum story displacements in Y direction due to increase of aspect ratio 1.5 and 2 times respectively from basic square shape of plan.

Table 4.38: Maximum story displacement in X and Y directions for Tabas 1978

Aspect Ratio	Maximum story displacement (mm)	
	X direction	Y direction
1	126	126
1.5	148	157
2	170	180

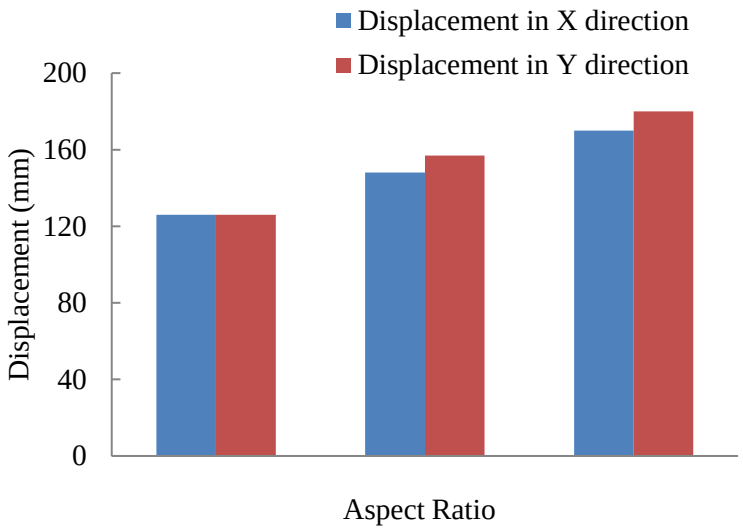

Fig. 4.38: Maximum story displacements along X and Y directions for Tabas 1978

4.4.2 Story Drift Ratio

4.4.2.1 El Centro 1940

The story drift ratio has been compared for all three building models with different aspect ratios (AR) in both X and Y directions are shown in Fig. 4.39 and Fig. 4.40 respectively. Similar to the maximum story displacement, story drift ratio are also increased in both X and Y directions with the increase of aspect ratios. However, story drift ratio are found maximum at 2nd story for ground motion time histories applied in both X and Y directions. Maximum story drift ratio values are found to be 0.014, 0.015 and 0.017 for building models with aspect ratios 1, 1.5 and 2 respectively in X direction. On the other hand, maximum story drift ratio values are found to be 0.014, 0.017 and 0.018 for building models with aspect ratios 1, 1.5 and 2 respectively in Y direction. It is observed that, there are 8% and 21% increase of maximum story drift ratio in X direction due to increase of aspect ratio 1.5 and 2 times respectively from basic square shape of plan. Similarly, there are 22% and 30% increase of

maximum story drift ratio in Y direction due to increase of aspect ratio 1.5 and 2 times respectively from basic square shape of plan. As building models become less stiff in Y direction with the increase of aspect ratios in X direction, maximum story displacements and story drift ratio are largely increased in Y direction compared to that in X direction.

Table 4.39: Story drift ratio in X direction for different aspect ratios for El Centro

Story No.	Story drift ratio		
	AR=1	AR=1.5	AR=2
6	0.0053	0.0070	0.0080
5	0.0060	0.0090	0.0097
4	0.0090	0.01	0.012
3	0.013	0.013	0.015
2	0.014	0.015	0.017
1	0.0047	0.0057	0.0077
0	0	0	0

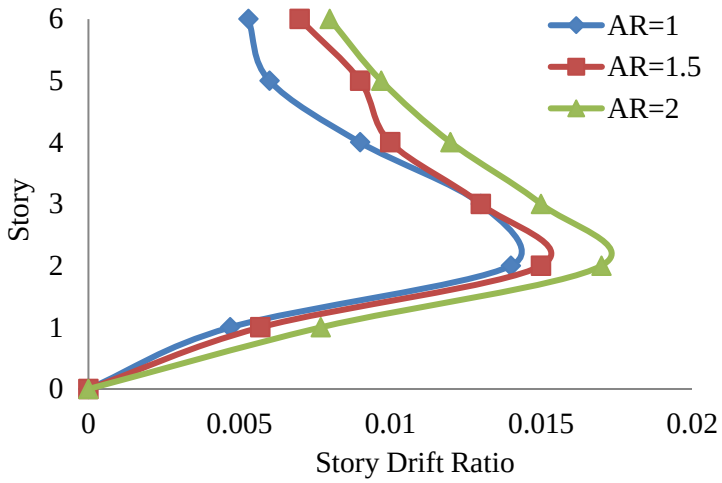

Fig. 4.39: Story drift ratio in X direction for different aspect ratios for El Centro 1940

Table 4.40: Story drift ratio in Y direction for different aspect ratios for El Centro

Story No.	Story drift ratio		
	AR=1	AR=1.5	AR=2
6	0.0053	0.0073	0.0090
5	0.006	0.0093	0.010
4	0.009	0.010	0.015
3	0.013	0.014	0.016
2	0.014	0.017	0.018
1	0.0047	0.0067	0.0083
0	0	0	0

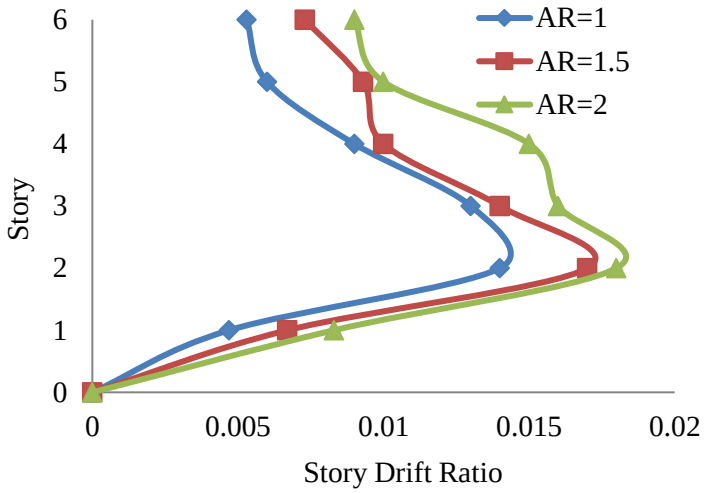

Fig. 4.40: Story drift ratio in Y direction for different aspect ratios for El Centro 1940

4.4.2.2 Kobe 1995

The story drift ratio has been compared for all three building models with different aspect ratios (AR) in both X and Y directions are shown in Fig. 4.41 and Fig. 4.42 respectively. Similar to the maximum story displacement, story drift ratio are also increased in both X and Y directions with the increase of aspect ratios. However, story drift ratio are found maximum at 2nd story for ground motion time histories applied in both X and Y directions. Maximum story drift ratio values are found to be 0.011, 0,013 and 0.014 for building models with aspect ratios 1, 1.5 and 2 respectively in X direction. On the other hand, maximum story drift ratio values are found to be 0.011, 0.014 and 0.015 for building models with aspect ratios 1, 1.5 and 2 respectively in Y direction. It is observed that, there are 18% and 27% increase of maximum story drift ratio in X direction due to increase of aspect ratio 1.5 and 2 times respectively from basic square shape of plan. Similarly, there are 28% and 36% increase of maximum story drift ratio in Y direction due to increase of aspect ratio 1.5 and 2 times respectively from basic square shape of plan. As building models become less stiff in Y direction with the increase of aspect ratios in X direction, maximum story displacements and story drift ratio are largely increased in Y direction compared to that in X direction.

Table 4.41: Story drift ratio in X direction for different aspect ratios for Kobe 1995

Story No.	Story drift ratio		
	AR=1	AR=1.5	AR=2
6	0.0040	0.0053	0.0060
5	0.0043	0.0063	0.0068
4	0.0090	0.0093	0.010
3	0.010	0.011	0.012
2	0.011	0.013	0.014
1	0.0020	0.0030	0.0036
0	0	0	0

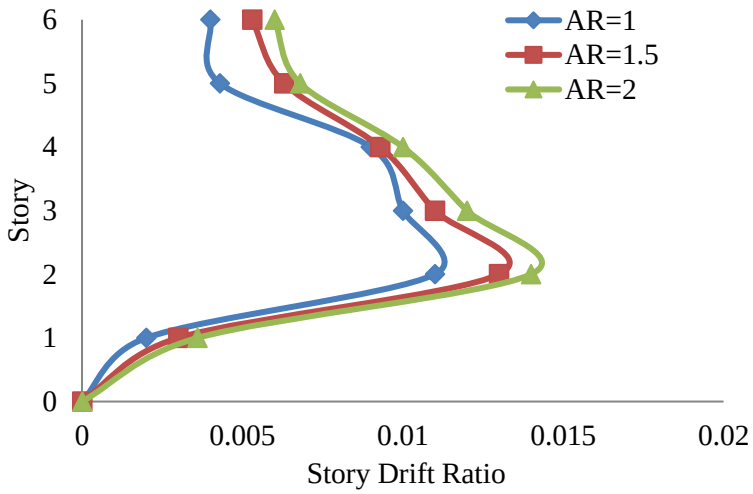

Fig. 4.41: Story drift ratio in X direction for different aspect ratios for Kobe 1995

Table 4.42: Story drift ratio in Y direction for different aspect ratios for Kobe 1995

Story No.	Story drift ratio		
	AR=1	AR=1.5	AR=2
6	0.0040	0.0056	0.0063
5	0.0043	0.0067	0.0073
4	0.0090	0.010	0.0093
3	0.010	0.012	0.013
2	0.011	0.014	0.015
1	0.0020	0.0023	0.0023
0	0	0	0

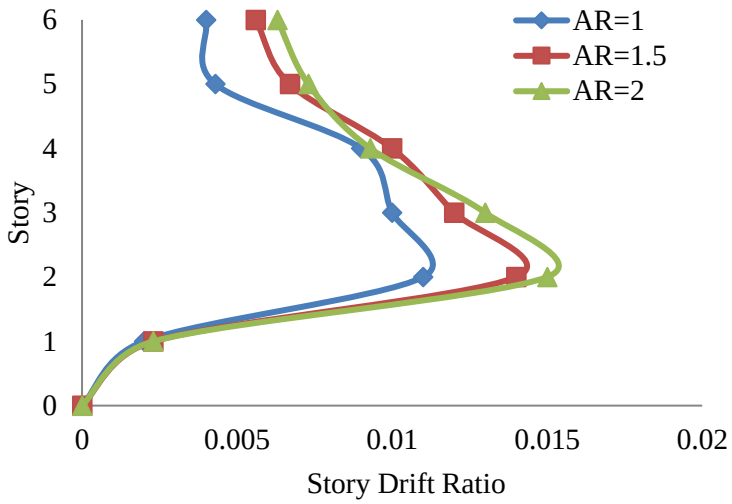

Fig. 4.42: Story drift ratio in Y direction for different aspect ratios for Kobe 1995

4.4.2.3 Tabas 1978

The story drift ratio has been compared for all three building models with different aspect ratios (AR) in both X and Y directions are shown in Fig. 4.43 and Fig. 4.44 respectively. Similar to the maximum story displacement, story drift ratio are also increased in both X and Y directions with the increase of aspect ratios. However, story drift ratio are found maximum at 2nd story for ground motion time histories applied in both X and Y directions. Maximum story drift ratio values are found to be 0.012, 0.014 and 0.015 for building models with aspect ratios 1, 1.5 and 2 respectively in X direction. On the other hand, maximum story drift ratio values are found to be 0.012, 0.015 and 0.016 for building models with aspect ratios 1, 1.5 and 2 respectively in Y direction. It is observed that, there are 17% and 25% increase of maximum story drift ratio in X direction due to increase of aspect ratio 1.5 and 2 times respectively from basic square shape of plan. Similarly, there are 26% and 34% increase of maximum story drift ratio in Y direction due to increase of aspect ratio 1.5 and 2 times respectively from basic square shape of plan. As building models become less stiff in Y direction with the increase of aspect ratios in X direction, maximum story displacements and story drift ratio are largely increased in Y direction compared to that in X direction.

Table 4.43: Story drift ratio in X direction for different aspect ratios for Tabas 1978

Story No.	Story drift ratio		
	AR=1	AR=1.5	AR=2
6	0.0030	0.0043	0.0060
5	0.0060	0.0083	0.0086
4	0.0093	0.0087	0.011
3	0.010	0.011	0.013
2	0.012	0.014	0.015
1	0.0020	0.0023	0.0033
0	0	0	0

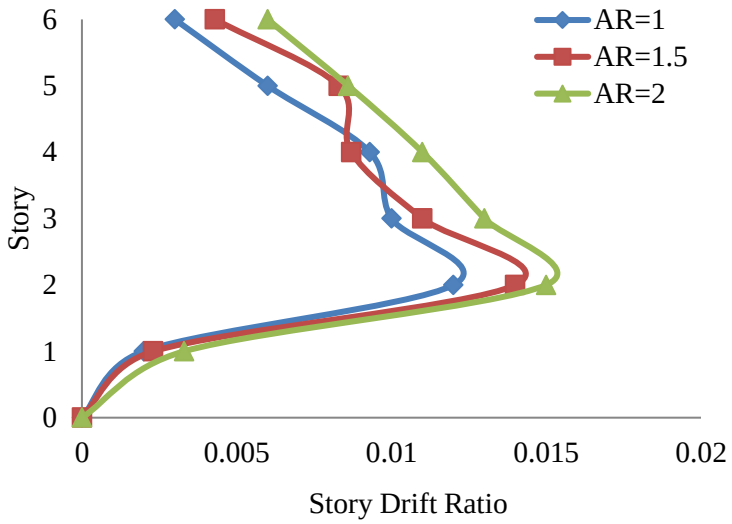

Fig. 4.43: Story drift ratio in X direction for different aspect ratios for Tabas 1978

Table 4.44: Story drift ratio in Y direction for different aspect ratios for Tabas 1978

Story No.	Story drift ratio		
	AR=1	AR=1.5	AR=2
6	0.0030	0.0050	0.0070
5	0.0060	0.0086	0.0090
4	0.0093	0.0096	0.010
3	0.010	0.011	0.014
2	0.012	0.015	0.016
1	0.0020	0.0027	0.0040
0	0	0	0

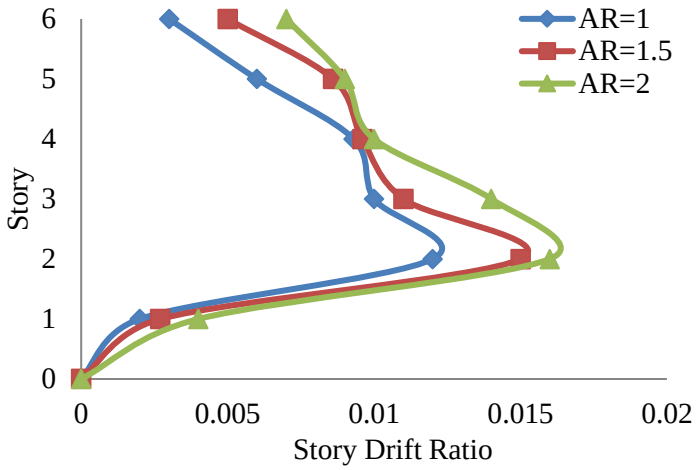

Fig. 4.44: Story drift ratio in Y direction for different aspect ratios for Tabas 1978

4.4.3 Comparison of Story Displacement for Different Ground Motions

4.4.3.1 All Models in X direction

The maximum story displacement values in X direction for building model 1, model 2 and model 3 (AR = 1, AR=1.5 and AR= 2) with three ground motions are shown in Fig. 4.45. For El Centro 1940, maximum story displacement model 1 is found to be 157 mm, model 2 is found to be 181 mm and model 3 is found to be 210 mm in X direction. For Kobe 1995, maximum story displacement model 1 is found to be 123 mm, model 2 is found to be 140 mm and model 3 is found to be 150 mm in X direction. For Tabas 1978, maximum story displacement model 1 is found to be 126 mm, model 2 is found to be 148 mm and model 3 is found to be 170 mm in X direction. Although, all three building models consist of same plan area, story displacement maximum El Centro 1940 in model 3. Seismic responses of buildings are assessed in terms of maximum story displacement in X direction. The maximum displacement value between these three ground motions (El Centro, Kobe and Tabas), that will do work with response.

Table 4.45: Maximum story displacement in X direction for all Models

Model	Maximum story displacement (mm)		
	El Centro 1940	Kobe 1995	Tabas 1978
Model 1	157	123	126
Model 2	181	140	148
Model 3	210	158	170

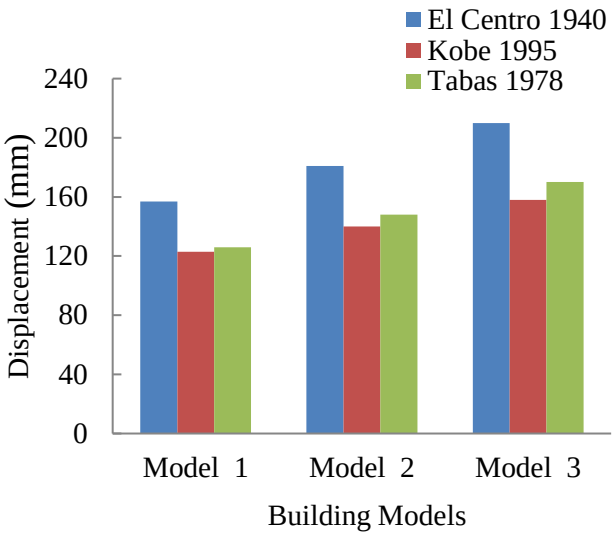

Fig. 4.45: Maximum story displacement in X direction for all Models

4.4.3.2 All Models in Y direction

The maximum story displacement values in Y direction for building model 1, model 2 and model 3 (AR = 1, AR=1.5 and AR= 2) with three ground motions are shown in Fig. 4.46. For El Centro 1940, maximum story displacement model 1 is found to be 157 mm, model 2 is found to be 193 mm and model 3 is found to be 233 mm in Y direction. For Kobe 1995, maximum story displacement model 1 is found to be 123 mm, model 2 is found to be 151 mm and model 3 is found to be 159 mm in Y direction. For Tabas 1978, maximum story displacement model 1 is found to be 126 mm, model 2 is found to be 157 mm and model 3 is found to be 180 mm in Y direction. Although, all three building models consist of same plan area, story displacement maximum El Centro 1940 in model 3. Seismic responses of buildings are assessed in terms of maximum story displacement in Y direction. The maximum displacement value between these three ground motions (El Centro, Kobe and Tabas), that will do work with response.

Table 4.46: Maximum story displacement in Y direction for all Models

Model	Maximum story displacement (mm)		
	El Centro 1940	Kobe 1995	Tabas 1978
Model 1	157	123	126
Model 2	193	151	157
Model 3	233	164	180

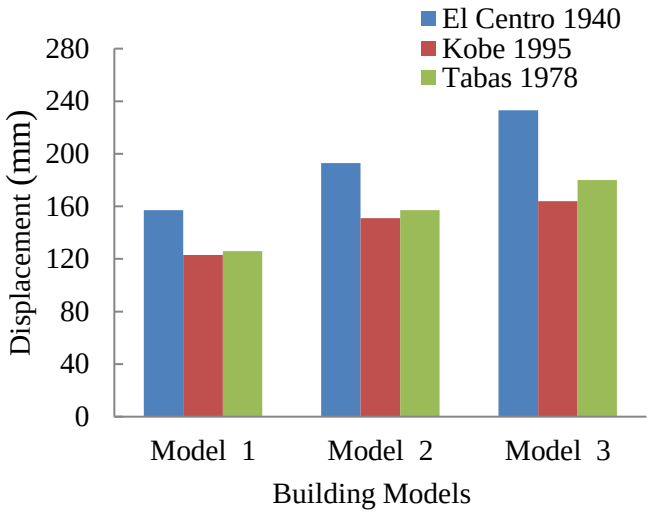

Fig. 4.46: Maximum story displacement in Y direction for all Models

4.4.4 Comparison of Story Drift Ratio

4.4.4.1 Model 1 (X direction)

The story drift ratio have been compared for building model 1 (AR = 1) with three ground motions in X direction are shown in Fig. 4.47. However, story drift ratio is found maximum at 2nd story for ground motion time histories applied in X direction. Maximum story drift ratio values are found to be 0.014, 0.011 and 0.012 for building model 1 with ground motions El Centro, Kobe and Tabas respectively in X direction. El Centro 1940 shows the highest story drift ratio values among all the three ground motions.

Table 4.47: Story drift ratio in X direction for Model 1

Story No.	Story drift ratio		
	El Centro 1940	Kobe 1995	Tabas 1978
6	0.0053	0.0040	0.0030
5	0.0060	0.0043	0.0060
4	0.0090	0.0090	0.0093
3	0.013	0.010	0.010
2	0.014	0.011	0.012
1	0.0047	0.0020	0.0020
0	0	0	0

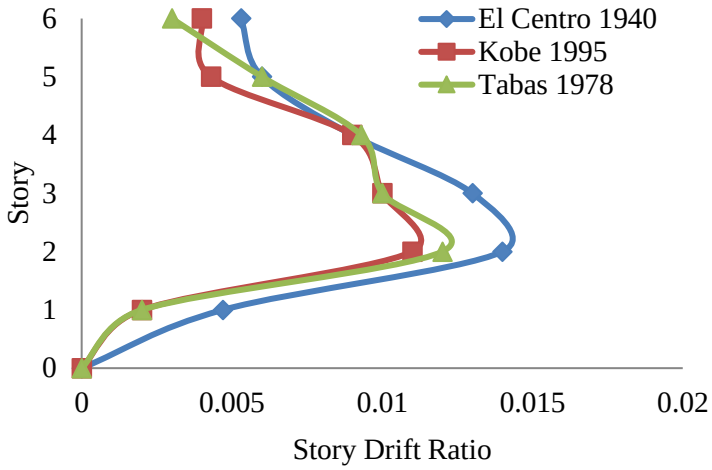

Fig. 4.47: Story drift ratio in X direction for Model 1

The maximum permissible limit for story drift ratio is 0.020 (BNBC, 2020). The maximum story drift ratio among all the cases is 0.014 ≤ 0.020; hence Building Model 1 in X direction is found safe for all ground motions in term of story drift ratio as shown in the Table 4.48, 4.49 and 4.50.

Table 4.48: El Centro 1940 in X direction

Story No.	Displacement δ_x	$\Delta_x=\delta_x-\delta_{x-1}$	Floor height	Story drift ratio	Story drift ratio limit	Remarks
6	157 mm	16 mm	3 m	0.0053	≤ 0.020	Ok
5	141 mm	18 mm	3 m	0.0060	≤ 0.020	Ok
4	123 mm	27 mm	3 m	0.0090	≤ 0.020	Ok
3	96 mm	40 mm	3 m	0.013	≤ 0.020	Ok
2	56 mm	42 mm	3 m	0.014	≤ 0.020	Ok
1	14 mm	14 mm	3 m	0.0047	≤ 0.020	Ok

Table 4.49: Kobe 1995 in X direction

Story No.	Displacement δ_x	$\Delta_x=\delta_x-\delta_{x-1}$	Floor height	Story drift ratio	Story drift ratio limit	Remarks
6	123 mm	12 mm	3 m	0.0040	≤ 0.020	Ok
5	111 mm	13 mm	3 m	0.0043	≤ 0.020	Ok
4	98 mm	28 mm	3 m	0.0090	≤ 0.020	Ok
3	70 mm	30 mm	3 m	0.010	≤ 0.020	Ok
2	40 mm	34 mm	3 m	0.011	≤ 0.020	Ok
1	6 mm	6 mm	3 m	0.0020	≤ 0.020	Ok

Table 4.50: Tabas 1978 in X direction

Story No.	Displacement δ_x	$\Delta_x=\delta_x-\delta_{x-1}$	Floor height	Story drift ratio	Story drift ratio limit	Remarks
6	126 mm	9 mm	3 m	0.0030	≤ 0.020	Ok
5	117 mm	18 mm	3 m	0.0060	≤ 0.020	Ok
4	99 mm	28 mm	3 m	0.0093	≤ 0.020	Ok
3	71 mm	30 mm	3 m	0.010	≤ 0.020	Ok
2	41 mm	35 mm	3 m	0.012	≤ 0.020	Ok
1	6 mm	6 mm	3 m	0.0020	≤ 0.020	Ok

4.4.4.2 Model 1 (Y direction)

The story drift ratio have been compared for building model 1 (AR = 1) with three ground motions in Y direction are shown in Fig. 4.48. However, story drift ratio is found maximum at 2nd story for ground motion time histories applied in Y direction. Maximum story drift ratio values are found to be 0.014, 0.011 and 0.012 for building model 1 with ground motions El Centro, Kobe and Tabas respectively in Y direction. El Centro 1940 shows the highest story drift ratio values among all the three ground motions.

Table 4.51: Story drift ratio in Y direction for Model 1

Story No.	Story drift ratio		
	El Centro 1940	Kobe 1995	Tabas 1978
6	0.0053	0.0040	0.0030
5	0.0060	0.0043	0.0060
4	0.0090	0.0090	0.0093
3	0.013	0.010	0.010
2	0.014	0.011	0.012
1	0.0047	0.0020	0.0020
0	0	0	0

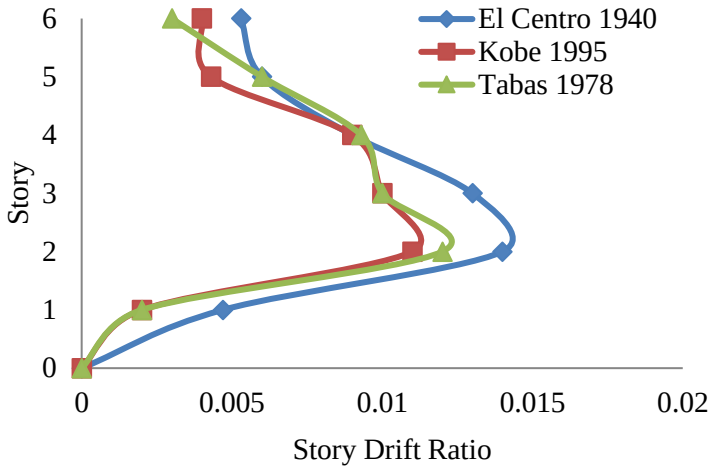

Fig. 4.48: Story drift ratio in Y direction for Model 1

The maximum permissible limit for story drift ratio is 0.020 (BNBC, 2020). The maximum story drift ratio among all the cases is 0.014 ≤ 0.020; hence Building Model 1 in Y direction is found safe for all ground motions in term of story drift ratio as shown in the Table 4.52, 4.53 and 4.54.

Table 4.52: El Centro 1940 in Y direction

Story No.	Displacement δ_x	$\Delta_x=\delta_x-\delta_{x-1}$	Floor height	Story drift ratio	Story drift ratio limit	Remarks
6	157 mm	16 mm	3 m	0.0053	≤ 0.020	Ok
5	141 mm	18 mm	3 m	0.0060	≤ 0.020	Ok
4	123 mm	27 mm	3 m	0.0090	≤ 0.020	Ok
3	96 mm	40 mm	3 m	0.013	≤ 0.020	Ok
2	56 mm	42 mm	3 m	0.014	≤ 0.020	Ok
1	14 mm	14 mm	3 m	0.0047	≤ 0.020	Ok

Table 4.53: Kobe 1995 in Y direction

Story No.	Displacement δ_x	$\Delta_x=\delta_x-\delta_{x-1}$	Floor height	Story drift ratio	Story drift ratio limit	Remarks
6	123 mm	12 mm	3 m	0.0040	≤ 0.020	Ok
5	111 mm	13 mm	3 m	0.0043	≤ 0.020	Ok
4	98 mm	28 mm	3 m	0.0090	≤ 0.020	Ok
3	70 mm	30 mm	3 m	0.010	≤ 0.020	Ok
2	40 mm	34 mm	3 m	0.011	≤ 0.020	Ok
1	6 mm	6 mm	3 m	0.0020	≤ 0.020	Ok

Table 4.54: Tabas 1978 in Y direction

Story No.	Displacement δ_x	$\Delta_x=\delta_x-\delta_{x-1}$	Floor height	Story drift ratio	Story drift ratio limit	Remarks
6	126 mm	9 mm	3 m	0.0030	≤ 0.020	Ok
5	117 mm	18 mm	3 m	0.0060	≤ 0.020	Ok
4	99 mm	28 mm	3 m	0.0093	≤ 0.020	Ok
3	71 mm	30 mm	3 m	0.010	≤ 0.020	Ok
2	41 mm	35 mm	3 m	0.012	≤ 0.020	Ok
1	6 mm	6 mm	3 m	0.0020	≤ 0.020	Ok

4.4.4.3 Model 2 (X direction)

The story drift ratio have been compared for building model 2 (AR = 1.5) with three ground motions in X direction are shown in Fig. 4.49. However, story drift ratio is found maximum at 2nd story for ground motion time histories applied in X direction. Maximum story drift ratio values are found to be 0.015, 0.013 and 0.014 for building model 2 with ground motions El Centro, Kobe and Tabas respectively in X direction. El Centro 1940 shows the highest story drift ratio values among all the three ground motions.

Table 4.55: Story drift ratio in X direction for Model 2

Story No.	Story drift ratio		
	El Centro 1940	Kobe 1995	Tabas 1978
6	0.0070	0.0053	0.0043
5	0.0090	0.0063	0.0083
4	0.010	0.0093	0.0087
3	0.013	0.011	0.011
2	0.015	0.013	0.014
1	0.0057	0.0030	0.0023
0	0	0	0

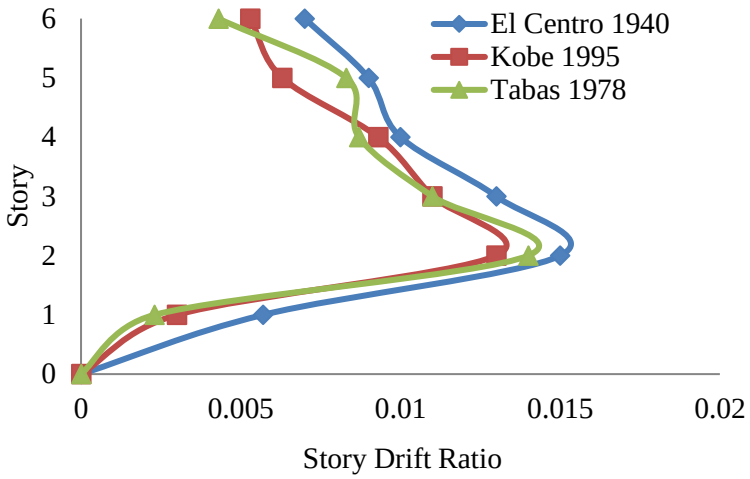

Fig. 4.49: Story drift ratio in X direction for Model 2

The maximum permissible limit for story drift ratio is 0.020 (BNBC, 2020). The maximum story drift ratio among all the cases is 0.015 ≤ 0.020; hence Building Model 2 in X direction is found safe for all ground motions in term of story drift ratio as shown in the Table 4.56, 4.57 and 4.58.

Table 4.56: El Centro 1940 in X direction

Story No.	Displacement δ_x	$\Delta_x=\delta_x-\delta_{x-1}$	Floor height	Story drift ratio	Story drift ratio limit	Remarks
6	181 mm	21 mm	3 m	0.0070	≤ 0.020	Ok
5	160 mm	27 mm	3 m	0.0090	≤ 0.020	Ok
4	133 mm	30 mm	3 m	0.010	≤ 0.020	Ok
3	103 mm	40 mm	3 m	0.013	≤ 0.020	Ok
2	63 mm	46 mm	3 m	0.015	≤ 0.020	Ok
1	17 mm	17 mm	3 m	0.0057	≤ 0.020	Ok

Table 4.57: Kobe 1995 in X direction

Story No	Displacement δ_x	$\Delta_x=\delta_x-\delta_{x-1}$	Floor height	Story drift ratio	Story drift ratio limit	Remarks
6	140 mm	16 mm	3 m	0.0053	≤ 0.020	Ok
5	124 mm	22 mm	3 m	0.0063	≤ 0.020	Ok
4	102 mm	28 mm	3 m	0.0093	≤ 0.020	Ok
3	74 mm	30 mm	3 m	0.011	≤ 0.020	Ok
2	44 mm	35 mm	3 m	0.013	≤ 0.020	Ok
1	9 mm	9 mm	3 m	0.0030	≤ 0.020	Ok

Table 4.58: Tabas 1978 in X direction

Story No.	Displacement δ_x	$\Delta_x=\delta_x-\delta_{x-1}$	Floor height	Story drift ratio	Story drift ratio limit	Remarks
6	148 mm	13 mm	3 m	0.0043	≤ 0.020	Ok
5	135 mm	25 mm	3 m	0.0083	≤ 0.020	Ok
4	110 mm	26 mm	3 m	0.0087	≤ 0.020	Ok
3	84 mm	34 mm	3 m	0.011	≤ 0.020	Ok
2	50 mm	43 mm	3 m	0.014	≤ 0.020	Ok
1	7 mm	7 mm	3 m	0.0023	≤ 0.020	Ok

4.4.4.4 Model 2 (Y direction)

The story drift ratio have been compared for building model 2 (AR = 1.5) with three ground motions in Y direction are shown in Fig. 4.50. However, story drift ratio is found maximum at 2nd story for ground motion time histories applied in Y direction. Maximum story drift ratio values are found to be 0.017, 0.014 and 0.015 for building model 2 with ground motions El Centro, Kobe and Tabas respectively in Y direction. El Centro 1940 shows the highest story drift ratio values among all the three ground motions.

Table 4.59: Story drift ratio in Y direction for Model 2

Story No.	Story drift ratio		
	El Centro 1940	Kobe 1995	Tabas 1978
6	0.0073	0.0056	0.0050
5	0.0097	0.0067	0.0086
4	0.010	0.010	0.0096
3	0.014	0.012	0.011
2	0.017	0.014	0.015
1	0.0067	0.0023	0.0027
0	0	0	0

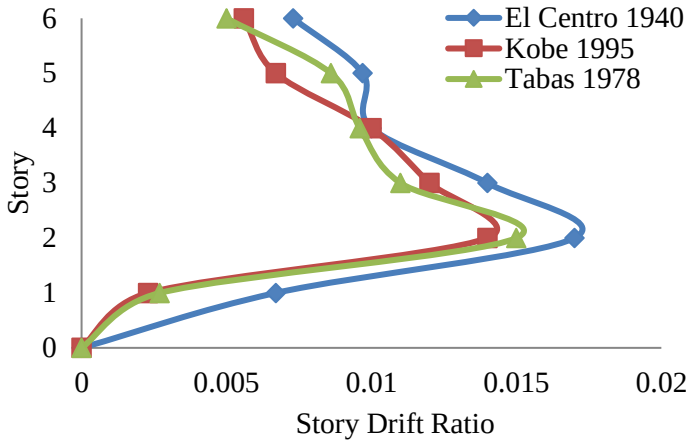

Fig. 4.50: Story drift ratio in Y direction for Model 2

The maximum permissible limit for story drift ratio is 0.020 (BNBC, 2020). The maximum story drift ratio among all the cases is 0.017 ≤ 0.020; hence Building Model 2 in Y direction is found safe for all ground motions in term of story drift ratio as shown in the Table 4.60, 4.61 and 4.62.

Table 4.60: El Centro 1940 in Y direction

Story No.	Displacement δ_x	$\Delta_x=\delta_x-\delta_{x-1}$	Floor height	Story drift ratio	Story drift ratio limit	Remarks
6	193 mm	22 mm	3 m	0.0073	≤ 0.020	Ok
5	171 mm	29 mm	3 m	0.0097	≤ 0.020	Ok
4	142 mm	30 mm	3 m	0.010	≤ 0.020	Ok
3	112 mm	42 mm	3 m	0.014	≤ 0.020	Ok
2	70 mm	50 mm	3 m	0.017	≤ 0.020	Ok
1	20 mm	20 mm	3 m	0.0067	≤ 0.020	Ok

Table 4.61: Kobe 1995 in Y direction

Story No.	Displacement δ_x	$\Delta_x=\delta_x-\delta_{x-1}$	Floor height	Story drift ratio	Story drift ratio limit	Remarks
6	151 mm	17 mm	3 m	0.0056	≤ 0.020	Ok
5	134 mm	20 mm	3 m	0.0067	≤ 0.020	Ok
4	114 mm	29 mm	3 m	0.010	≤ 0.020	Ok
3	85 mm	37 mm	3 m	0.012	≤ 0.020	Ok
2	48 mm	41 mm	3 m	0.014	≤ 0.020	Ok
1	7 mm	7 mm	3 m	0.0023	≤ 0.020	Ok

Table 4.62: Tabas 1978 in Y direction

Story No.	Displacement δ_x	$\Delta_x=\delta_x-\delta_{x-1}$	Floor height	Story drift ratio	Story drift ratio limit	Remarks
6	157 mm	15 mm	3 m	0.0050	≤ 0.020	Ok
5	142 mm	26 mm	3 m	0.0086	≤ 0.020	Ok
4	116 mm	29 mm	3 m	0.0096	≤ 0.020	Ok
3	87 mm	34 mm	3 m	0.011	≤ 0.020	Ok
2	53 mm	45 mm	3 m	0.015	≤ 0.020	Ok
1	8 mm	8 mm	3 m	0.0027	≤ 0.020	Ok

4.4.4.5 Model 3 (X direction)

The story drift ratio have been compared for building model 3 (AR = 2) with three ground motions in X direction are shown in Fig. 4.51. However, story drift ratio is found maximum at 2nd story for ground motion time histories applied in X direction. Maximum story drift ratio values are found to be 0.017, 0.014 and 0.015 for building model 3 with ground motions El Centro, Kobe and Tabas respectively in X direction. El Centro 1940 shows the highest story drift ratio values among all the three ground motions.

Table 4.63: Story drift ratio in X direction for Model 3

Story No.	Story drift ratio		
	El Centro 1940	Kobe 1995	Tabas 1978
6	0.0080	0.0060	0.0060
5	0.0097	0.0068	0.0086
4	0.012	0.010	0.011
3	0.015	0.012	0.013
2	0.017	0.014	0.015
1	0.0077	0.0036	0.0033
0	0	0	0

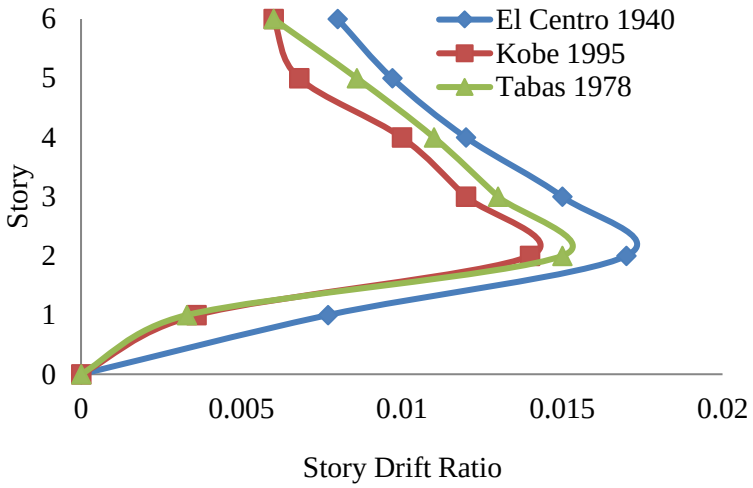

Fig. 4.51: Story drift ratio in X direction for Model 3

The maximum permissible limit for story drift ratio is 0.020 (BNBC, 2020). The maximum story drift ratio among all the cases is 0.017 ≤ 0.020; hence Building Model 3 in X direction is found safe for all ground motions in term of story drift ratio as shown in the Table 4.64, 4.65 and 4.66.

Table 4.64: El Centro 1940 in X direction

Story No.	Displacement δ_x	$\Delta_x=\delta_x-\delta_{x-1}$	Floor height	Story drift ratio	Story drift ratio limit	Remarks
6	210 mm	24 mm	3 m	0.0080	≤ 0.020	Ok
5	186 mm	29 mm	3 m	0.0097	≤ 0.020	Ok
4	157 mm	38 mm	3 m	0.012	≤ 0.020	Ok
3	119 mm	46 mm	3 m	0.015	≤ 0.020	Ok
2	73 mm	50 mm	3 m	0.017	≤ 0.020	Ok
1	23 mm	23 mm	3 m	0.0077	≤ 0.020	Ok

Table 4.65: Kobe 1995 in X direction

Story No.	Displacement δ_x	$\Delta_x=\delta_x-\delta_{x-1}$	Floor height	Story drift ratio	Story drift ratio limit	Remarks
6	158 mm	18 mm	3 m	0.0060	≤ 0.020	Ok
5	140 mm	20 mm	3 m	0.0068	≤ 0.020	Ok
4	120 mm	30 mm	3 m	0.010	≤ 0.020	Ok
3	90 mm	37 mm	3 m	0.012	≤ 0.020	Ok
2	53 mm	42 mm	3 m	0.014	≤ 0.020	Ok
1	11 mm	11 mm	3 m	0.0036	≤ 0.020	Ok

Table 4.66: Tabas 1978 in X direction

Story No.	Displacement δ_x	$\Delta_x=\delta_x-\delta_{x-1}$	Floor height	Story drift ratio	Story drift ratio limit	Remarks
6	170 mm	18 mm	3 m	0.0060	≤ 0.020	Ok
5	152 mm	26 mm	3 m	0.0086	≤ 0.020	Ok
4	126 mm	33 mm	3 m	0.011	≤ 0.020	Ok
3	93 mm	38 mm	3 m	0.013	≤ 0.020	Ok
2	55 mm	45 mm	3 m	0.015	≤ 0.020	Ok
1	10 mm	10 mm	3 m	0.0033	≤ 0.020	Ok

4.4.4.6 Model 3 (Y direction)

The story drift ratio have been compared for building model 3 (AR = 2) with three ground motions in Y direction are shown in Fig. 4.52. However, story drift ratio is found maximum at 2nd story for ground motion time histories applied in Y direction. Maximum story drift ratio values are found to be 0.018, 0.015 and 0.016 for building model 3 with ground motions El Centro, Kobe and Tabas respectively in Y direction. El Centro 1940 shows the highest story drift ratio values among all the three ground motions.

Table 4.67: Story drift ratio in Y direction for Model 3

Story No.	Story drift ratio		
	El Centro 1940	Kobe 1995	Tabas 1978
6	0.0090	0.0063	0.0070
5	0.010	0.0073	0.0090
4	0.015	0.0093	0.010
3	0.016	0.013	0.014
2	0.018	0.015	0.016
1	0.0083	0.0023	0.0040
0	0	0	0

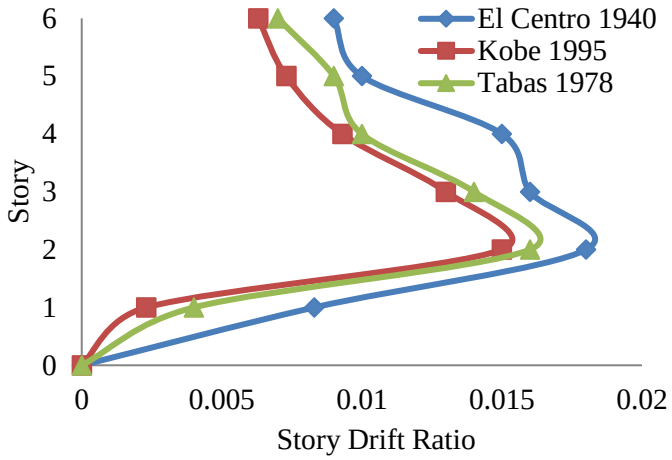

Fig. 4.52: Story drift ratio in Y direction for Model 3

The maximum permissible limit for story drift ratio is 0.020 (BNBC, 2020). The maximum story drift ratio among all the cases is 0.018 ≤ 0.020; hence Building Model 3 in Y direction is found safe for all ground motions in term of story drift ratio as shown in the Table 4.33, 4.34 and 4.35.

Table 4.68: El Centro 1940 in Y direction

Story No.	Displacement δ_x	$\Delta_x=\delta_x-\delta_{x-1}$	Floor height	Story drift ratio	Story drift ratio limit	Remarks
6	233 mm	27 mm	3 m	0.0090	≤ 0.020	Ok
5	206 mm	30 mm	3 m	0.010	≤ 0.020	Ok
4	176 mm	47 mm	3 m	0.015	≤ 0.020	Ok
3	129 mm	50 mm	3 m	0.016	≤ 0.020	Ok
2	79 mm	54 mm	3 m	0.018	≤ 0.020	Ok
1	25 mm	25 mm	3 m	0.0083	≤ 0.020	Ok

Table 4.69: Kobe 1995 in Y direction

Story No.	Displacement δ_x	$\Delta_x=\delta_x-\delta_{x-1}$	Floor height	Story drift ratio	Story drift ratio limit	Remarks
6	164 mm	19 mm	3 m	0.0063	≤ 0.020	Ok
5	145 mm	22 mm	3 m	0.0073	≤ 0.020	Ok
4	123 mm	28 mm	3 m	0.0093	≤ 0.020	Ok
3	95 mm	41 mm	3 m	0.013	≤ 0.020	Ok
2	54 mm	47 mm	3 m	0.015	≤ 0.020	Ok
1	7 mm	7 mm	3 m	0.0023	≤ 0.020	Ok

Table 4.70: Tabas 1978 in Y direction

Story No.	Displacement δ_x	$\Delta_x=\delta_x-\delta_{x-1}$	Floor height	Story drift ratio	Story drift ratio limit	Remarks
6	180 mm	21 mm	3 m	0.0070	≤ 0.020	Ok
5	159 mm	27 mm	3 m	0.0090	≤ 0.020	Ok
4	132 mm	30 mm	3 m	0.010	≤ 0.020	Ok
3	102 mm	42 mm	3 m	0.014	≤ 0.020	Ok
2	60 mm	48 mm	3 m	0.016	≤ 0.020	Ok
1	12 mm	12 mm	3 m	0.0040	≤ 0.020	Ok

4.5 Synopsis

In this chapter, Seismic responses of all building models are evaluated in terms of maximum story displacements and story drift ratio. Maximum story displacement is increased in Y direction compared to that in X direction. Story drift ratio are found maximum at 2nd story for ground motion time histories applied in both X and Y directions. Moreover, maximum story drift ratio is governed on the second story of all building models in both directions. So, for this particular study, the location of occurrence of maximum story drift ratio is independent of plan aspect ratios as the total plan area are same for all building models concentrating same seismic weight on similar floors of different models.

Chapter 5
CONCLUSION

5.1 General

Three different aspect ratios in three different six storied building models have been considered in the study. Aspect ratios of 1, 1.5 and 2 are considered for this purpose. These buildings are modeled using nonlinear seismic analysis software, SeismoStruct and ETABS. Three ground motion time histories have been considered for the time history analysis of the building models in accordance with current building codes. In this regard, El Centro 1940, Kobe 1995, Tabas 1978 ground motions records are matched with design response spectrum of a specific seismic zone and site class according to Bangladesh National Building Code. Nonlinear time history analysis has been conducted using matched ground motion records applied at the fixed base of all columns in X and Y direction separately. Seismic responses of building models are evaluated in terms of maximum story displacements and story drift ratio.

5.2 Summary

- In Seismostruct Software, for matched El Centro 1940 ground motion, maximum story displacement and story drift ratio have been compared for all three building models with different aspect ratios (AR) in both X and Y directions. There are 35% and 50% increase of maximum story displacements in X direction due to increase of aspect ratio 1.5 and 2 times respectively from basic square shape of plan. However, there are 55% and 95% increase of maximum story displacements in Y direction due to increase of aspect ratio 1.5 and 2 times respectively. On the other hand, there are 35% and 50% increase of maximum story drift ratio in X direction due to increase of aspect ratio 1.5 and 2 times respectively. Similarly, there are 65% and 100% increase of maximum story drift ratio in Y direction due to increase of aspect ratio 1.5 and 2 times respectively. As building models become less stiff in Y direction with the increase of aspect ratios in X direction, maximum story displacements and story drift ratio are largely increased in Y direction compared to that in X direction.

- In Etabs Software, for matched El Centro 1940 ground motion, maximum story displacement and story drift ratio have been compared for all three building models with different aspect ratios (AR) in both X and Y directions. There are 15% and 35% increase of maximum story displacements in X direction due to increase of aspect ratio 1.5 and 2 times respectively from basic square shape of plan. However, there are 23% and 50% increase of maximum story displacements in Y direction due to increase of aspect ratio 1.5 and 2 times respectively. On the other hand, there are 8% and 21% increase of maximum story drift ratio in X direction due to increase of aspect ratio 1.5 and 2 times respectively. Similarly, there are 22% and 30% increase of maximum story drift ratio in Y direction due to increase of aspect ratio 1.5 and 2 times respectively. As building models become less stiff in Y direction with the increase of aspect ratios in X direction, maximum story displacements and story drift ratio are largely increased in Y direction compared to that in X direction.
- In Seismostruct Software, for matched Kobe 1995 ground motion, maximum story displacement and story drift ratio have been compared for all three building models with different aspect ratios (AR) in both X and Y directions. There are 20% and 6% increase of maximum story displacements in X direction due to increase of aspect ratio 1.5 and 2 times respectively from basic square shape of plan. However, there are 3% and 16% increase of maximum story displacements in Y direction due to increase of aspect ratio 1.5 and 2 times respectively. On the other hand, there are 26% and 8% increase of maximum story drift ratio in X direction due to increase of aspect ratio 1.5 and 2 times respectively. Similarly, there are 4% and 17% increase of maximum story drift ratio in Y direction due to increase of aspect ratio 1.5 and 2 times respectively. For Model 2 (AR = 1.5), maximum story displacements and story drift ratio are increased in X direction compared to that in Y direction and For Model 3 (AR = 2), maximum story displacements and story drift ratio are increased in Y direction compared to that in X direction.
- In Etabs Software, for matched Kobe 1995 ground motion, maximum story displacement and story drift ratio have been compared for all three building models with different aspect ratios (AR) in both X and Y directions. There are 15% and 30% increase of maximum story displacements in X direction due to

increase of aspect ratio 1.5 and 2 times respectively from basic square shape of plan. However, there are 23% and 35% increase of maximum story displacements in Y direction due to increase of aspect ratio 1.5 and 2 times respectively. On the other hand, there are 18% and 27% increase of maximum story drift ratio in X direction due to increase of aspect ratio 1.5 and 2 times respectively. Similarly, there are 28% and 36% increase of maximum story drift ratio in Y direction due to increase of aspect ratio 1.5 and 2 times respectively. As building models become less stiff in Y direction with the increase of aspect ratios in X direction, maximum story displacements and story drift ratio are largely increased in Y direction compared to that in X direction.

- In Seismostruct Software, for matched Tabas 1978 ground motion, maximum story displacement and story drift ratio have been compared for all three building models with different aspect ratios (AR) in both X and Y directions. There are 17% and 34% increase of maximum story displacements in X direction due to increase of aspect ratio 1.5 and 2 times respectively from basic square shape of plan. However, there are 48% and 56% increase of maximum story displacements in Y direction due to increase of aspect ratio 1.5 and 2 times respectively. On the other hand, there are 32% and 57% increase of maximum story drift ratio in X direction due to increase of aspect ratio 1.5 and 2 times respectively. Similarly, there are 57% and 76% increase of maximum story drift ratio in Y direction due to increase of aspect ratio 1.5 and 2 times respectively. As building models become less stiff in Y direction with the increase of aspect ratios in X direction, maximum story displacements and story drift ratio are largely increased in Y direction compared to that in X direction.
- In Etabs Software, for matched Tabas 1978 ground motion, maximum story displacement and story drift ratio have been compared for all three building models with different aspect ratios (AR) in both X and Y directions. There are 18% and 35% increase of maximum story displacements in X direction due to increase of aspect ratio 1.5 and 2 times respectively from basic square shape of plan. However, there are 25% and 43% increase of maximum story displacements in Y direction due to increase of aspect ratio 1.5 and 2 times respectively. On the other hand, there are 17% and 25% increase of maximum

story drift ratio in X direction due to increase of aspect ratio 1.5 and 2 times respectively. Similarly, there are 26% and 34% increase of maximum story drift ratio in Y direction due to increase of aspect ratio 1.5 and 2 times respectively. As building models become less stiff in Y direction with the increase of aspect ratios in X direction, maximum story displacements and story drift ratio are largely increased in Y direction compared to that in X direction.

- The story drift ratio have been compared for all building models with three ground motions (El Centro, Kobe, Tabas) in both X and Y directions. Story drift ratio is found maximum at 2nd story for ground motion time histories applied in both X and Y directions. The maximum permissible limit for story drift ratio is 0.020 (BNBC, 2020). However, all building models in both X and Y directions are found safe for all ground motions in term of story drift ratio.

In general it can be concluded that, seismic response of buildings increases with the increase of plan aspect ratio if the building is analyzed by time history method.

REFERENCES

Ansary MA and Sadek A (2006) Assessment of 2003 Rangamati Earthquake, Bangladesh. 8th USNCEE, San Francisco, USA.

Alashker Y, Nazar S and Ismaiel M (2015) Effects of building configuration on seismic performance of RC buildings by pushover analysis. Open Journal of Civil Engineering, 5: 203-213. http://dx.doi.org/10.4236/ojce.2015.52020

Arnold C and Reitherman R (1982) Building Configuration and Seismic Design. NY, USA.

Ahmed MM, Ahmed NS, Roy A, Haque M and Bashar I (2019) Comparative Study on Various Horizontal Aspect Ratios on Seismic Performance of Regular Shape G+10 Storey RCC Building. Journal of Earthquake Science and Soil Dynamic Engineering, 4(1): 338-342.

Ahirwal A, Gupta K and Singh V (2019) Effect of irregular plan on seismic vulnerability of reinforced concrete buildings. AIP Conference Proceedings 2158, 020012: 1-5. https://doi.org/10.1063/1.5127136

BNBC (2020) Bangladesh National Building Code, Part 6: Structural Design (In Press). Ministry of Housing and Public Works, Dhaka, Bangladesh

Bolt BA (1987) Site specific study of seismic intensity and ground motion parameters for proposed Jamuna river bridge, Bangladesh. Report Submitted to Jamuna Multipurpose Bridge Authority, Bangladesh.

Bozorgnia Y and Bertero VV (2004) Earthquake engineering. From engineering seismology to performance-based engineering, Boca Raton, etc.

CDMP (2009) Seismic hazard & vulnerability assessment of Dhaka, Chittagong & Sylhet City Corporation. Comprehensive Disaster Management Program, Bangladesh.

Chopra AK (1995) Dynamics of structures: Theory and applications to earthquake engineering. Upper Saddle River, NJ, Prentice Hall.

Chakravorti BK, Kundar M, Moloy DJ, Islam J and Faruque SB (2015) Earthquake Forecasting in Bangladesh and its Surrounding Regions, European Scientific Journal, 18(11): 273-278.

COSMOS Virtual Data Center (2012) Consortium of organizations for strong-motion observation systems (COSMOS). Center for Engineering Strong Motion Data (CESMD), available from https://strongmotioncenter.org/vdc/scripts/earthquakes.plx

Drazic J and Vatin N (2016) The influence of configuration on to the seismic resistance of a building. Procedia Engineering, 165: 883-890. https://doi.org/10.1016/j.proeng.2016.11.788

Eurocode 8 (2004) Design of structures for earthquake resistance - Part 1: General rules, seismic actions and rules for buildings. EN 1998-1, European Standards (EN).

Hossain A (1998) Earthquake Database and Seismic Zoning of Bangladesh. Bangkok, 59-74.

Hussaini TMA and Al-Noman MN (2012) Proposed Changes to the Geotechnical Earthquake Engineering Provisions of the Bangladesh National Building Code. Geotechnical Engineering Journal of the SEAGS & AGSSEA, 43(2): 1-7.

Haselton CB, Whittaker AS, Hortacsu A, Baker JW, Bray J and Grant DN (2012) Selecting and scaling earthquake ground motions for performing response-history analyses, Proceedings of the 15th World Conference on Earthquake Engineering, September 24-28, 2012, Lisbon, Portugal.

Hujare RB and Tande SN (2017) Seismic performance of multi-storied RC moment resisting frames based on plan aspect ratio by pushover analysis. International Journal of Recent Research Aspects, 4(4): 418-422.

Karmakar S (2003) Trends in the frequency and magnitude of earthquake recorded at Chittagong and development of empirical formula for magnitude. Seminar on Earthquake monitoring and loss mitigation in Bangladesh, Dhaka, Bangladesh.

Karim MF (2003) Seismo-tectonic evaluation of Barkal Rangamati earthquakes, its engineering geological significance and some disaster management strategies. Seminar on 2003 Rangamati Earthquakes, September 4, Dhaka, Bangladesh.

Khan AA (2003) Earthquake scenario of Bangladesh in reference to Kolabunia earthquake of july 27, 2003 vulnerability assessment of megacities. Seminar on 2003 Rangamati Earthquake, September 4, Dhaka, Bangladesh.

Modi A, Palia F and Desai M (2016) Effect of aspect ratio on seismic performance of reinforced concrete building using pushover analysis. International Journal of Emerging Technology and Advanced Engineering, 6(10): 235-246.

Murty CVR, Goswami R and Mehta VV (2013) Earthquake Behaviour of Buildings. Gujarat State Disaster Management Authority, Government of Gujarat.

Pecker A (2007) Advanced earthquake engineering analysis. Wien, Springer.

Raheem EA, Ahmed MMM, Ahmed MM and Abdel-shafy AGA (2018) Evaluation of plan configuration irregularity effects on seismic response demands of L-shaped MRF buildings. Bulletin of Earthquake Engineering, 16: 3845–3869. https://doi.org/10.1007/s10518-018-0319-7

Roy S (2014) Probabilistic Prediction for Earthquake in Bangladesh. Open Journal of Earthquake Research, 3(2): 7.

Sadh SK and Pendharkar U (2016) Influence of aspect ratio & plan configurations on seismic performance of multistoryed regular RCC buildings: An evaluation by response spectrum analysis. International Research Journal of Engineering and Technology, 3(1): 293-299.

Sabri MSA (2001) Earthquake intensity-attenuation relationship for Bangladesh and its surrounding region. A thesis of master in engineering in civil engineering, BUET, Bangladesh.

SeismoStruct (2018) Civil engineering software for structural assessment and structural retrofitting. Available from http://www.seismosoft.com

SeismoStruct (2018) Technical information sheet, Nonlinear analysis and assessment of structures. Available from https://seismosoft.com/wp-content/uploads/prods/lib/SEISMOSTRUCT-Technical-Information-Sheet-ENG.pdf

SeismoMatch (2020) Earthquake software for response spectrum matching. Available from http://www.seismosoft.com

Vimala A and Kumar RP (2015) Effects of aspect ratio on nonlinear seismic performance of RC buildings. International Journal of Research in Engineering and Technology, 4(13): 297-304.

Wilkinson and Hiley (2006) A non-linear response history model for the seismic analysis of high-rise framed buildings. Computers & Structures, 84(5): 318-329. https://doi.org/10.1016/j.compstruc.2005.09.021

Wilson EL (2002) Three-dimensional static and dynamic analysis of structures, A physical approach with emphasis on earthquake engineering. Berkeley, Calif.

Wikimedia Commons File, Map plate tectonics world.gif, published 10 September 2007. This page was last edited on 18 February, 2017. https://commons.wikimedia.org/wiki/File:Map_plate_tectonics_world.gif